# The detection of two *Plasmodium falciparum* metabolic enzymes using chicken antibodies

by

**Robert Gerd Erich Krause**

BSc. (*Hons*) Biochemistry

Submitted in fulfilment of the academic requirements for the degree of Master of Science in the School of Biochemistry, Microbiology and Genetics

University of KwaZulu-Natal

Pietermaritzburg

As the candidate's supervisor I have approved this dissertation for submission.

Signed: _____ Name: Prof. J.P.D. Goldring Date:_____

## Abstract

Three protein targets are used in malaria rapid diagnostic tests (RDTs). These are *Plasmodium falciparum* histidine rich protein 2, *Plasmodium* lactate dehydrogenase and aldolase. A thrust of research in RDTs is to improve on their specificity and sensitivity. In this study the current diagnostic target, *P. falciparum* lactate dehydrogenase (*Pf*LDH) was compared to a new target glyceraldehyde-3-phosphate dehydrogenase (*Pf*GAPDH) that was identified based on transcriptional data. These proteins are conserved amongst all *Plasmodium* species, with minor amino acid sequence variations which were evaluated as possible species-specific peptide epitopes for *Pf*LDH: LISDAELEAIFDRC and *Pf*GAPDH: CADGFLLIGEKKVSVFA; CAEKDPSQIPWGKCQV, where common peptides were identified as pan-malarial epitopes for *p*LDH: APGKSDKEWNRDDLC and *p*GAPDH: CKDDTPIYVMGINH. The chosen peptides were located on the surface of their predicted 3D crystal structure models. Antibodies were raised against these peptides in chickens (IgY) and affinity purified.

*Pf*LDH and *Pf*GAPDH were recombinantly expressed in *E. coli* BL21(DE3) cells and their coding inserts confirmed by sequencing. The recombinant proteins were detected in Western blots with specific anti-$His_6$ tag antibodies at approximately 35 kD (*Pf*LDH ~ 36 kD and *Pf*GAPDH ~ 39 kD) which compared with their expected values. Both recombinant proteins were found to form tetramers in solution and were used to raise IgY antibodies for comparison of Pheroids™ and Freund's adjuvants. Pheroids™, like Freund's appeared to exhibit a depot effect, however Freund's adjuvant gave higher affinity purified IgY yields. The anti-recombinant and anti-peptide IgY specifically detected their respective recombinant and native antigens and did not cross-react with other human blood proteins. Immunoprecipitation detected higher levels of *Pf*GAPDH to *Pf*LDH in *P. falciparum* culture lysates. A double antibody sandwich ELISA detected 17.3 ng/ml *Pf*LDH and 138.5 ng/ml *Pf*GAPDH at 1% parasitemia in *in vitro* cultures, however this needs to be further evaluated.

These findings suggest *Pf*GAPDH to be at least as good a protein target as *Pf*LDH for malaria diagnosis and further trials using it as a target in an RDT format should be considered.

## Preface

The experimental work described in this dissertation was carried out in the Discipline of Biochemistry, School of Biochemistry, Microbiology and Genetics, University of KwaZulu-Natal, Pietermaritzburg from February 2010 to February 2012 under the supervision of Prof. J.P.D. Goldring.

These studies represent original work by the author and have not otherwise been submitted in any form to another University. Where use has been made of the work by other authors it has been duly acknowledged in the text.

Signed:

_____

Date:

_____

**Faculty of Science and Agriculture**

**Declaration of Plagiarism**

I, Robert Gerd Erich Krause declare that:

1. The research reported in this thesis, except where otherwise indicated, is my original research.

2. This thesis has not been submitted for any degree or examination at any other university.

3. This thesis does not contain other persons' data, pictures, graphs or other information, unless specifically acknowledged as being sourced from other persons.

4. This thesis does not contain other persons' writing, unless specifically acknowledged as being sourced from other researchers. Where other written sources have been quoted, then:
   a. Their words have been re-written but the general information attributed to them has been referenced
   b. Where their exact words have been used, then their writing has been placed in italics and inside quotation marks, and referenced.

5. This thesis does not contain text, graphics or tables copied and pasted from the Internet, unless specifically acknowledged, and the source being detailed in the thesis and in the References sections.

Signed:

_____

Date:

_____

*Declaration Plagiarism 22/05/08 FHDR Approved*

**Acknowledgements**

I would like to thank my supervisor Professor J.P.D. Goldring for all his assistance and support throughout my studies, from undergrad to my MSc. I hope that we can continue working together in the same way in future!

As for the rest of the malaria lab, I thank all of you for the good times in the lab and I apologise if I caused any "malaria" (*bad air*) from all the bacterial cultures and IgY isolations…well done for holding your breath!

To my other lecturers, supervisors and demonstrators, especially Professor Coetzer, Dr. Niesler, Professor Anderson and Dr. Elliott, thank you for your time and willingness to answer questions.

I would like to thank everyone involved in running the department, from the cleaning staff, to the administrative and technical staff. Thank you for all the effort you put into making our life as easy as it is!

Thank you to the South African Malaria Initiative (SAMI), the National Research Foundation of South Africa, the Medical Research Council and the University of KwaZulu-Natal for their financial assistance, without which this study would not have been possible.

To all my friends I appreciate the support and good will that you all express. Thank you for all the good times, and "cheers to many more!".

Ich möchte meine Eltern, meinen Bruder und den Rest meiner Familie danken für all die Unterstützung und Liebe die es vielfach von gab! "*Aanhouer wen!*"

"*Danket dem Herrn, denn Er ist freundlich und Seine Güte währet ewiglich!*"

# CONTENTS

## List of tables

## List of figures

## Abbreviations and symbols

| | |
|---|---|
| ABC | ATP-binding cassette |
| ABTS | di-Ammonium 2,2'-azino-bis(3-ethybenzothiazolinesulfonate) |
| ACT | artemisinin combination therapy |
| bp | base pairs |
| BSA | bovine serum albumin |
| cAMP | cyclic adenosine monophosphate |
| CDC | centre for disease control |
| DAS ELISA | double antibody sandwich enzyme-linked immunosorbent assay |
| DMSO | dimethyl sulfoxide |
| DTT | dithiothreitol |
| ECL | enhanced chemiluminescence |
| ELISA | enzyme-linked immunosorbent assay |
| EtBr | ethidium bromide |
| FCA | Freund's complete adjuvant |
| FIA | Freund's incomplete adjuvant |
| GAPDH | glyceraldehyde-3-phosphate-dehydrogenase (*Pf*GAPDH *Plasmodium falciparum* glyceraldehyde-3-phosphate-dehydrogenase; r*Pf*GAPDH recombinant *Plasmodium falciparum* glyceraldehyde-3-phosphate-dehydrogenase; pGAPDH *Plasmodium* glyceraldehyde-3-phosphate-dehydrogenase) |
| HRP-2 | histidine rich protein 2 |
| HRPO | horseradish peroxidase |
| IgG | immunoglobulin G |
| IgY | egg yolk immunoglobulin |
| IPTG | isopropyl thioglucopyranoside |
| kD | kilo Dalton |
| *kdr* | knock down resistance mutation |
| LDH | lactate dehydrogenase (*Pf*LDH *Plasmodium falciparum* lactate dehydrogenase; r*Pf*LDH recombinant *Plasmodium falciparum* lactate dehydrogenase; pLDH *Plasmodium* lactate dehydrogenase) |

| | |
|---|---|
| MBS | maleimidobenzoyl-N-hydroxysuccinimide ester |
| MEC | molecular exclusion chromatography |
| mRNA | messenger ribonucleic acid |
| NA | not available |
| NAD | nicotinamide adenine dinucleotide ($NAD^+$ oxidised form; NADH reduced form) |
| PAMP | pathogen associated molecular patterns |
| PBS | phosphate buffered saline |
| PCR | polymerase chain reaction *Pf*CRT *Plasmodium falciparum* chloroquine resistance transporter |
| PEG | polyethylene glycol |
| *Pf*MRP1 | *Plasmodium falciparum* multidrug resistance-associated protein 1 |
| *Pf*MDR1 | *Plasmodium falciparum* multidrug resistance protein 1 |
| RA | rabbit albumin |
| rbc | red blood cell |
| RDT | rapid diagnostic test |
| SDS | sodium dodecyl sulphate |
| SDS-PAGE | sodium dodecyl sulphate polyacrylamide gel electrophoresis |
| TEMED | N,N,N',N'-tetramethylethylenediamine |
| TM | trade mark |
| UV | ultra violet |
| WHO | world health organisation |
| 3D | three dimensional |

# Chapter 1
# Introduction and Literature Review

## 1.1 An overview of malaria

Malaria is caused by a eukaryotic parasite from the genus *Plasmodium* (Miller *et al.*, 1994; Bannister *et al.*, 2000), and is transmitted by the *Anopheles* mosquito (Kiszewski *et al*., 2004). Malaria caused an estimated 1 million deaths worldwide out of 247 million reported cases in 2006 (WHO The Global Burden of Disease, 2008). The disease is especially severe in children under the age of 5, claiming a child's life nearly every 30 seconds, totalling approximately 700,000 deaths each year (Black *et al*., 2003;WHO The Global Burden of Disease, 2008; WHO malaria fact sheet no. 94, January 2009). In endemic countries adults develop natural immunity against malaria. However, this is non-sterilizing, meaning that individuals remain susceptible to infection but remain asymptomatic, making them important reservoirs of malaria (Hafalla *et al*., 2011; Miller *et al*., 1994).

Progress on an anti-malarial vaccine has proven slow although various strategies are being investigated ranging from anti-protein or sub-unit vaccines to using attenuated whole parasites (Friesen *et al.*, 2010; Nussenzweig *et al*., 1967). Some groups believe a humoral immune response should suffice for sterile immunity, while others have demonstrated the need for stimulation of both humoral and innate immune systems as reviewed by Anders (2011) and Good (2011). Until a vaccine is found, diagnosis and anti-malarial drugs remain the main tools in the treatment of a malaria infection.

### 1.1.1 The malaria life cycle

It was initially believed that malaria was caused by inhaling bad air, which in Italian translates to "*mal aria*". Since then it was discovered that the parasite life cycle is divided between a human host and a mosquito vector. The first microscopic record of the red blood cell stage of the parasite was made by Laveran in 1880. The vector responsible for transmitting avian malaria was identified as the female *Anopheles* mosquito by Ross in 1897, which quickly lead to identification of the human malaria vector, also from the *Anopheles* genus, by Grassi in

1900. The human liver stage of the infection was only identified in 1948 by Shortt and Garnham, thus completing the life cycle as shown in Figure 1.1.

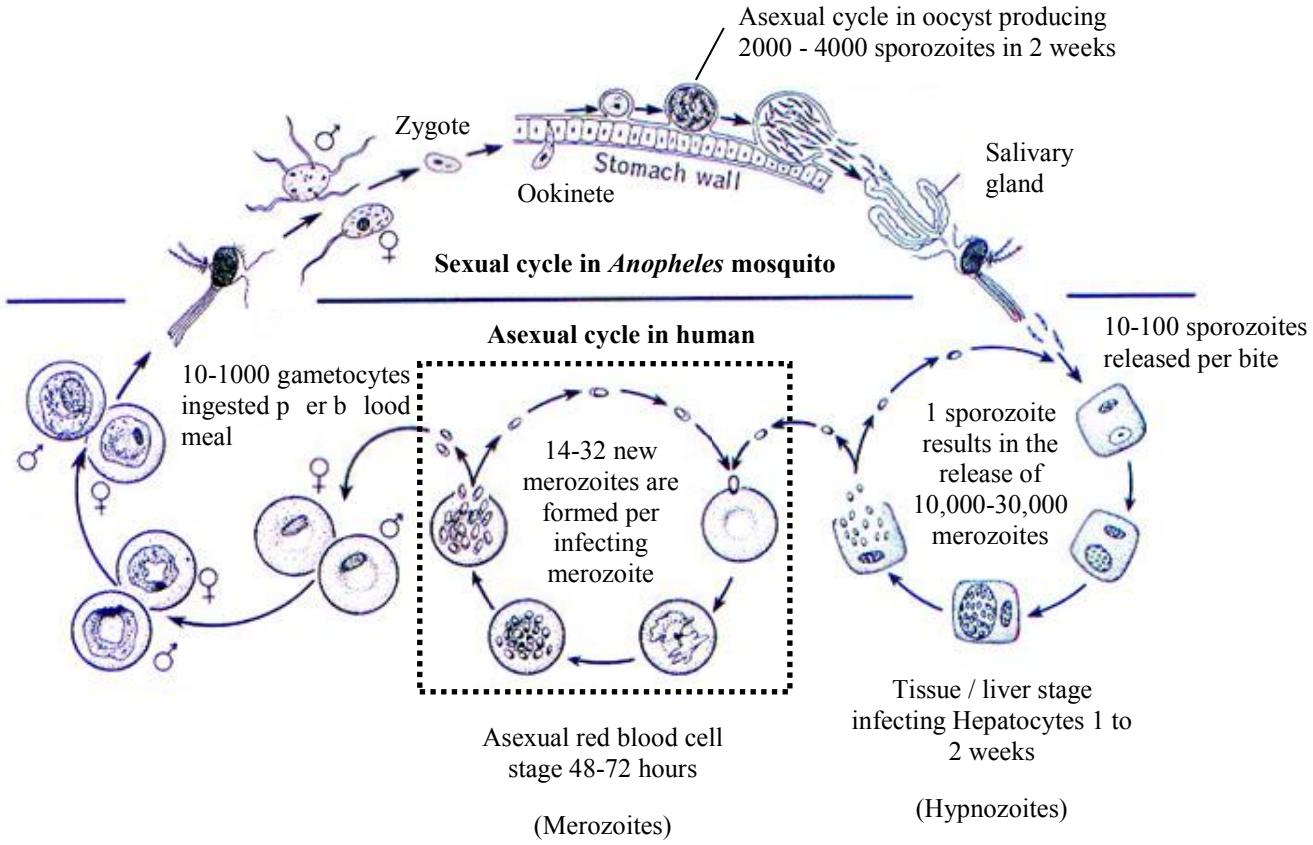


**Figure1.1 The malaria life cycle, highlighting the asexual red blood cell stage as the target for diagnostics.**

The approximate numbers of parasites per stage were taken from (Antia *et al.*, 2008; Baldacci and Menard, 2004; Fujioka and Aikawa, 2002; Kappe *et al.*, 2010; Miller *et al.*, 1994; Smith and Craig, 2005). The boxed red blood cell stage is responsible for disease symptoms and is the stage targeted for diagnostics. (adapted from R.D. Barnes).

Female mosquitoes require blood as a source of protein for egg production, and produce eggs throughout their life. This means they feed regularly, which makes them an ideal vector for transmission of malaria from one host to another. The female *Anopheles* mosquito injects salivary fluid containing anti-coagulants into the blood as part of its feeding process (Miller *et al.*, 1994). If infected it injects malarial sporozoites with its saliva into host tissue or directly into the blood (Baldacci and Menard, 2004). Around 10 to 100 sporozoites are injected per mosquito bite (Baldacci and Menard, 2004; Kappe *et al.*, 2010) and this marks the start of the life cycle within the human host.

Sporozoites migrate to the liver within 60 minutes either by entering the blood stream or the lymphatic system by active gliding motility (Baldacci and Menard, 2004; Kebaier *et al.*, 2009) and invade liver hepatocytes (Baldacci and Menard, 2004; Miller *et al*., 1994). At this stage the parasites mature into schizonts, or they remain dormant in which case they are referred to as hypnozoites. The schizonts eventually occupy the entire cytoplasm of a hepatocyte, at which stage the hepatocyte bursts and releases thousands of merozoites (10,000 to 30,000) into the host blood stream (Fujioka and Aikawa, 2002; Miller *et al*., 1994). This completes the liver stage of the infection except in the case of *P. vivax* and *P. ovale* as these have dormant liver stages referred to as hypnozoites (Fujioka and Aikawa, 2002).

The next stage takes place in the red blood cell stage and has a 48 to 72 hour cycle, depending on the species of *Plasmodium* (see Table 1.1). For each successful merozoite that infects a red blood cell, 8 to 32 new merozoites are formed (Antia *et al.*, 2008; Baldacci and Menard, 2004; Collins and Jeffery, 2005), and given the short turn-over time in the red cell, the parasitemia increases rapidly. This erythrocytic stage is responsible for the symptoms in the patient and is targeted for diagnosis (Antia *et al.*, 2008; Baldacci and Menard, 2004; Miller *et al*., 1994; Murray *et al*., 2008). The time taken for the expression of disease symptoms after the initial infective bite is referred to as the incubation period and ranges between 12 to 28 days dependent on the species of *Plasmodium* and the number of sporozoites initially injected. The greater the numbers of infective sporozoites the faster the symptoms appear. After 3 to 10 red blood cell cycles of the infection the first male and female gametocytes appear. The life cycle returns to the mosquito vector when both male and female gametocytes are ingested by a female *Anopheles* mosquito on its next blood meal where the gametocytes mature into male and female gametes (Fujioka and Aikawa, 2002).

This starts the sexual cycle of the parasite within the mosquito where the gametes form a zygote. The zygote becomes a motile ookinete approximately 18 hours after feeding, and passes through the stomach wall, settling in the mid gut as a sessile oocyst. Within 10 to 24 days dependent on the ambient temperature and the species of *Anopheles* and *Plasmodium*, 2000 to 4000 sporozoites are produced within the oocyst (Fujioka and Aikawa, 2002). These then become actively motile and migrate to the salivary gland of the mosquito until its next blood meal, upon which the life cycle is completed.

### 1.1.2 Which malaria species infect humans?

Only 5 out of over 100 species of *Plasmodium* infect humans (Suh *et al*., 2004). These are *Plasmodium falciparum*; *P. vivax*; *P. ovale*; *P. malariae* and *P. knowlesi* (Daneshvar *et al.*, 2009; Sabbatani *et al*., 2010). *P. knowlesi* is common to monkeys, and has only recently been accepted as a naturally infective human species (Cox-Singh *et al*., 2008; Lee *et al.*, 2009; Singh *et al*., 2004; van Hellemond *et al.*, 2009).

*P. knowlesi* was first isolated from long-tailed macaques in India in 1931, and was shown to be infectious to humans by blood passage in 1932 (Lee *et al*., 2009). The first case of a natural *P. knowlesi* infection in humans was reported in 1965 in Pahang (Malaysia) (Chin *et al*., 1965). The first full description of *P. ovale* was published in 1922 (Collins and Jeffery, 2005). Humans are the only natural host of this species and the Donaldson strain was used as a treatment of neurosyphilis before the advent of penicillin. The first separate description of *P. vivax* and *P. malariae* was done by Grassi and Feletti in 1890 (Collins and Jeffery, 2007). The malignant tertian malaria was named *P. falciparum* by Welch and Thayer in 1897.

Each of these species has slightly different life cycle characteristics as summarized in Table 1.1. *P. falciparum* has by far the most aggressive infective characteristics of the 5 species infectious to man and leads to the most deaths (Suh *et al*., 2004). Little is known of the *P. knowlesi* infection characteristics in man, but the short erythrocytic cycle suggests it to cause severe and rapid progression of disease, as well as daily fever spikes (Ng *et al*., 2008). *P. knowlesi* has been shown to share symptoms with *P. falciparum* and *P. vivax* and fatal cases have been reported (Daneshvar *et al.*, 2009; Sabbatani *et al.*, 2010).

**Table 1.1 Life cycle characteristics of the 5 human infective *Plasmodium* species.**

| | ***P. falciparum*** | ***P. vivax*** | ***P. ovale*** | ***P. malariae*** | ***P. knowlesi*** |
|---|---|---|---|---|---|
| **Pre-erythrocytic cycle (days)** | 5 to 6 | 8 | 9 | 13 | NA |
| **Dormant liver stage** | no | yes | yes | no | no |
| **Merozoite number released per infected hepatocyte** | 30,000 | 10,000 | 15,000 | 10,000 | NA |
| **Rbc cycle (hours)** | 48 | 48 | 49 | 72 | 24 |
| **Maximum number of merozoites per rbc** | 32 | 24 | 20 | 14 | 16 |
| **Average parasitemia / µl** | 20 to 500,000 | 20,000 | 9000 | 6000 | NA |
| **Maximum parasitemia / µl** | 2,000,000 | 100,000 | 100,000 | 20,000 | > 100,000 |

The life cycle data was assembled from the following sources: Chin *et al*., 1965; Daneshvar *et al*., 2009; Fujioka and Aikawa, 2002; Lee *et al*., 2009; Murray *et al*., 2008. Abbreviations used: rbc. = red blood cell(s); NA = not currently available.

The WHO defined severe malaria in 2000 as a patient who shows one or more of the following symptoms: prostration (patient cannot sit up without help); impaired consciousness; difficulty breathing or pulmonary edema; seizures; collapse of blood circulation and abnormal bleeding; jaundice; haemoglobinuria and severe anemia (< 15 % hematocrit). In severe malaria, even with proper treatment, the mortality rate exceeds 20 % (Antia *et al*., 2008; Suh *et al*., 2004). These effects are due to high parasite numbers in the blood and in the case of *P. falciparum*, parasite sequestration also occurs (Baldacci and Menard, 2004; David *et al*., 1983; Suh *et al*., 2004). Sequestration is a phenomenon unique to *P. falciparum*. As the parasite matures within the red blood cell it exports HRP-2 and EMP1 (among other proteins) to the surface of the infected red blood cell which form visible knobs on the surface of the cell (Bannister *et al*., 2000). These cause the infected red blood cells to adhere to each other as well as uninfected red blood cells, described as rosetting (Leitgeb *et al*., 2011). The infected red blood cells also adhere to endothelial cells lining arterioles. This results in cerebral malaria and organ failures in severe malaria (David *et al*., 1983; Leitgeb *et al*., 2011).

Only *P. vivax* and *P. ovale* have liver dormant stages as seen in Table 1.1 (Perkins and Bell, 2008). These stages are not susceptible to drugs targeting the blood stage therefore drugs targeting hypnozoites are additionally required to clear all stages of these species. As a result diagnostic tests have to differentiate between the species of malaria responsible for infection to allow appropriate treatment and to avoid a possible relapse. This task is further complicated as co-infections of different malaria species are common (Chuangchaiya *et al.*, 2009; Murray *et al*., 2008). Hypnozoites can often emerge from the liver and cause relapse up to two years after clearance of the initial blood stage infection (Fujioka and Aikawa, 2002).

### 1.1.3 Where is malaria found?

As mentioned before, all 5 species are transmitted by the *Anopheles* mosquito vector (Kiszewski *et al.*, 2004) and as a result malaria endemic regions overlap with the *Anopheles* mosquito's natural habitat (Hay *et al*., 2009). *P. knowlesi* is transmitted by *Anopheles latens* and *An. leucospherus* which feed on humans as well as macaque monkeys (Anderios, 2009, Sabbatani *et al.*, 2010, Van den Eede *et al.*, 2010,). *Anopheles latens* is predominantly found in South-East Asian countries, where *An. leucospherus* is more wide spread and has been found in island countries of Australasia (Kiszewski *et al.*, 2004). The major *Anopheles* vectors

and malaria distribution are illustrated in Figure 1.2. This shows that malaria is endemic to the tropics. Currently an estimated 1.38 billion people live in high-risk malaria endemic areas, and are affected by the disease, excluding the millions of travellers visiting these countries each year (Hay *et al*., 2009).

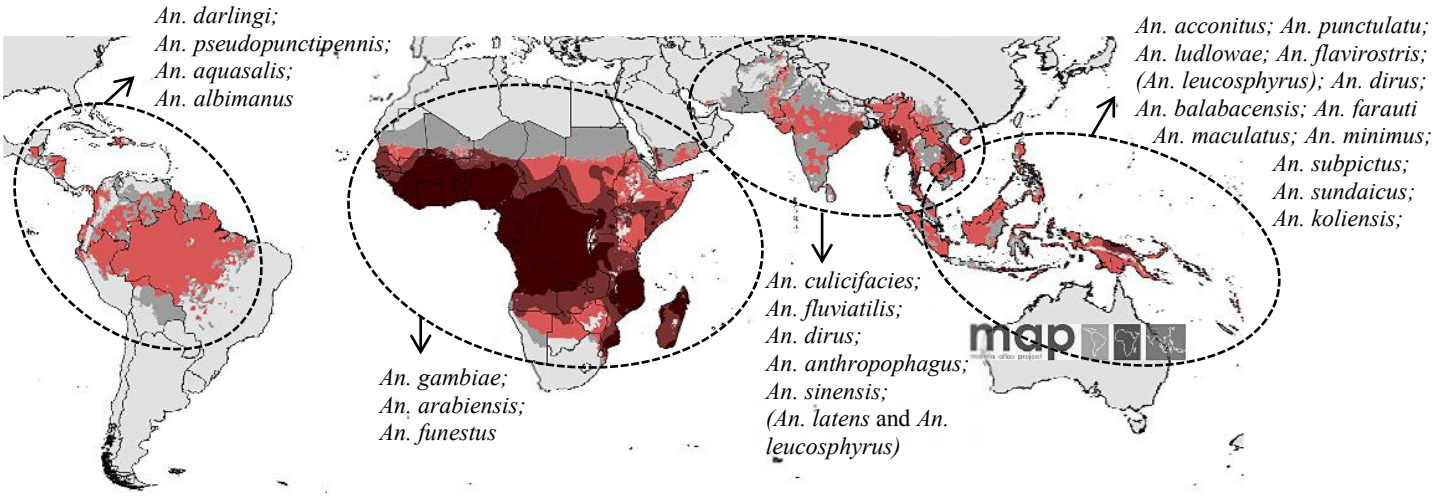


**Figure1.2 Global malaria distribution, including primary *Anopheles* mosquito vectors.**

Key to the malaria prevalence is as follows, where % values indicate the proportion of the human population likely to be affected by malaria: malaria free; 0.1 %; 0 – 5 %; > 5 - < 40 %; > 40 % (Hay *et al.*, 2009). Primary vectors were defined as: species that feed on humans; frequently contained sporozoites and were more prevalent than other species (Kiszewski *et al.*, 2004). The *An. latens* and *An. leucosphyrus* species were listed in brackets as these are the main *P. knowlesi* vectors responsible for transmission between macaque monkeys and humans (Daneshvar *et al.*, 2010; Sabbatani *et al.*, 2010).

From Figure 1.2, it is clear that Sub-Saharan Africa and some East-Asian countries have the highest malaria burden. Of the 1.38 billion, people living in high-risk endemic areas, 0.041 billion are in the Americas; 0.657 billion in Africa and 0.686 billion in central and south east Asia. Africa has the highest risk of *P. falciparum* infection accounting for 90 % all fatalities and amounts to an estimated annual loss of around 12 billion US Dollars in Africa alone (Hay *et al*., 2009; Suh *et al*., 2004). An important factor for malaria severity is that most tropical countries are still developing and have vast rural areas which lack adequate healthcare infrastructure. As such diagnosis in these areas has to be "low-tech", simple to perform and interpret, yet reliable and sensitive at the same time (Murray *et al*., 2008; Perkins and Bell, 2008).

### 1.1.4 What is the effect of malaria on South Africa?

Due to changing climate patterns, the distribution of the *Anopheles* vector may spread more to the east and south-east coast of South Africa (Tonnang *et al*., 2010). Figure 1.3 shown here, depicts the current distribution and worst case scenarios of climate change on the *An. arabiensis* and *An. gambiae* distributions in South Africa. These two species are seen as the major vectors within Sub-Saharan Africa and form part of the *An. gambiae* complex (Betson *et al*., 2009; Levine *et al*., 2004; Tonnang *et al*., 2010).

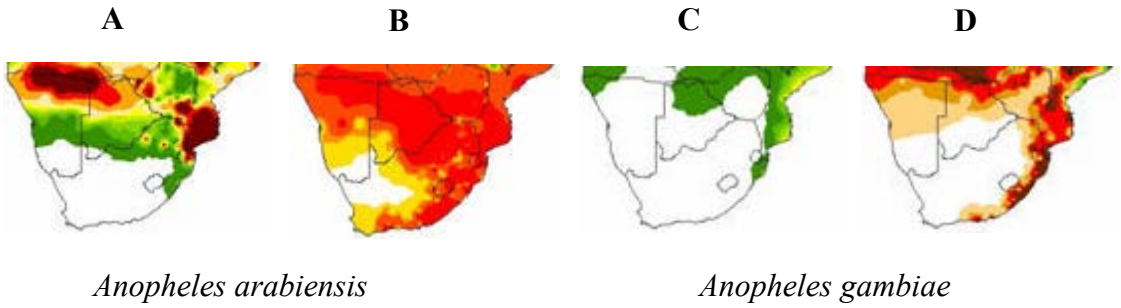


**Figure1.3 The present and future distribution models of the two major Sub-Saharan African *Anopheles* vectors.**

The key indicates distribution of *Anopheles* vectors, with green being low populations and brown being high populations ( ). Each map had individual values per colour, which were omitted here for simplicity. (A and C) show present conditions where (B and D) show the change in distribution after a 4 ºC rise in temperature and a 20 % increase in summer rains with a 20 % decrease in winter rains. The maps were taken from (Tonnang *et al*., 2010).

The north-eastern regions of South Africa have the highest risks of malaria transmission especially along the border with Mozambique. In 2006 the estimated population at risk of malaria infection in South Africa (including Lesotho and Swaziland) totalled 6.15 million people (Teklehaimanot *et al*., 2007). The implementation of indoor residual spraying using dichlorodiphenyltrichloroethane (DDT) and malaria treatment with artemether-lumefantrine in 2003 has reduced malaria cases in the KwaZulu-Natal province by more than 99 % from over 30,000 cases between 1991 and 1992 to around 300 annual cases (Duffy and Mutabingwa, 2005). South Africa is fortunate, in that it has better health care infrastructure and is economically stronger than many other African countries, and as such is better suited to implement malaria control measures.

This is an example of the successful implementation of combined control measures. Malaria was also eradicated from North America and Europe by draining swamps and large scale

spraying of insecticides. These control measures are still implemented in Florida and in Australia today (Rozendaal, 1997).

### 1.1.5 Malaria vector control

The main methods of vector control include insecticide treated bed nets and indoor residual spraying. Only a limited number of insecticides are available for indoor residual spraying (12 in total from 4 classes, organochlorides; organophosphates; carbamates and pyrethroids), where only pyrethroids have been approved for treatment of bed nets (Betson *et al.*, 2009). Reduced susceptibility of mosquitoes has been reported since mid-1950, and resistance to all 4 classes of insecticide have been recorded in Africa (Betson *et al.*, 2009; Blanford *et al*., 2011). This is due to a pyrethroid knockdown resistance (*kdr*) mutation in *An. gambiae* (Martinez-Torres *et al*., 1998).

The use of alternate vector control measures, such as bio-control methods are being developed against *Anopheles*. These include entomopathogenic soil-borne fungi such as *Beauveria bassiana* and *Metarhizium anisopliae*, which are found worldwide (Blanford *et al*., 2011; Kanzok and Jacobs-Lorena, 2006). These infect and kill mosquitoes within 2 weeks, which corresponds to the time taken for the development of infective malaria sporozoites within the mosquito (Blanford *et al*., 2011; Fujioka and Aikawa, 2002). Both fungi are currently used as bio-control agents against termites and aphids (Khetan, 2000). The downfall with current formulations is that the viability of spores decreased by 63 % in 3 weeks after spraying. This will have to be improved for large scale implementation. No resistance has been reported in *Anopheles* against these agents so far, although cases of reduced susceptibility have been observed (Kanzok and Jacobs-Lorena, 2006). Even where mosquitoes develop resistance against these agents, it is unlikely that the same population would develop resistance against insecticides and *vice versa* for insecticide resistant populations. Thus by rotational use of insecticides and entomopathogenic fungi, vector control could become a lot more effective (Blanford *et al*., 2011).

Encounters between humans and *Anopheles* mosquito vectors are almost inevitable, especially in cases where people work or hunt in forests, or work in agricultural plantations. For this reason transmission remains a very real threat and occurs frequently in spite of vector control

measures, especially in malaria endemic countries and effective treatment with antimalarial drugs is essential.

### 1.1.6 Treatment of malaria

The classical treatment strategy adopted in malaria endemic countries since the discovery and development of chloroquine in the 1930-1940's was: "fever equals malaria unless proven otherwise" (Perkins and Bell, 2008). The majority of fever cases in the tropics were therefore treated with chloroquine. This "liberal" use of chloroquine has resulted in the development of resistant strains of malaria as summarised in Table 1.2 (Okiro and Snow, 2010; Perkins and Bell, 2008).

**Table 1.2 Stages targeted by antimalarial drugs and geographical regions in which drug resistance has been reported.**

| Antimalarial drug | Parasite target stage | Resistant species | Distribution of resistance |
|---|---|---|---|
| Chloroquine / amodiaquine | Blood | *P. falciparum* | All *P. falciparum* endemic regions except: Mexico, Dominican Republic, Haiti, Central America west and north of the Panama Canal, Argentina, North Africa, most of the Middle East and China. |
| | | *P. vivax* | *P. vivax* resistance: Oceania, Myanmar, Guyana, Colombia and Brazil |
| Mefloquine / quinine | Blood | *P. falciparum* | Thai borders with Cambodia and Myanmar |
| Pyrimethamine / chlorproguanil; Sulfadixine | Blood | *P. falciparum* | |
| Artemisinin | Blood and gametocyte | | |
| Primaquine | Liver and gametocyte | *P. vivax* | Oceania, Southeast Asia and Somalia |
| Ciprofloxacin; Clindamycin / doxycycline; Fosmidomycin; Rifampicin; Atovaquone | Liver and blood | | |
| Fatty acid synthesis inhibitors | Liver | | |

Data was collected from: Lalloo *et al.*, (2007); Kappe *et al*., (2010); Suh *et al*., (2004); Peterson *et al*., (1998); Kublin *et al*., (2002).

Malaria treatment is dependent on the infecting species of malaria as well as the geographical region in which the infection was contracted. The species is important due to the presence of liver dormant stages or hypnozoites in both *P. vivax* and *P. ovale* infections as mentioned

previously in Table 1.1. To clear hypnozoites, a 14-day course of primaquine is required to avoid relapse (Lalloo *et al*., 2007). The geographical region is important as resistant strains have been identified in specific areas of the world as shown in Table 1.2 and alternate drug treatments have been recommended accordingly (Lalloo *et al*., 2007; Kappe *et al*., 2010; Suh *et al*., 2004;).

Protein transporters involved in drug resistance have been identified in *P. falciparum*. These include the chloroquine resistance transporter (*Pf*CRT); two ATP-binding cassette (ABC) transporter family members called the multidrug resistance protein 1 (*Pf*MDR1) and the multidrug resistance-associated protein 1 (*Pf*MRP1). Single nucleotide polymorphisms change the specificity of the ABC proteins, stopping transport of drugs into the parasite cytosol and thereby making the parasite resistant to the drug. Studying these A/T-rich and transmembrane proteins of malaria is difficult due to expression difficulties (Koenderink *et al*., 2010).

To counter drug resistance "Treatment of Malaria (Guidelines for Clinicians)" was published by the centre for disease control in 2007 and more recently "Guidelines for the treatment of malaria 2010" (Reyburn H., 2010), both emphasizing the need for a parasitological diagnosis of malaria before treatment. The WHO has recommended artemisinin combination therapy (ACT) in drug resistant areas. This includes quinoline compounds or derivatives such as amodiaquine and mefloquine. These drugs prevent haematin polymerisation into haemozoin. As the parasite degrades haemoglobin the ferriprotoporphyrin groups accumulate (Bannister *et al*., 2000) and kill the parasite by inhibiting metabolic enzymes such as glyceraldehyde-3-phosphate dehydrogenase (GAPDH) and lactate dehydrogenase (LDH) (Campanale *et al*., 2003; Egan and Ncokazi, 2005; Penna-Coutinho *et al*., 2011). Pyrimethamine and proguanil are also incorporated and inhibit the tetrahydrofolic acid cycle, resulting in the inhibition of DNA synthesis (Kappe *et al*., 2010). Artemisinin itself has been shown to reduce gametocyte formation as well as reducing their infectivity to mosquitoes as reviewed by Golenser *et al*., (2006). Artemisinin is hypothesised to interfere with a calcium ion transporter called sarcoplasmic / endoplasmic calcium ATPase (SERCA) Golenser *et al*., (2006).

Development of drug resistance remains a constant challenge in the treatment of malaria. There have been recent reports of reduced artemisinin susceptibility as well as artesunate-mefloquine resistance in Cambodia which are concerning, however these have yet to be confirmed (Akler *et al*., 2007; Koenderink *et al*., 2010). For this reason it is essential that

diagnostic tests allow clinicians to monitor patients while treating them. An increase in parasitemia during treatment would therefore suggest treatment failure and alternate treatments could be lifesaving. The increased cost of combination therapies has also made diagnosis before treatment more essential, while this will also curb the "liberal" use of antimalarials, as has been the case with chloroquine (Perkins and Bell, 2008).

## 1.2 Malaria diagnosis

### 1.2.1 What are the main factors impacting malaria diagnosis?

The important points highlighting the need for malaria diagnosis so far were:

- Malaria causes severe disease and there is currently no available vaccine.
- Patients only seek medical attention once disease symptoms appear, which is during the red blood cell stage of malaria, making this the stage targeted for diagnostics.
- There are 5 species of malaria infective to humans, 2 of which have dormant liver stages that require alternative treatments to avoid relapse, therefore they have to be differentiated by diagnosis.
- Malaria is endemic to the tropics and rural areas of developing countries are worst affected. In this setting diagnostic tests have to be "low tech", quick and easy to perform and interpret.
- Although South Africa has implemented a successful prevention program, climate change models predict a spread in the prevalence of the *Anopheles* vector, thus diagnosis in South Africa will also become more important.
- Vector control methods are effective, however, insecticide resistance in mosquitoes is increasing and there is still a risk of exposure "out of reach" of control measures, therefore transmission remains a risk and makes treatment essential.
- Increasing malarial drug resistance has forced the implementation of combination therapies. With the increasing cost of treatment and efforts to curb the spread of anti-malarial drug resistance, it has become important to diagnose malaria before treatment.
- Diagnostic tests should ideally be able to track disease progress, which will aid in assessing treatment success, which can be lifesaving in drug resistant regions.

### 1.2.2 Criteria for comparison of diagnostic tests

Before describing the different diagnostic tests available, definitions of the criteria used to compare these tests are important. These are specificity, sensitivity and limits of detection. Specificity refers to the accuracy of the particular test to correctly identify the infecting species of *Plasmodium* (Murray *et al*., 2008). Sensitivity refers to the ability of the particular test to correctly detect infection out of a total number of positive and negative samples (Murray *et al*., 2008). Both specificity and sensitivity are usually expressed as percentages in terms of the total number of samples diagnosed correctly out of the overall number of test samples. Finally, the limit of detection refers to the lowest level of infection in terms of % parasitemia or parasites per microliter of blood that the method can detect. Microscopy is still the gold standard for comparison although some groups additionally use PCR as a standard (Murray *et al*., 2008).

### 1.2.3 A closer look at the red blood cell stage as the target for diagnosis

Due to the nature of the parasite life-cycle, diagnosis focuses on the red blood cell stage of the infection, which was boxed in Figure 1.1 and is shown in more detail in Figure 1.4. This stage has the highest parasite count throughout the lifecycle and is responsible for disease symptoms as described before (Antia *et al*., 2008; Baldacci and Menard, 2004; Miller *et al*., 1994).

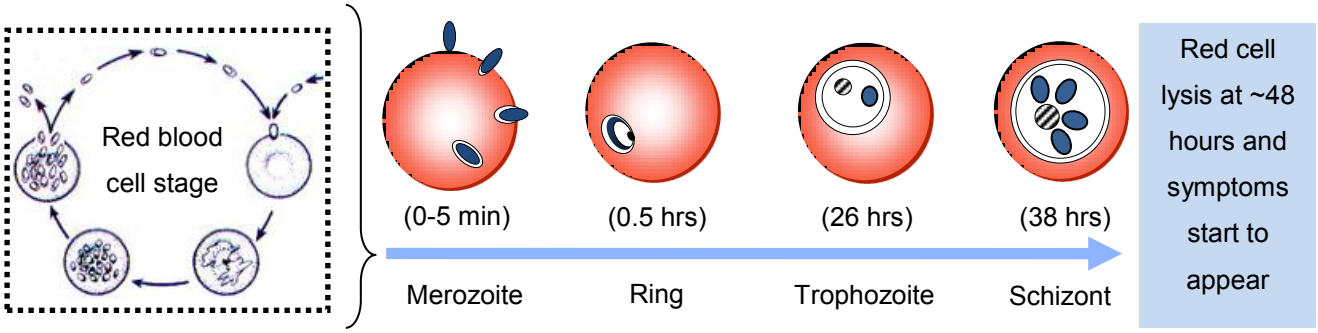


**Figure1.4 Maturation of the red blood cell stage (erythrocytic schizogony) of the *Plasmodium falciparum* parasite.**

The diagram was based on descriptions from Bannister *et al.,* (2000) and depicts the progress of the *P. falciparum* parasite through its 48 hour red blood cell cycle, from the initial invading merozoite stage, to the mature late trophozoite stage known as the schizont. ● depicts the parasite, which during the ring stage has a ring-shaped cytoplasm with a punctate nucleus. ◍ depicts haemozoin formation.

From the initial infection of a red blood cell, a merozoite undergoes several morphologically distinct changes until maturation (Bannister *et al*., 2000), followed by rupture of the red blood cell. These different stages can be identified under a light microscope (see section 1.3.3) and are used in diagnosis of the species of malaria. This is done by comparison of different morphological characteristics of the parasites at each stage in the red blood cell cycle as summarised in Table 1.4. Once the merozoite invades the red blood cell, which is a rapid process, taking at most a few minutes, it enters its trophozoite stage (Bannister *et al*., 2000).

The first of these is the ring-stage (Bannister *et al*., 2000), which has a characteristic vacuole in the centre of the parasite. At around 26 hours post-invasion of the red blood cell the first pigments of haemozoin appear, which is yet another characteristic that has been exploited for diagnosis (see section 1.3.5). The morphology of the parasite assumes an early trophozoite stage in which it has a single nucleus and a large cytoplasm with no vacuole (Bannister *et al*., 2000). At 38 hours post invasion the morphology assumes that of a schizont, which has multiple nuclei, and multiple merozoites are produced. The number of merozoites released is also dependent on the species of malaria, with the number ranging from 14 to 32 as shown in Table 1.1 (Antia *et al.*, 2008).

Upon completion of one erythrocytic cycle the red blood cells rupture and release the parasites into the blood stream. This causes disease symptoms, where fever is the first of these (Miller *et al*., 1994). The time taken from initial infection to the presentation of symptoms is known as the incubation period (Suh *et al*., 2004). In the field this is of little use as the clinician will have no idea as to when the patient was initially bitten. Clinical diagnosis of malaria is therefore based on the time between fever episodes (see 1.3.1).

## 1.3 How is malaria diagnosed?

### 1.3.1 Clinical diagnosis

Rupturing infected red blood cells release parasites into the blood stream resulting in fever as was shown by Golgi in 1886 and reviewed by Miller *et al.,* (1994). Fever was used for diagnosis because it is the earliest symptom to present during a malaria infection (Antia *et al*., 2008). The red blood cell cycles of the 5 species of human malaria differ in length. As a result the time between fever episodes is different as shown in Table 1.3.

**Table 1.3 Characteristic fevers of the 5 human malaria species.**

| | *P. vivax* | *P. ovale* | *P. malariae* | *P. falciparum* | *P. knowlesi* |
|---|---|---|---|---|---|
| **Erythrocytic cycle (hours)** | 48 | 49 | 72 | 48 | 24 |
| **Time between fevers (days)** | 2 | 2 | 3-4 | 2 | 1 |
| **Fever description** | tertian | tertian | quartan | tertian | daily |

The data were taken from Collins and Jeffery, (2005); Daneshvar *et al*., (2009); Sabbatani *et al*., (2010).

As was shown by Källander *et al.,* in 2004, fever is a common symptom of pneumonia and other tropical diseases and as a diagnostic for malaria it is less than 20 to 30 % accurate (Gwer *et al*., 2007; Perkins and Bell, 2008). Clinical diagnosis is highly presumptive as a result, but has had success as demonstrated by Kidane and Morrow in 2000 and Sirima *et al*., in 2003, reporting a 40 % reduction in mortality and reduced risk of severe disease in children under five years old. Treatment of children exhibiting overlapping disease symptoms using both antimalarials and antibiotics, known as an integrated management of childhood illness (IMCI), was described by Gove in 1997 to improve the success of presumptive treatment.

In African children alone the annual number of fever episodes was estimated to around 870 million (Snow *et al.*, 2003). Presumptive treatment inevitably leads to high rates of misdiagnosis and several negative consequences. These included: 1) the treatment of the wrong disease resulting in the onset of severe disease and death and 2) an increased frequency of drug resistance due to the "liberal" use of antimalarial drugs (Murray *et al.*, 2008; Perkins and Bell, 2010).

More accurate diagnostic techniques have been developed, each with its advantages and disadvantages as summarised in Table 1.4 and each of these methods will be briefly described.

**Table 1.4 Parameters of the main malaria diagnostic tests.**

| Parameter | Microscopy | Fluorescence | PCR | RDTs |
|---|---|---|---|---|
| **Sensitivity (parasites / µl)** | 50 | ≥ 100 | ≤ 5 | 100 to 200 |
| **Specific** | yes | no | yes | yes |
| **Quantification** | yes | no | no | possible |
| **Time** | up to 60 min | up to 60 min | 2 to 3 hours | 15 to 20 min |
| **Equipment / infrastructure required** | yes | yes | yes | no (kit format) |
| **Expertise level** | moderate-high | moderate | high | low |
| **Cost / test** | R1 - R3.20 | R0.60 - R13.60 | R20.00 | R4.40 - R12.00 |

Data were taken from Demas *et al.*, (2011); Makler *et al.*, (1998); Moody (2002); Perkins and Bell (2008); Wongsrichanalai *et al.*, (2007).

### 1.3.3 Microscopy

Microscopy is based on the visual detection and identification of malaria parasites in red blood cells. This is usually done using Giemsa staining, where Wright's or Field's stains are alternative methods. All three methods stain DNA, take advantage of the terminal nature of the mature red blood cell, which does not contain DNA, and the parasites are easily visible (Figure 1.5) (Moody, 2002; Suh *et al.*, 2004).

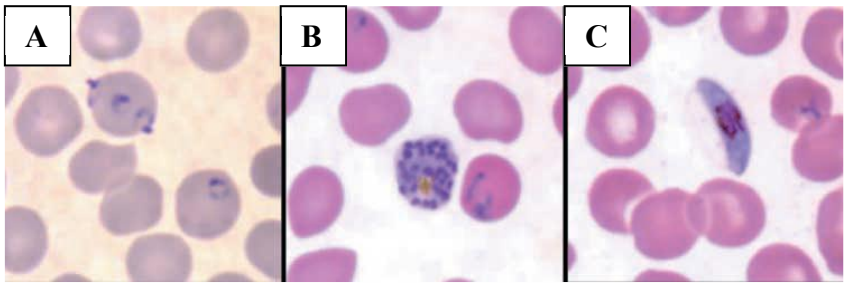


**Figure1.5 View of a thin blood smear showing Giemsa stained red blood cell stages of *P. falciparum* using light microscopy.**

Early trophozoites (ring stage) are visible in (A), followed by a mature schizont in (B) and a gametocyte in (C). The images were taken from Suh *et al.*, (2004).

Slides are prepared either as thick or thin blood films. In the case of thick smears the red blood cells are stained but not fixed and are concentrated by a factor of 20 to 30 on the slide. Alternatively the thin film preparations are fixed with methanol and then stained. Thick films

are more suited to gross quantification, whereas thin films are usually used for identifying the infecting species of malaria and more accurate quantification (Moody, 2002).

Calculating the parasite load or % parasitemia of the patient, which is a measure of the extent of infection, allows the clinician to track response to treatment (Murray *et al*., 2008). The most common method of determining parasite load is to count the number of parasites and white blood cells in a thick film preparation. The number of parasites in relation to 200 white blood cells is extrapolated by multiplying by 40, which assumes that a normal blood sample has approximately 8000 white blood cells per microliter (Makler *et al*., 1998; Moody, 2002). Alternatively % parasitemia is estimated using thin film preparations. This is done by counting the total number of parasites seen in 10,000 red blood cells or 40 fields of view using a normal light microscope at 100X magnification. It is then assumed that 1 µl of blood contains an estimated 5 x $10^6$ red blood cells. The following equation is therefore used: 1 % parasitemia = 5000 parasites/µl of blood (Moody, 2002).

In naïve patients, symptoms will start to appear at around 100 parasites/µl (0.0002 % parasitemia) whereas in immune patients symptoms are expressed around 2500 to 30,000 parasites/µl (0.05-0.7 % parasitemia). Severe malaria generally occurs in patients with a parasitemia greater than 5 % (Miller *et al*., 1994; Murray *et al*., 2008; Suh *et al*., 2004). Since patients will only seek treatment after the presence of symptoms, the sensitivity of microscopy at around 50 parasites per microliter (Table 1.4) makes this a good diagnostic method. It is also a very simple protocol to follow, which is why it is still regarded as the gold standard for comparison of new alternate diagnostic tests (Moody, 2002).

Various visual characteristics are used to identify the different species of malaria, which is summarised in Table 1.5. These are usually viewed in thin film microscope slides. In the case of *P. falciparum* only ring stages are usually visible due to sequestration of late trophozoites (Bannister *et al*., 2000; David *et al.*, 1983). Only *P. vivax* and *P. ovale* visibly enlarge the red blood cell and characteristic stippling of the red blood cell cytoplasm also known as Schüffner's granules appear (Gkrania-Klotsas and Lever, 2007).

**Table 1.5 Differentiating features of the 5 *Plasmodial* species infecting humans.**

| | ***P. falciparum*** | ***P. vivax*** | ***P. ovale*** | ***P. malariae*** | ***P. knowlesi*** |
|---|---|---|---|---|---|
| Parasites / red blood cell | multiple | single | single | single | multiple |
| Size of red blood cell | normal | enlarged | enlarged with fimbriated ends | normal | normal |
| Typical asexual red blood cell stages present and shape | predominant ring stages, very few trophozoites and schizonts | all stages present, with typical amoeboid trophozoites | all stages present, with compact trophozoites | all stages present with compact "band form" trophozoites; "rosetting" merozoites | all stages present with compact band form trophozoites |
| Gametocytes | banana / sickle shaped | present | present | present | present |
| Other characteristics | Knobs on red blood cells of late trophozoite stages | Schüffner's granules | Schüffner's granules | Fine stippling of red blood cells | Fine stippling of red blood cells |

Data taken from: Anderios *et al*., (2009); David *et al*., (1983); Gkrania-Klotsas and Lever (2007); Lee *et al*., (2009).

Microscopy based diagnosis of malaria is a case where "practice makes perfect" and the level of experience affects both the specificity and sensitivity of the method. For example *P. knowlesi* resembles *P. malariae* morphologically during late stages of infection (mature trophozoites, schizonts and gametocytes), where early ring stages resemble those of *P. falciparum* (Anderios *et al*., 2009; Lee *et al.*, 2009). Since co-infections of different malaria species are also possible, correctly identifying the individual species in such cases is even more challenging (Chuangchaiya *et al.*, 2009).

Microscopy also requires electricity which often not available in a field setting and it can take up to 60 minutes to prepare slides. It is still the cheapest method available in terms of cost per test, although the microscope itself is a large initial cost.

### 1.3.4 Fluorescence microscopy

Fluorescence microscopy is another method used to visualise the parasite by staining DNA. Two fluorochromes are commercially available, namely acridine orange and benzothiocarboxypurine, which are excited at 490 nm and emit an apple green or yellow fluorescence (Makler *et al*., 1998; Moody, 2002). Examples of these were shown in Figure 1.6.

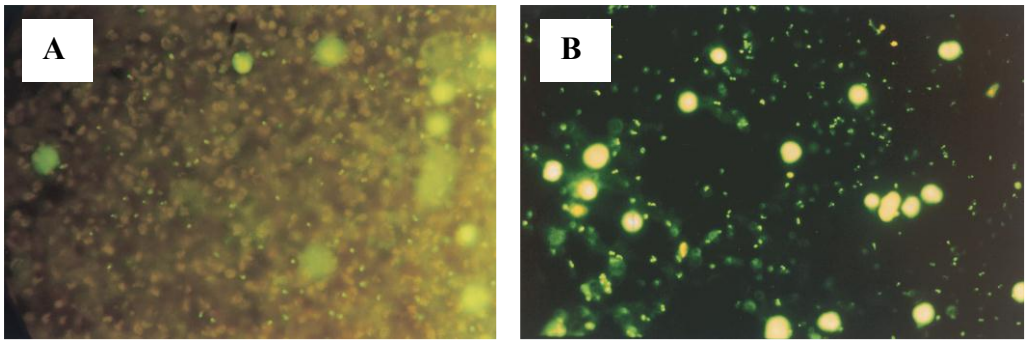


**Figure1.6 A representation of fluorescence microscopy showing detection of *P. falciparum* trophozoites.**

The image in (A) was stained with acridine orange and that in (B) was stained with benzothiocarboxypurine. The images were taken from Moody (2002).

Acridine orange is not specific to living parasites and stains all DNA containing cells. An alternative method called the quantitative buffy coat method separates parasites from white blood cells using a capillary tube, making it easier to differentiate the two (Moody, 2002). Acridine orange is toxic, making its handling and safe disposal problematic (Moody, 2002). Alternatively benzothiocarboxypurine is used to identify viable parasites as it depends on active adsorption through the parasite membrane to stain the DNA. It also does not stain white blood cells as strongly as acridine orange does (Moody, 2002). Rhodamine-123 is an alternative dye used for parasite viability, but it is not commercially available. Rhodamine-123 is a cationic permeant dye which selectively accumulates inside the parasite due to its high membrane potential (Moody, 2002). Fluorescence microscopy is not quantitative and can thus not be used to track infections during drug treatment. Differentiating the species of malaria is difficult with fluorescence and this method is not preferred for this purpose (Moody, 2002). This method also requires electricity, although filters have been developed enabling the use of sunlight (Moody, 2002). A portable battery powered assay was developed (CyScope®) and showed good sensitivity, but a high rate of false positives and requires further development (Sousa-Figueiredo *et al*., 2010).

### 1.3.5 Detection of haemozoin

The malaria parasite digests haemoglobin as a source of amino acids within a lysosome-type body called a food vacuole (Bannister *et al*., 2000; Olszewski *et al*., 2011). As a by-product of haemoglobin catalysis large amount of free haem is produced, which is toxic as it inhibits various enzymes and also results in the generation of free radicals. The parasite therefore polymerises haem into a compound known as haemozoin or malaria pigment and stores it in the food vacuole (Dostert *et al*., 2009). Haemozoin accumulates to visually detectable levels as a black or brown pigment in late trophozoites, as was illustrated in Figure 1.4 (Bannister *et al*., 2000).

Besides being visible under the microscope in thin blood films, haemozoin can also be detected in white blood cells of infected patients. Following lysis of an infected red blood cell the haemozoin is released into the blood stream (Dostert *et al*., 2009). These particles are then phagocytosed by white blood cells (Hänscheid *et al*., 2001). Haemozoin was detected in white blood cells using a cell analyser / counter due to the depolarising properties of the pigment and gave 95 % sensitivity and 88 % specificity in comparison to microscopy (Hänscheid *et al*., 2001).

### 1.3.6 Molecular diagnosis

PCR involves either single or multiplex methods, detecting malarial DNA (Demas *et al*., 2011). This method traditionally uses the small-subunit ribosomal RNA (18S rRNA) or circumsporozoite genes as targets (Ng *et al*., 2008). Pvr47 and Pfr364 have also been identified as alternate targets (Demas *et al*., 2011). Nested or reverse transcription PCR allows differentiation of the *Plasmodial* species. The use of fluorescein or radiolabeled probes allows detection, or alternatively samples are run and visualised on agarose gels with ethidium bromide. Nested PCR to detect malaria infections using saliva and urine samples is also possible (Buppan *et al*., 2010).

PCR takes a long time, between 2-3 hours to complete and requires a sterile lab environment and technical competence for reliable results, making it unsuitable for field clinics. It is an essential technique for studies of drug resistance, however and blood samples can be dried and stored on filter paper for later analysis (Moody, 2002).

Alternative methods have been developed to simplify the PCR reactions, which include loop-mediated and helicase dependent isothermal amplification reactions. Both methods still require a 95 ºC DNA denaturation step as well as subsequent incubations at 37 or 65 ºC respectively (Notomi *et al*., 2000; Vincent *et al*., 2004). The loop mediated isothermal amplification has been used to detect a human *P. knowlesi* infection of < 0.01 % parasitemia and was performed in less than an hour (Lau *et al*., 2011). The high cost and expertise required remain a deterrent for use of PCR in the field.

### 1.3.7 Serodiagnosis

These methods entail the detection of antibodies in serum. Antibodies are usually produced within one week of onset of the red blood cell stage of the infection. At the same time however these antibodies may persist for up to a year after clearance of infection (She *et al*., 2007). This is impractical as it is not clear if antibodies in serum are against a current or past infection, especially in endemic countries where populations may often have persistent low level infections and thus constant levels of antibodies (Makler *et al*., 1998). The assay is based on a direct ELISA format in which ELISA plates are coated with the target malarial antigen, such as merozoite-surface protein in the case of the Newmarket Malaria EIA test (She *et al*., 2007). The reverse of this assay would be to detect the immunogenic antigens of the malaria parasite by raising antibodies against these antigens and using them to capture and detect these antigens.

### 1.3.8 Antigen based diagnosis

Antigen based diagnosis relies on the specificity of antibodies for their target antigen. An antibody is used to capture its target antigen out of solution, followed by a second antibody for detection such as in a double antibody sandwich (DAS) ELISA for example. Alternatively if the target antigen is an enzyme, then the enzyme activity of the target antigen can be measured such as the immunocapture malarial LDH assay described by (Makler *et al*., 1998). ELISA based methods are complex to perform and require some expertise as well as being laboratory based techniques and taking a few hours to perform.

The setting in field hospitals requires diagnostic tests to be "low tech", quick to perform and easy to interpret. Malaria rapid diagnostic tests were thus developed in the 1990's and were designed to allow for "point of care" diagnosis and treatment (Perkins and Bell, 2008).

## 1.4 Immunochromatographic tests or rapid diagnostic tests

### 1.4.1 Basic principle of RDTs

The basic principle of RDTs is outlined in the Figure 1.7.

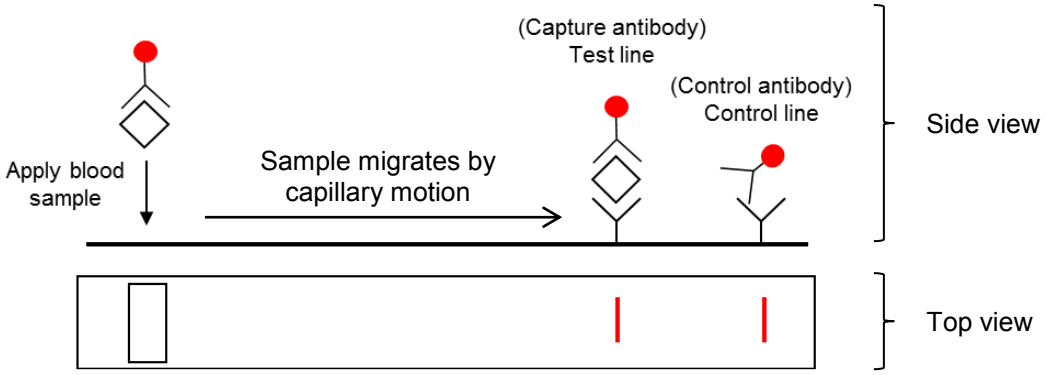


**Figure1.7 Basic outline of a simple rapid diagnostic test (RDT), both top and side view.**

RDTs are antibody based diagnostic tests which exploit the interaction between an antibody and its specific antigen, for the detection of malaria. There are various tests on the market today, and all make use of a colloidal gold labelled detection antibody which is prepared in a lysis buffer and mixed with the test blood sample. If the test sample is infected with malaria, then the detection antibody will bind to its specific malarial antigen. This solution is then added to one end of the test strip (the end on the left in Figure 1.7), and migrates up the strip by capillary action. On the other end of the strip are two bands of capture antibodies which are fixed to the nitrocellulose strip (the end on the right in Figure 1.7). The first capture antibody binds a separate epitope on the same malarial antigen as the detection antibody. As the lysed malaria positive sample migrates up the strip, the antigen-detection-antibody complex is bound by the capture antibody. The colloidal gold particles attached to the detection antibody then form the test line. Any unbound detection antibody migrates further up the strip and is captured by the second antibody (control antibody) fixed to the test strip

and forms a control line. The second line shows that the test sample has moved completely across the strip and that the test is working (Makler *et al*., 1998; Murray *et al*., 2008).

### 1.4.2 Malarial RDT target proteins and examples of commercially available tests

More involved tests have since been developed based on the basic outline in Figure 1.7. These allow differentiation between malaria species, and include up to four line detection. The antigens targeted for diagnosis are histidine rich protein 2 (HRP-2) which is specific to *P. falciparum*. These tests include Paracheck Pf®; ParaHIT *f*® and *Para*Sight-F for example (Murray *et al*., 2008). Two other proteins commonly used include lactate dehydrogenase (LDH) and aldolase, which are both metabolic enzymes conserved among all 5 species of human malaria. Tests targeting LDH alone include OptiMAL® or OptiMAL-IT® tests. Other tests detect HRP-2 as a *P. falciparum* specific target, and detect LDH as a pan-malarial target, such as the CARESTART™ test, or alternatively tests target aldolase such as the BinaxNOW® test for example (Ashley *et al*., 2009; Khairnar, 2009; Murray *et al*., 2008).

### 1.4.3 Problems associated with RDTs

Problems associated with malaria RDTs can be divided into practical problems with their implementation, or problems associated with the diagnostic target antigen used in RDTs.

#### 1.4.3.1 Practical problems associated with the use of RDTs

**False negative test results**

The tropical setting of malaria endemic areas exposes RDTs to temperatures ranging from 35 to 60 ºC (Jorgensen *et al*., 2006). An assay by Chiodini *et al.,* in 2007 showed LDH based tests to be more heat-susceptible than HRP-2 based tests and the biggest concern was that tests showed positive control lines but no test lines, thus giving false negative results. They highlighted the need for a cold chain to supply RDTs to field clinics, which is also required for antimalarial drugs.

**False positive test results**

Buffer vials are often lost in the field and often saline, distilled water or tap water are used instead. This was assessed by Gillet *et al.,* in 2010, who found that RDTs gave false positive reactions in such cases. This could be rectified by supplying multiple buffer vials per kit as opposed to a single vial.

### 1.4.3.2 Problems associated with the diagnostic target antigen

**False negative test results**

The prozone effect, also known as the high dose hook phenomenon causes false negatives or faint positive tests at high parasitemia due to excessive antigen concentrations. The capture antibody fixed to the test strip binds more "free" antigen from solution than antigens bound by the detection antibody, thus resulting in a low signal. This affected HRP-2 based tests and not LDH tests in a study by Gillet *et al.*, in 2009. HRP-2 levels have been quantified to approximately 6:1 in comparison to LDH (Martin *et al.*, 2009), explaining why HRP-2 based tests are prone to this phenomenon. The prozone effect can be avoided by simple dilution of the test sample.

Both gene deletions and antigenic variation (variation in the amino acid composition of the target antigen) have been reported for HRP-2 (Baker *et al*., 2010; Gamboa *et al*., 2010; Lee *et al*., 2006a) and resulted in false negative test results. Sequence analyses of LDH and aldolase from malaria field isolates showed both proteins to be conserved among malaria species (Lee *et al*., 2006b) thus tests targeting these antigens were not affected.

**False positive test results**

False positive results are common in HRP-2 based tests after drug treatment and clearance of infection as HRP-2 persists in serum for between 14 to 28 days (Iqbal *et al*., 2004; Kodisinghe *et al*., 1997; Murray *et al*., 2008; Tjitra *et al*., 2001). LDH and aldolase based tests revert back to negative within 2 to 7 days, as both antigens have shorter half-lives and are involved in parasite metabolism, thus their presence indicate a current infection (Ashley *et al*., 2009; Iqbal *et al*., 2004, Murray *et al*., 2008). All three antigens are produced during the gametocyte stage of the infection thus low levels of the proteins may persist if gametes are present (Murray *et al*., 2008, Tjitra *et al*., 2001).

**Cross-reactivity reactions**

Cross reactivity reactions have been recorded with RDTs and Rheumatoid factor or anti-nuclear antibodies, giving false positive results. Rheumatoid factors are autoantibodies raised against the Fc portion of IgG molecules and react with the mouse IgG isotype monoclonal antibodies often used in RDTs (Iqbal *et al*., 2000). The Fc portion (fragment crystalline) of IgG molecules consists of the carboxyl termini of the heavy chains and is involved in the activation of complement by binding effector molecules or immune cell Fc receptors (Delves *et al*., 2006).

Another issue was cross-reaction of RDTs between malarial species. This has only been recorded for LDH and aldolase based RDTs, since HRP-2 is only expressed by *P. falciparum*. *P. falciparum*-specific as well as *P. vivax*-specific LDH based RDTs cross-reacted and detected *P. knowlesi* (Kawai *et al.*, 2009; McCutchan *et al.*, 2008). Six out of nine *P. vivax*-specific LDH based RDTs also cross-reacted and detected high parasitemia (> 2 %) *P. falciparum* infections (Maltha *et al.*, 2010).

**Quality assurance of malaria RDTs**

To improve confidence in RDTs, quality assurance is very important and has also been recommended by the WHO (WHO, 2008). These measures include buying RDTs from manufacturers with evidence of good manufacturing practice as well as "in the field testing" of RDTs. Positive controls have been developed which make use of recombinant antigens or peptides reconstituted in uninfected blood (Lon *et al*., 2005, Murray *et al*., 2008). Alternatively Versteeg and Mens in 2009 used dried infected blood spots as positive controls, and found this format to work best for HRP-2 based tests due to the stability of the antigen. The purpose of positive controls is not only to give a positive result on the RDT, but also to ensure RDT sensitivity is maintained after delivery to the field (Lon *et al*., 2005; McMorrow *et al.*, 2008).

### 1.4.3.3 Further development and advantages of RDTs

Finding alternatives to blood for diagnosis was investigated by Rodriguez-del Valle *et al.,* in 1991 and Wilson *et al.,* in 2008 who found detectible levels of protein antigens in urine and

saliva samples of infected patients. This may address safety issues surrounding diagnosis using blood samples from patients, as well as avoiding cultural objections to blood collection in some rural populations.

RDTs also serve as diagnostic records for the patients, as isolation of DNA for PCR reactions is also possible (Ishengoma *et al.*, 2011; Veron and Carme, 2006). This would allow for more accurate mapping of disease prevalence, as well as subsequent analyses of resistance markers within a certain malaria area for example, which are invaluable data for controlling malaria (Bisoffi *et al*., 2009).

### 1.4.4 Improving malaria RDTs

Detection of asymptomatic infections is essential for the elimination of malaria. This requires detection of parasite loads of < 100 / µl which may act as reservoirs of malaria (Hafalla *et al*., 2011; Harris *et al.*, 2010; Miller *et al*., 1994). The current malaria RDTs will have to be improved in order to allow for such low detection. This will also allow for earlier detection and treatment of infections which may be lifesaving.

Strategies to improve the limits of detection of RDTs are based on the identification of new antigenic targets that are present at higher concentrations than the current targets. This would allow RDTs to detect infections at lower parasite loads.

#### 1.4.4.1 GAPDH as an alternative RDT target antigen to LDH

According to transcriptional data from Le Roch *et al*., (2003) *P. falciparum* GAPDH (*Pf*GAPDH) messenger RNA (mRNA) levels are around 3 to 4 times higher than *P. falciparum* LDH (*Pf*LDH) levels (Figure 1.8). This is suggestive of higher protein levels of *Pf*GAPDH to *Pf*LDH since proteins are usually translated immediately from mRNA in the parasite (Bozdech *et al*., 2003).

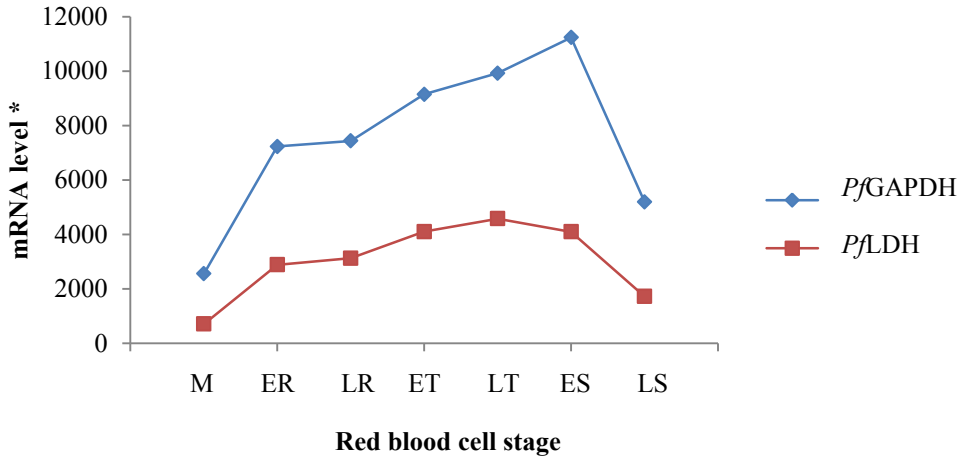


**Figure 1.8 Comparative mRNA levels of glyceraldehyde-3-phosphate dehydrogenase (*Pf*GAPDH) and lactate dehydrogenase (*Pf*LDH).**
The mRNA levels of *Pf*GAPDH and *Pf*LDH were plotted for the different red blood cell stages of *P. falciparum* 3D7 parasites. The data was taken from Le Roch *et al.*, (2003). The red blood cell stages were annotated as follows: M (merozoite); ER (early ring); LR (late ring); ET (early trophozoite); LT (late trophozoite); ES (early schizont); LS (late schizont). * The mRNA levels were assigned arbitrary units.

There are only semi-quantitative data available on the relative protein levels of *Pf*GAPDH and *Pf*LDH. These data suggest increasing protein levels during the development of the erythrocytic stage, similar to the increasing mRNA levels (Aebersold and Mann, 2003; Lasonder *et al.*, 2002; Nirmalan *et al.*, 2004; Smit *et al.*, 2009).

Targeting metabolic proteins for diagnosis has the advantage, at least in theory, of allowing the RDTs to monitor the treatment of infection. This was shown with RDTs using LDH as the target antigen, where they returned to negative within 2 to 7 days after clearance of infection (Iqbal *et al.*, 2004, Murray *et al.*, 2008).

GAPDH is similar to LDH in that both proteins are dehydrogenase enzymes involved in glycolysis (Berwal *et al.*, 2008; Daubenberger *et al.*, 2000; Satchell *et al.*, 2005). Structurally both proteins form tetramers in solution, where the size of the native *Pf*LDH monomer is approximately 34.4 kD and that of the *Pf*GAPDH monomer is approximately 36 kD (Berwal *et al.*, 2008; Daubenberger *et al.*, 2000; PlsamoDB; Satchell *et al.*, 2005). Both proteins bind $NAD^{+}(H)$ N-terminally thus sharing a common dinucleotide binding domain known as a Rossman fold for this purpose (Akinyi *et al.*, 2008; Daubenberger *et al.*, 2000; Granchi *et al.*, 2010). The catalytic sites are located C-terminally in both proteins, where they bind their

respective substrates (Granchi *et al*., 2010; Daubenberger *et al*., 2000; Akinyi *et al*., 2008). The reactions catalysed by each enzyme are shown in Figure 1.9.

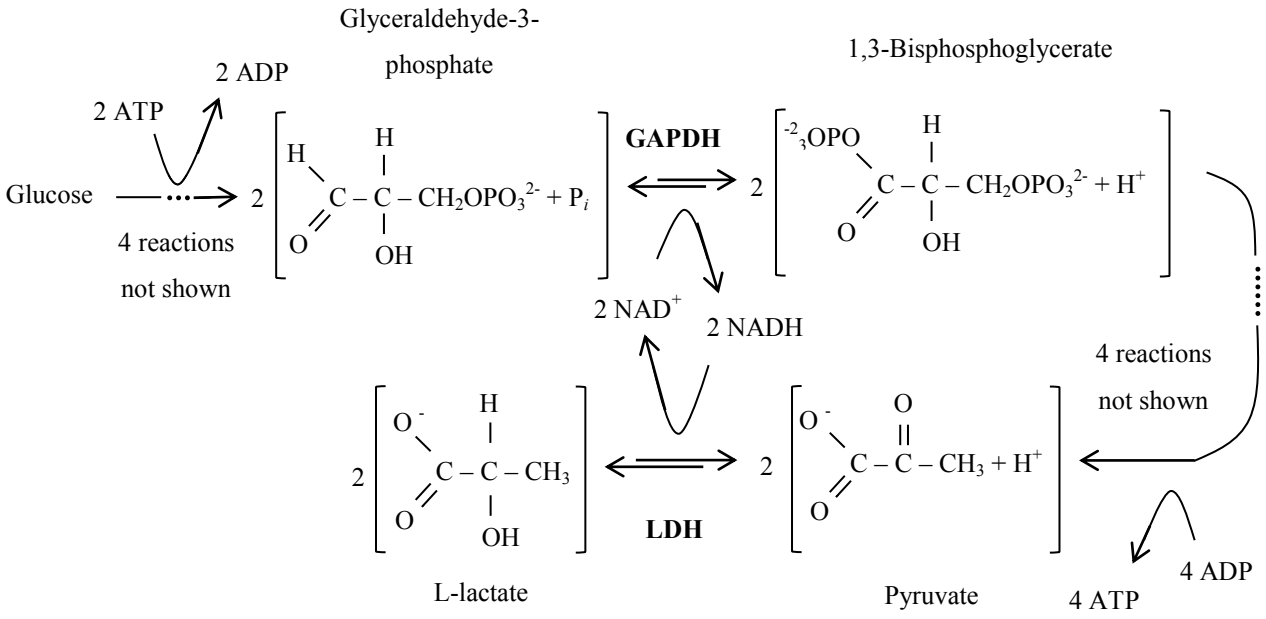


**Figure 1.9 Basic glycolytic reactions involving GAPDH and LDH, producing 2 ATP molecules and recycling $NAD^+(H)$.**

The figure was prepared according to the description of glycolysis by Voet and Voet, 2004. Glucose is a 6–carbon sugar, thus its catalysis results in 2 of each of the 3–carbon moieties shown in the figure.

The parasite relies primarily on glycolysis for energy production (Daubenberger *et al*., 2000; Granchi *et al*., 2010; Olszewski *et al*., 2011; Satchell *et al*., 2005), where the rate of glycolysis in an infected red blood cell is between 50 to 100 times greater than that of an uninfected cell (Daubenberger *et al*., 2000; Gomez *et al*., 1997; Olszewski *et al*., 2011). Glycolysis entails the breakdown of glucose (6 carbon sugar) into two molecules of pyruvate (3- carbon moiety), which is then converted to two L-lactate molecules by LDH in an anaerobic homolactic fermentation pathway in the malaria parasite (Berwal *et al*., 2008; Daubenberger *et al*., 2000; Granchi *et al*., 2010). This pathway requires two ATP molecules (energy investment) to generate 4 molecules of ATP, thus yielding two ATP molecules per glucose molecule. GAPDH reduces $NAD^+$ to NADH and LDH then oxidises NADH to $NAD^+$ allowing GAPDH to catalyse further reactions. This is important as the $NADH/NAD^+$ ratio is maintained within the cell.

Both GAPDH and LDH have been assessed as drug targets, where both are inhibited by ferriprotoporphyrin (unpolymerised haeme) as mentioned earlier in the introduction (Campanale *et al.*, 2003; Egan and Ncokazi, 2005; Penna-Coutinho *et al.*, 2011).

GAPDH has been shown to be involved in alternate roles besides glycolysis. Daubenberger *et al.,* (2003) showed the N-terminal domain of *Pf*GAPDH to be involved in membrane recruitment by binding Rab2. This suggested that *Pf*GAPDH may be involved in vesicle transport within the parasite, by interacting with Rab2, tubulin and actin (Tristan *et al*., 2010). Alternative functions of mammalian GAPDH also include association with mitochondria during stressed cellular conditions, thereby mediating cell death. Alternatively GAPDH has also been located in the nucleus where it is involved in DNA repair or transcription as well as telomere protection and cell cycle regulation and cell death (Tristan *et al*., 2010). These alternate roles may explain the higher mRNA levels of *Pf*GAPDH in comparison to *Pf*LDH (Le Roch *et al*., 2003).

*Pf*GAPDH shares 63.5 % sequence identity with its human red blood cell counterpart (Daubenberger *et al*., 2003). One of the major differences between human and *Plasmodial* GAPDH is the presence of a two amino acid (K194; G195) insert within a structural region called the S-loop (residue 188 to 203) in the *Plasmodial* protein (Satchell *et al*., 2005). The S-loop separates the Rossman folds of the adjacent subunits in the tetrameric form of the enzyme (Akinyi *et al*., 2008). Another difference is a substitution of two amino acids (L187; V188 for K187; T188) in the same region of the *Plasmodial* protein. These changes are thought to be responsible for the ferriprotoporphyrin susceptibility of the *Plasmodial* protein (Akinyi *et al*., 2008; Satchell *et al*., 2005).

## 1.5 Aims and objectives of the current study

A wide range of diagnostic methods can be used to diagnose malaria, each with their individual advantages and disadvantages. An ideal RDT should be easy to perform and interpret and have adequate sensitivity and specificity to allow for rapid and correct treatment of patients that present with malaria-like symptoms (Makler *et al*., 1998; Moody, 2002; Murray *et al*., 2008).

One of the methods of addressing sensitivity of RDTs is by identifying protein targets which are more abundant than the present targets. This would lower the limit of detection of the test and in so doing should increase the sensitivity. Thus the first aim was to identify a new diagnostic target, using transcriptional data from Le Roch *et al*., (2003) as a starting point (Figure 1.8). GAPDH was identified as a possible new target.

Another issue with RDTs is cross reactivity with Rheumatoid factor and anti-nuclear antibodies as a result of cross reaction with Fc portions of mammalian IgG (Gillet *et al*., 2009; Iqbal *et al*., 2000). The second aim was to use polyclonal antibodies raised in chickens (IgY), which lack an Fc portion and thus should not cross react with these factors (Schade *et al*., 1991, 1993). Since monoclonal antibodies are preferred for RDTs due to their high specificity, the polyclonal IgY antibodies raised here were raised against specific peptide epitopes to improve their specificity. An alternative adjuvant called Pheroids$^{TM}$ was also assessed in comparison to Freund's adjuvant, with an aim to improve IgY yields, or to reduce stress on the experimental animals as Freund's is known to cause hypersensitivity reactions (Wilson-Welder *et al.*, 2009; Reed *et al.*, 2008).

The objectives of the current study were therefore to:

- Recombinantly express and affinity purify both *Pf*GAPDH and *Pf*LDH (Chapter 3).
- Identify specific immunogenic peptide epitopes on the surface of both *Pf*GAPDH and *Pf*LDH and to raise and affinity purify polyclonal IgY antibodies against both the whole recombinant proteins as well as the selected peptides and measure final yields for comparison of adjuvants (Chapter 4).
- To compare the levels of the current RDT target *Pf*LDH to that of *Pf*GAPDH within parasite lysate samples (Chapter 5).

# Chapter 2
# Materials and Methods

This chapter describes the molecular, biochemical, immunochemical and bioinformatics methods used in this study.

## 2.1 Materials

### 2.1.1 Equipment

Poly Prep® affinity column, Mini Protean II™ vertical PAGE unit and the VersaDoc™ imaging system were purchased from BioRad (California, USA). Orbital shaking incubator was purchased from New Brunswick Scientific (New Jersey, USA). Ultraspec 2100pro UV/visible spectrophotometer was purchased from GE Healthcare (Buckinghamshire, England). VersaMax™ ELISA plate reader was purchased from Molecular Devices Corporation (California, USA). Avanti™ J-26 XPI centrifuge was from Beckman Coulter (California, USA). GeneAmp™ PCR thermocyler was from Applied Biosystems (California, USA). BIOER Lifepro thermal cycler was purchased from United Scientific (Pty) Ltd. (Johannesburg, RSA). Virosonic™ cell disruptor was purchased from VirTis (New York, USA). Edwards One Stage 5 A.C. pump from GEC. Machines Ltd. (Newcastle, UK). Micro Tube Peristaltic pump MP-3 from EYELA Tokyo Rikakikai co. Ltd. (Tokyo, Japan).

### 2.1.2 Reagents

Ethidium bromide (EtBr), β-mercarptoethanol, 4-chloro-1-naphthol, acrylamide, ampicillin, Biomax® X-ray film, bisacrylamide, bromophenol blue, Coomassie Brilliant Blue G-250, Coomassie Brilliant Blue R-250, Ellman's Reagent, formamide, Freund's complete adjuvant (FCA), Freund's incomplete adjuvant (FIA), glycine, isopropyl thioglucopyranoside (IPTG), L-cysteine, kanamycin, maleimidobenzoyl-N-hydroxysuccinimide ester (MBS), ovalbumin, p-iodophenol, luminol, ponceau S, rabbit albumin (RA), saponin, Sephadex G-25, Sephadex G-10, Sephacryl S200, N,N,N',N'-tetramethylethylenediamine (TEMED), Triton X-100, tryptone, Tween-20, and yeast extract were purchased from Sigma-Aldrich-Fluka (Steinheim, Germany). Bovine serum albumin (BSA) was purchased from Roche (Mannheim, Germany). The following were purchased from Fermentas (Vilinius, Lithuania): agarose, DNA MassRuler™, 10mM dNTP mix, EcoR1, Pst1, Nde1, Xho 1, molecular biology grade DTT,

Buffer O™ and an unstained protein molecular weight marker, containing: 116 kD β-galactosidase; 66.2 kD bovine serum albumin; 45 kD ovalbumin; 35 kD lactate dehydrogenase; 25 kD REase Bsp981; 18.4 kD β-lactoglobulin and 14.4 kD lysozyme. Molecular biology reagents were purchased from Solis Biodyne (Tartu, Estonia), which included the 10× PCR buffer ($MgCl_2$ and detergent-free), PCR $MgCl_2$ stock solution (25mM) and Taq polymerase. The *Escherichia coli* host cells, plasmids and antibodies purchased from Novagen (Damstadt, Germany) were: BL21(DE3) (glycerol stock), pET-23a and pET-28a plasmids; mouse monoclonal anti-His-Tag IgG and peroxidase conjugated sheep monoclonal anti mouse IgG. Polyethylene glycol 6000 (PEG 6000) was purchased from Merck Biosciences (Damstadt, Germany). 2,2'-azino-bis(3-ethybenzothiazolinesulfonate) (ABTS) was purchased from Boehringer (Mannheim, Germany). SulfoLink™ and AminoLink™ coupling gels and Snake skin™ dialysis membrane were purchased from Pierce Perbio Science (Erembodegem, Belgium). Hybond-C™ Extra nitrocellulose membrane purchased from GE Healthcare (Buckinghamshire, England). Peroxidase-conjugated rabbit anti-IgY, peroxidase-conjugated rabbit ant-mouse IgG antibodies were from Jackson Immunochemicals (Pennsylvania, USA). TALON® cobalt metal affinity resin was from Clontech Laboratories Inc. (California, USA). Synthetic peptides for lactate dehydrogenase and glyceraldehyde-3-phosphate dehydrogenase proteins were synthesized by GL Biochem (Shanghai, China). Nunc Maxi Sorp™ 96-well ELISA plates were from Nunc products (Roskilde, Denmark). DNA purification kit was purchased from PEQLAB Biotechnologie (Erlangen, Germany).

## 2.2 Molecular biology methods

These methods include expression and purification of the recombinant proteins used in this study. Both expression vectors were provided and the plasmid vectors and expression hosts are described first.

### 2.2.1 Expression vectors/plasmids and *E. coli* hosts

*Escherichia coli* BL21(DE3) was used as the expression host, where the plasmids used were as follows: For recombinant *Plasmodium falciparum* lactate dehydrogenase (r*Pf*LDH) a pKK223-3 plasmid vector was used, whereas a pET-15(b) plasmid expression vector was

used for recombinant *P. falciparum* glyceraldehyde-3-phosphate dehydrogenase (r*Pf*GAPDH). The plasmid vectors were shown in the Figures 2.1 and 2.2.

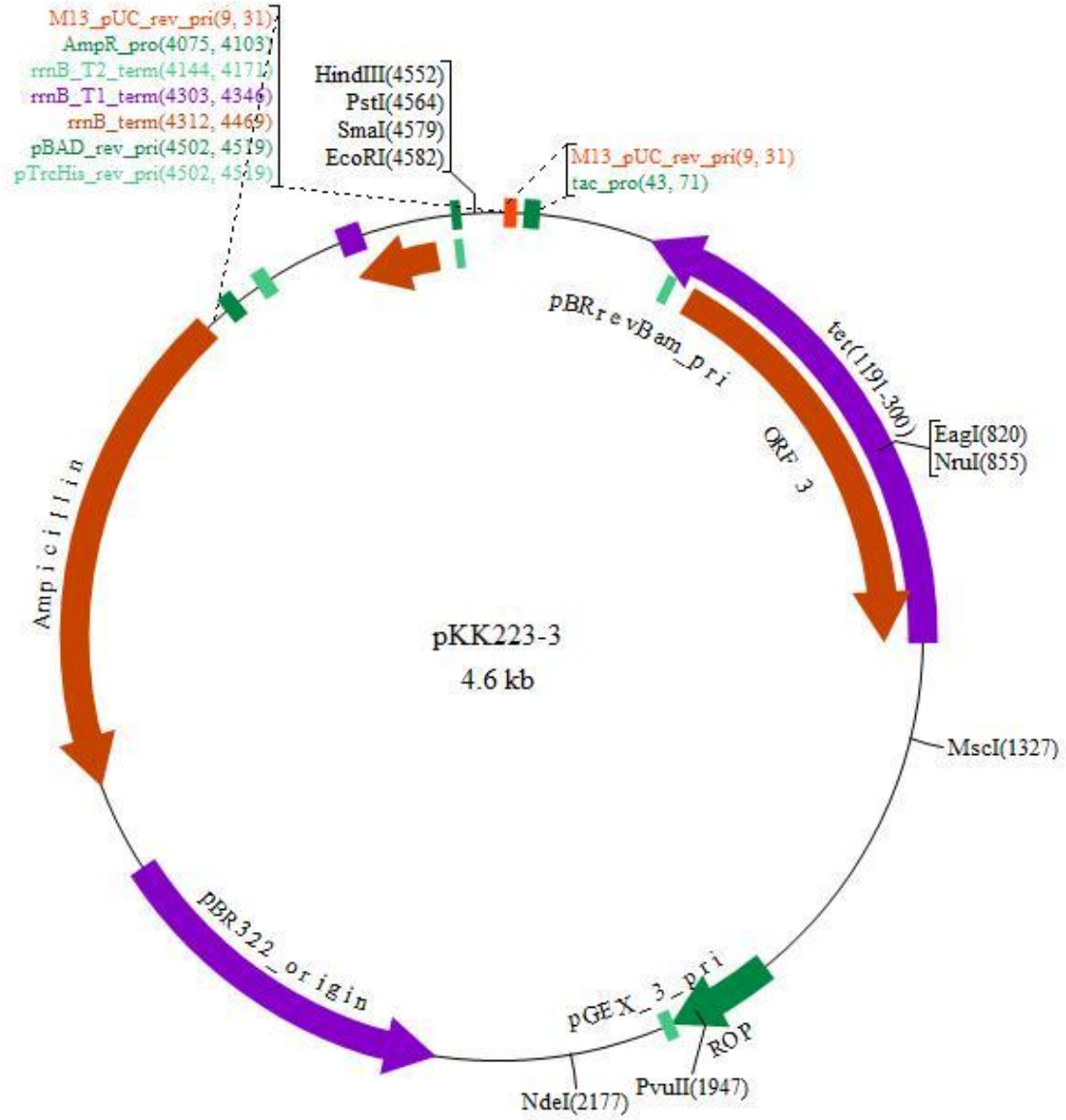


**Figure 2.1 r*Pf*LDH expression plasmid vector map (pKK223-3 vector).**
The vector map depicts the restriction sites available for inserting the desired coding sequence. The *Pf*LDH sequence was inserted between the *Pst*I and *Eco*RI restriction sites. The vector codes for Ampicillin resistance, which is used as the selective maker for transformed cells. The size of the plasmid without insert was 4.6 kb as shown in the centre of the map.

The *Pf*LDH sequence was inserted between the *Eco*RI (base 4582) and *Pst*I (base 4564) sites in the pKK223-3 plasmid shown in Figure 2.1, where the size of the plasmid without an insert was 4.6 kb. The *Pf*GAPDH sequence was inserted between the *Xho*I (base 324) and *Nde*I (331) sites in the pET-15(b) vector shown in Figure 2.2, which was 5.7 kb in size without an insert.

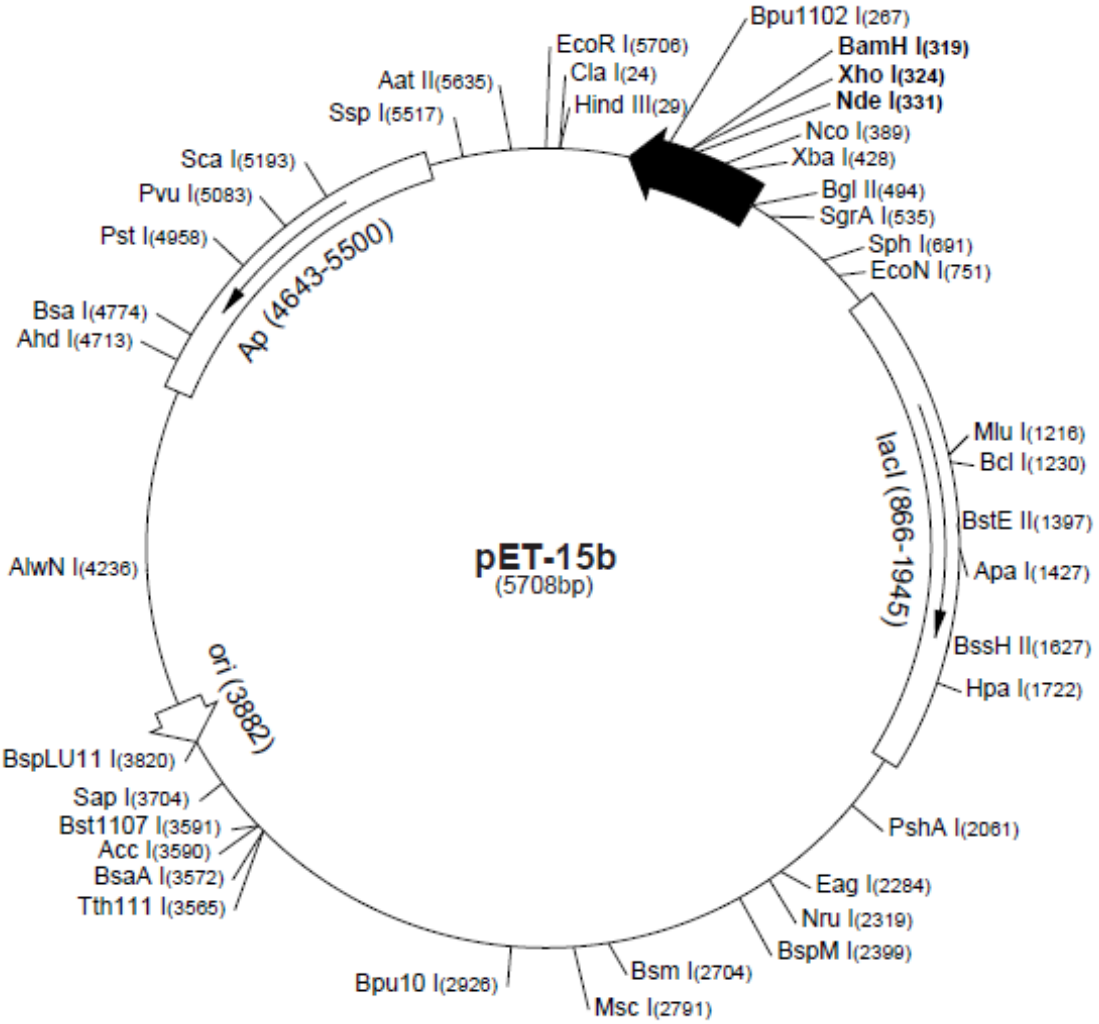


**Figure 2.2 pET-15(b) expression plasmid vector map.**
The vector map depicts the restriction sites available for inserting the desired coding sequence. The *Pf*GAPDH sequence was inserted between the *Xho*I and *Nde*I restriction sites. The vector codes for Ampicillin resistance, which is used as the selective maker for transformed cells. The size of the plasmid without an insert was given as 5.7 kb as shown in the centre of the map.

### 2.2.2 Vector verification

This includes several molecular techniques which were performed on overnight (16 hour) culture samples of the respective *E. coli* BL21(DE3) transformed hosts. The overnight cultures were inoculated with single colonies picked from LB agar plates supplemented with ampicillin.

#### 2.2.2.1 Agarose gel electrophoresis

For 1 % (w/v) agarose gels with dimensions of 7 x 6.5 cm gels 0.3 g agarose was dissolved in 30 ml TAE buffer (2M Tris; 50 mM EDTA; 0.95 M glacial acetic acid, pH 8.0) and heated in a microwave until the agarose had completely melted. Once the agarose solution cooled sufficiently, ethidium bromide (1 % (w/v) ethidium bromide in TAE buffer) was added to a final concentration of around 0.7 µg/ml, and the solution was poured into the gel casting tray and allowed to solidify at RT. Samples were prepared by diluting 5:1 in Fermentas sample loading buffer (0.25 % (w/v) bromophenol blue and 40 % (w/v) sucrose in TAE buffer). Gels were visualised under UV light and images captured using a VersaDoc$^{TM}$ gel imaging system. Sizes of bands in base pairs (bp) were extrapolated from a graph of relative distance travelled from the well to log of the band size in bp of DNA standards run on the same gel.

#### 2.2.2.2 Plasmid isolation

The 10 ml overnight (16 hour) culture grown at 37 ºC was centrifuged (1210 x *g*, 4 ºC, 5 min) and the supernatant discarded. The pellet was suspended in 200 µl GTE solution (25 mM Tris; 1 mM EDTA; 50 mM glucose at pH 8.0) and left at room temperature (RT) for 5 min and transferred to a microfuge tube, to which 2 µl RNase A (10 mg/ml in 10 mM Tris; 1 mM EDTA at pH 8.0) and 400 µl NaOH/SDS solution (200 mM NaOH; 35 mM SDS) was added and left on ice for 5 min to allow cell lysis. Thereafter 300 µl potassium acetate (3 M potassium acetate at pH 4.8, titrated with glacial acetic acid) was added and mixed thoroughly and placed on ice for 5 min. At this stage a coarse white precipitate of cell debris and chromosomal DNA formed, after which the sample was centrifuged (17530 x *g*, RT, 5 min) and 800 µl of the supernatant was transferred to a fresh tube. Six hundred microliters isopropanol was added and mixed thoroughly, and the sample was left on ice for 30 min, after which it was centrifuged (17530 x *g*, RT, 5 min) to pellet the plasmid DNA. The pellet was then washed with ice cold 70% (v/v) ethanol and centrifuged (17530 x *g*, RT, 5 min), with the final plasmid pellet suspended in 50 µl TE buffer (10 mM Tris; 1 mM EDTA at pH 8.0) and run on a 1% agarose gel to check purity.

### 2.2.2.3 Restriction digest

Restriction digests were performed on plasmid DNA isolated as mentioned in 2.2.2.2.

For single restriction the isolated plasmid DNA was digested at 37 ºC for 2 hours by preparing the following reaction mixture: 10 µl isolated plasmid DNA; 0.5 µl restriction endonuclease (5 units); 2 µl 10 x digestion buffer and the solution was made up to 20 µl with MiliQ $dH_2O$. For double digests a suitable digestion buffer was chosen and the amount of each restriction endonuclease added was adjusted based on its activity within the chosen buffer (Fermentas restriction endonuclease buffers), and the digest time was left as 2 hours at 37 ºC. For the *P. falciparum* LDH vector (pKK223-3) a double digest using *Eco*RI and *Pst*I was performed to drop out the insert. In the case of the *P. falciparum* GAPDH vector (pET-15(b)) a double digest using *Nde*I and *Xho*I was attempted.

### 2.2.2.4 Polymerase Chain Reaction

Colony polymerase chain reaction (PCR) was performed to verify the presence of the insert within the expression host.

Single colonies were used to inoculate 5 ml LB media and cultured overnight (16 hours) at 37 °C. After centrifugation (1210 x *g*, RT, 5 min) the supernatant was discarded and the pellet suspended in 500 µl MiliQ $dH_2O$. Two microliters of this suspension was then removed and diluted further in 50 µl MiliQ $dH_2O$. After boiling for 5 min, the samples were centrifuged (17530 x *g*, RT, 10 min), and 3 µl of the supernatant was transferred to a PCR tube and used as the template in the PCR reaction. The reaction mixture was completed by addition of the following: 1 µl forward and reverse primers; 0.25 µl Taq polymerase (5 units / µl); 2 µl $MgCl_2$ (25 mM); 0.8 µl dNTPs; 2 µl 10 x PCR buffer ($MgCl_2$ free) and made up to 20 µl with MiliQ $dH_2O$. The reaction conditions were represented in Figure 2.4 below and a total of 30 cycles were run per reaction.

The specific annealing temperature of the primers used differed per reaction, and were optimised using gradient PCR if required. The primers were listed in Table 2.1, with the respective annealing temperatures used.

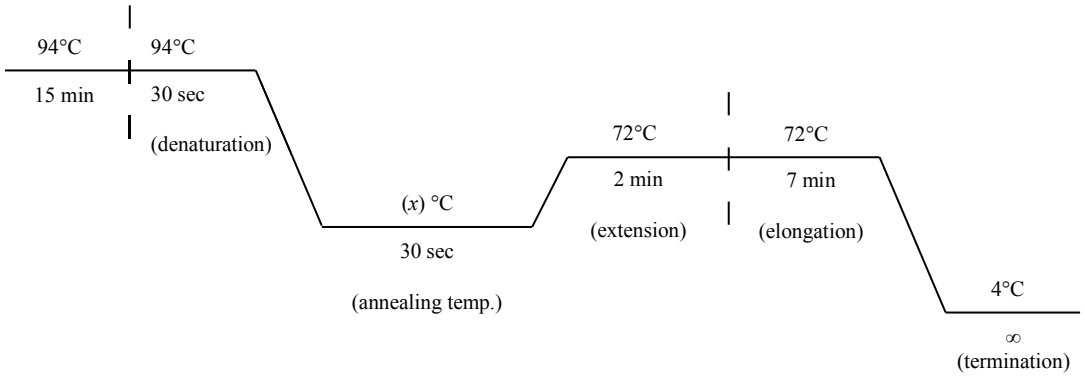


**Figure 2.3 PCR cycle conditions.**
The conditions were standard for all PCR reactions performed, except in the case of the annealing temperature "*x*" of the specific primers used, which were optimised if required.

**Table 2.1 Primer sequences and annealing temperatures.**

| Primer | Sequence | Annealing temp. (ºC) |
|---|---|---|
| T7 promoter primer #69348-3 | TAATACGACTCACTATAGGG | 55 |
| T7 terminator primer #69337-3 | GCTAGTTATTGCTCAGCGG | 55 |
| pLDH forward control primer | GGATCTGGTATGATTGGAGGTGTTATGGCC | 65 |
| pLDH reverse control primer | TTCGATTACTTGTTCTACACCATTACCACC | 65 |

### 2.2.2.5 Sequencing

Plasmid DNA was isolated as described in 2.2.2.2 and sent for sequencing to Central Analytical Facilities at Stellenbosch University. The *Pf*LDH sequencing was done using the pLDH primers from Table 2.1, whereas T7 promoter and terminator specific primers were supplied by Central Analytical Facilities at Stellenbosch University for the *Pf*GAPDH reactions. Consensus sequences were then identified using the forward and reverse sequences, and analysed by alignment using clustalW to assess their sequence identity with the corresponding coding sequences found in PlasmoDB.

### 2.2.3 Expression

Glycerol stocks (overnight culture pellets (centrifuged 4000 x *g*, 4 ºC, 10 min) suspended in 850 µl PBS (137 mM NaCl; 3 mM KCl; 7 mM $Na_2HPO_4$; 1.5 mM $KH_2PO_4$ at pH 7.2) 150 µl glycerol (50 % (v/v))) of the respective expression vectors were 3-way streaked onto LB agar (1 % (w/v) tryptone; 0.5 % (w/v) yeast extract; 85 mM NaCl; 11 mM glucose; 1.5 % (w/v) bacto-agar prepared in $dH_2O$ and autoclaved) plates and incubated overnight (16 hours) at 37

ºC. Single colonies were picked to inoculate 10 ml LB broth (1 % (w/v) tryptone; 0.5 % (w/v) yeast extract; 85 mM NaCl; 11 mM glucose; 1.5 % (w/v) prepared in $dH_2O$ and autoclaved) and incubated overnight at 37 ºC. These cultures were then used to inoculate large LB broth preparations (expression culture) using 1/100 dilutions of the overnight cultures. All LB broth and agar was supplemented with ampicillin (50 mg/ml stock prepared in $dH_2O$ and filter sterilised) to a final concentration of 50 µg/ml, and the expression cultures were re-supplemented with ampicillin every 2 hours to maintain selective pressure for transformed *E. coli* hosts. The expression cultures were monitored until absorbance values at 600 nm ($A_{600}$) of between 0.5-0.6 were reached (exponential growth phase of cultures), upon which expression was induced for 4 hours by supplementing with IPTG (0.1 M in $dH_2O$ and filter sterilised) to a final concentration of 0.3 mM. Cultures were then centrifuged (4000 x *g*, 4 ºC, 10 min) and suspended in 5 % of their original volume in resuspension buffer (50 mM $NaH_2PO_4$; 300 mM NaCl at pH 7.0 or pH 8.0) after which they were further processed for affinity purification of recombinant proteins or stored at -20 ºC until further use.

### 2.2.4 Affinity purification

Following vector verification, the recombinant proteins were expressed and passed over a TALON ($Co^{2+}$) affinity matrix, allowing the $His_6$-tagged recombinant proteins to be purified as described below.

The pelleted culture samples prepared as in 2.2.3 were suspended to 5 % of their original culture volume in wash buffer and lysed using 4 x 30 sec sonication steps (0.6-0.8 Watts). Samples were then centrifuged (12000 x *g*, 4 ºC, 20 min) and 10 ml of the supernatant was incubated for 20 min with 1 ml of a packed TALON ($Co^{2+}$) affinity resin (i.e. 2 ml of 50 % slurry). The resin was equilibrated earlier by washing twice with 10 ml wash buffer (50 mM $NaH_2PO_4$; 300 mM NaCl; 10 mM Imidazole; 0.02 % (w/v) $NaN_3$ at pH 7.0 or 8.0), with a 5 min centrifugation step at 1210 x *g* after each wash and removal of the supernatant buffer. After the incubation with the sample, the resin was washed twice with wash buffer as described above. The resin was then transferred to a column and the bound recombinant protein was eluted using 5 ml elution buffer (same as wash buffer except for the addition of 250 mM Imidazole as opposed to 10 mM). Eluants were analysed by measuring $A_{280}$ values, and protein concentration was determined by Bradford method as described in 2.3.1. The resin was regenerated by washing with 10 ml MES buffer (20 mM MES at pH 5.0) for 20

min, followed by a 10 ml wash with $dH_2O$ and storage at 4 ºC in storage buffer (20 % (v/v) ethanol; 0.1 % (w/v) $NaN_3$ prepared in $dH_2O$).

## 2.3 Biochemical techniques

This section outlines the different biochemical techniques used to examine both the recombinant and native *Plasmodium* proteins.

### 2.3.1 Bradford

This method was performed according to (Bradford, 1976). In order to obtain a standard curve, the 1mg/ml bovine serum albumin (BSA) stock solution was used to prepare BSA standards (0-50 µg) in triplicate. These were made up to 100 µl with $dH_2O$ after which 900 µl Bradford dye (0.12 % (w/v) Coomassie brilliant blue G-250 dissolved in 500 ml of a 2 % (v/v) perchloric acid solution) was added to each sample and vortexed. Samples were left to stand for 15 min after which their absorbance at 595 nm ($A_{595}$) was read and plotted against BSA concentration. Unknown samples were prepared in the same way as the standard samples in that an appropriate dilution of the unknown was prepared which allowed the concentration to be extrapolated from the standard curve shown in Figure 2.4.

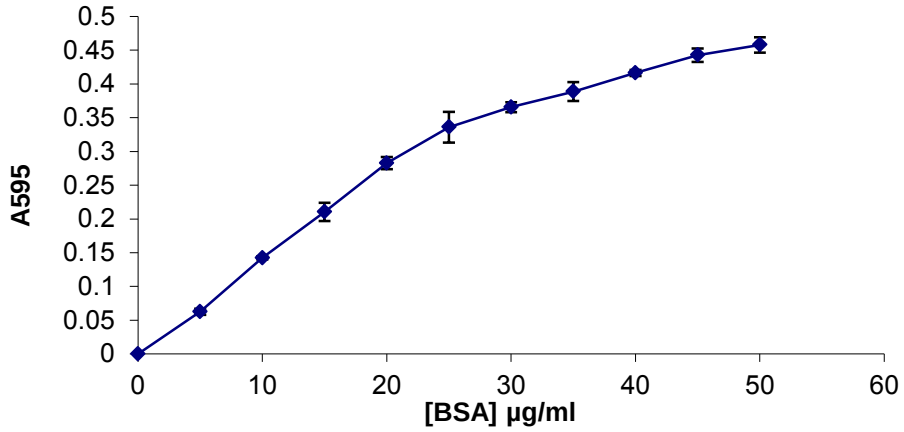


**Figure 2.4 Bradford standard curve.**
All values are average values of triplicate readings with standard deviations shown.

### 2.3.2 Sodium dodecyl sulphate polyacrylamide gel electrophoresis

Discontinuous SDS-PAGE as described by (Laemmli, 1970) was used to assess protein size and purity and was performed as follows.

Gels were prepared according to Table 2.2. The buffers were named A through E for simplicity of the table and were as follows: A (4.1 M acrylamide and 52 mM N,N'-methylenebisacrylamide); B (1.5 M Tris buffer at pH 8.8); C (495 mM Tris buffer at pH 6.8); D (1 % (w/v) SDS solution in $dH_2O$) and E (10 % (w/v) ammonium persulfate solution in $dH_2O$). Gels were set using a Bio-Rad Mini PROTEAN II® vertical slab apparatus, consisting of 4 glass plates (two with dimensions of 81.5 mm x 101.5 mm and two 72.5 mm x 101.5 mm); two 10 or 15 well combs; four spacer plates and a gel-casting stand with casting gaskets and plate cassettes. The gel-casting unit was assembled according to manufacturer's instructions after cleaning plates with detergent and rinsing under $dH_2O$, giving final gels of approximately 1.5 mm width.

**Table 2.2 Running and stacking gel recipes for SDS-PAGE.**

| | **12.5 % Running gel** | **4 % Stacking gel** |
|---|---|---|
| **A** | 6.25ml | 940 µl |
| **B** | 3.75ml | 0 |
| **C** | 0 | 1.75ml |
| **D** | 150µl | 70 µl |
| **E** | 75 µl | 35 µl |
| **$dH_2O$** | 4.75ml | 4.3ml |
| **TEMED** | 7.5 µl | 15 µl |

After addition of TEMED, the un-polymerised running gel solution was mixed and 6.6 ml of this was poured into the gel cassette between the glass plates and overlaid with 200 µl $dH_2O$. This allows the gels to set properly, as oxidation would otherwise inhibit gel polymerisation. Once set, the water was decanted and the freshly prepared stacking gel solution was overlaid to the top of the glass plates. The 10 or 15 well comb was then inserted immediately and the stacking gel was allowed to set. Samples to be run on the gel were prepared as follows: samples were diluted 1:1 in 50 % (v/v) sample buffer for non-reducing gels (2.5 ml solution C; 2 ml glycerol; 4 ml solution D; with few grains of bromophenol blue to colour the buffer). For reducing gels β-mercaptoethanol was added 1:10 to the sample buffer before mixing with the samples. After loading the samples the gels were run at 20 mA per gel in tank buffer (25

mM Tris; 192 mM glycine and 1 % (v/v) solution D) until the dye front had migrated to within 0.5 to 1 cm from the bottom of the gel. The gels were then removed immediately and stained with Coomassie stain (45 % (v/v) methanol; 10 % (v/v) acetic acid; 0.25 % (w/v) Coomassie brilliant blue R-250) and destained with several changes of destain I (50 % (v/v) methanol and 10 % (v/v) acetic acid) and left in destain II (5 % (v/v) methanol and 7 % (v/v) acetic acid) until the gels had swollen back to their original size. The sizes of protein bands were determined by extrapolation from a graph of log molecular weight of molecular weight standards run on the same gel, against their relative mobility (Rf values).

### 2.3.3 Sliver staining

Glassware used for staining was meticulously cleaned with detergent and then rinsed with fixing solution (50 % (v/v) methanol; 12 % (v/v) acetic acid and 0.5 % (v/v) formaldehyde) and allowed to dry. SDS-PAGE gels were transferred to glass petri dishes and fixed for 1 hour or overnight (16 hours). All incubations and washes were performed on a rocker. The gels were washed 3 times with wash solution (50 % (v/v) ethanol) after fixing, and then left in pre-treatment solution (4 mg/ml $Na_2S_2O_3.5H_2O$) for 1 min and 15 sec. Gels were then washed 3 times with $dH_2O$, 20 sec per wash and then left in impregnation solution (0.2 % (v/v) $AgNO_3$; 0.3 % (v/v) formaldehyde prepared just before use) for 20 min. Gels were washed 3 times with $dH_2O$, 20 sec per wash and then incubated with developing solution (566 mM $Na_2CO_3$; 0.2 % (v/v) formaldehyde; 2 % (v/v) pretreatment solution) until first bands appeared. The developing solution was then replaced with $dH_2O$ and bands were allowed to develop until the intensity was satisfactory, at which time the gels were incubated in stop solution (50 % (v/v) methanol; 12 % (v/v) acetic acid) for 10 min, and stored in 50% (v/v) methanol.

### 2.3.4 Molecular Exclusion Chromatography

Sephacryl S200 resin was packed using $dH_2O$ to a final column volume of approximately 309 ml. This was done using a peristaltic pump at half to maximum flow rate. Once packed the column was washed using half the column volume cleaning buffer (0.2 M NaOH). The MEC buffer (50 mM $NaH_2PO_4$; 150 mM NaCl at pH 8.0) was always degassed for 45 min at 4 °C prior to use, using an Edwards One Stage 5 A.C. pump, and all further working solutions were cooled to 4 °C prior to use. The column was then equilibrated with twice the column volume

MEC buffer at a set flow rate of 1 ml/min. For calibration of the column, the molecular weight standards were prepared to a final volume of 3 ml as follows: 6 mg blue dextran (2000 kD), and 15 mg each of sheep IgG (150 kD), bovine serum albumin (68 kD), ovalbumin (45 kD), and myoglobin (18.8 kD). The parameters for running the column were set to a flow rate of 1 ml/min and collection of 4 ml eluents. The absorbance at 280 nm ($A_{280}$) was read for each eluent fraction, to give a calibration curve of $A_{280}$ plotted against elution volume (ml). After calibration the r*Pf*LDH (5.6 mg) and r*Pf*RDP (3.8 mg) samples were prepared to a final volume of 4 ml and run over the column using the same parameters.

## 2.4 Bioinformatics

This section describes the *in silico* work done in identifying peptide epitopes for each of the target proteins, *Pf*LDH and *Pf*GAPDH.

### 2.4.1 Sequence alignments

Alignments DNA coding sequences as well as primary protein amino acid sequences were done using clustalW2 (www.ebi.ac.uk/Tools/msa/clustalw2/). The sequences were obtained either from NCBI (www.ncbi.org/) or PlasmoDB (www.plasmodb.org/) as indicated in text.

### 2.4.2 3D modelling

3D protein models were downloaded from the Swiss model repository (http://swissmodel.expasy.org/repository/) and manipulated with Deep view Swiss pdb viewer downloaded from (http://www.expasy.org/spdbv/).

### 2.4.3 Predict7™

Predict 7™ was used for analysis of protein primary amino acid sequences in order to identify immunogenic peptides on the surface of the target proteins *Pf*LDH and *Pf*GAPDH, which were used to raise antibodies in chickens. Graphs were generated, plotting peptide hydrofilicity, surface probability, antigenicity and flexibility of the peptide sequences.

## 2.5 Immunochemical techniques

The methods included in this section centre around the production and use of antibodies, in particular chicken antibodies (IgY).

### 2.5.1 Western blot

This method follows on from the SDS-PAGE method described in 2.3.2. After running protein samples on an SDS-PAGE gel, the proteins were transferred onto a nitrocellulose membrane. This was done by sandwiching the gel and nitrocellulose between two pairs of blotting paper and one set of sponges in a blotting cassette. The gels and nitrocellulose were soaked in blotting buffer (50 mM Tris; 192 mM glycine; 20 % (v/v) methanol) for 10 min prior to preparing the sandwich, and the nitrocellulose was carefully rolled onto the gel to avoid trapping air bubbles. The cassettes were inserted into the cassette holder and placed in the blotting tank, after which they were immersed in blotting buffer. Electrophoretic transfer was carried out overnight at 20 mA. The nitrocellulose pieces were then carefully removed and blocked with 10 ml of a 5 % (w/v) low fat milk powder in TBS (20 mM Tris; 200 mM NaCl at pH 7.4) solution for 1 hour. The nitrocellulose strips were then washed 3 times in 10 ml TBS for 5 min per wash. Primary antibody solutions were prepared in .05 % (w/v) BSA-TBS solutions as specified and nitrocellulose strips were incubated for 2 hours with these solutions, followed by 3 washes in TBS as described before. The nitrocellulose strips were then incubated for 1 hour with secondary antibody solution 1/12000 (unless stated otherwise) in 0.5 % (w/v) BSA-TBS, followed by three washes in TBS as described before. Finally the nitrocellulose strips were developed for 10 to 30 min using 2 ml of a substrate stock solution (0.3 % (w/v) 4-chloro-1-naphthol in methanol) diluted in 8 ml TBS containing 4 µl $H_2O_2$. After developing the nitrocellulose strips were washed with $dH_2O$ and left to dry.

### 2.5.2 Enhanced chemiluminescence

The procedure follows that of Western blotting, except that TTBS (0.1 % (v/v) Tween 20 added to the TBS buffer as described in 2.5.1) is used and the blocking is done with 8 % (w/v) low fat milk powder in TTBS, and wash steps are increased to 8 min per wash. After blocking for 1 hour and washing 3 times 8 min with TTBS, the blots were incubated with primary antibody overnight (16 hours) at 4 °C with rocking. The primary and secondary antibodies

were prepared in 0.5 % (w/v) BSA-TTBS to the desired concentrations, which were both optimised. Detection of the chemiluminescent signal was done in a dark room fitted with red lights. Film paper was used for detection, and blots were sandwiched between two sheets of plastic overheads and the MWM were traced. The chemiluminescent reagent was then prepared by mixing 50 µl of a luminol stock solution (40 mg/ml luminol in 1 % (v/v) DMSO), 25 µl of a p-iodophenol stock (0.1 M p-iodophenol in 1 ml DMSO) and 10 ml 0.1 M Tris-HCl pH 8.5 buffer directly onto the blots and the overhead sheets were folded slowly over the blot. Care was taken not to trap air bubbles and the blots were placed into an ECL exposure cassette. The film paper was then carefully laid on top of the blots and the exposure cassette was closed for the exposure time which was optimised. The film paper was then quickly removed and incubated in developing and fixing solution for 5 min and 2 min respectively. The film was then rinsed with water and left to dry.

### 2.5.3 Immunoprecipitation

Protein G beads were centrifuged (3000 x *g*, RT, 2 min), suspended in IP buffer (50 mM Tris; 150 mM NaCl; 0.1 % (v/v) Triton X-100 at pH 8.0) and washed for 30 min on a rocker. They were then centrifuged again (3000 x *g*, RT, 2 min) and suspended in their original volume with IP buffer. All sample incubations were done at room temperature (RT) with rocking. Parasite lysate samples (1 ml) were pre cleared by incubating with 20 µl protein G slurry for 30 min, centrifuged (3000 x *g*, RT, 2 min) and the pre-clarified supernatant samples were transferred to new eppendorfs. These samples were then incubated with 25 µg primary IgY antibody for 2 hours, followed by an hour incubation with 10 µg secondary / bridging antibody (rabbit anti-chicken IgY). Fifty microliters of the washed protein G beads were then added to the samples and incubated for one hour. Finally the samples were underlayed with 200 µl 1M sucrose and centrifuged (3000 x *g*, RT, 5 min). The supernatant samples were then either discarded, or in the case of sequential immunoprecipitation experiments they were transferred to new eppendorfs. The immunoprecipitation procedure was then repeated with a different primary antibody. The final precipitated pellets were washed twice by suspending the samples in 1 ml IP buffer and centrifuging (3000 x *g*, RT, 2 min), after which they were prepared for SDS-PAGE and Western blotting.

### 2.5.4 ELISA (direct and double antibody sandwich)

#### 2.5.4.1 Direct ELISA method

Antigen concentrations were prepared to 1 µg / ml in PBS (137 mM NaCl; 3 mM KCl; 7 mM $Na_2HPO_4$; 1.5 mM $KH_2PO_4$ at pH 7.2) and 150 µl was pipetted to each well. The plates were incubated overnight at 4 °C to allow coating of the wells. All wash steps were done with 0.1 % (v/v) PBS-Tween 20 and repeated 3 times and all incubations subsequent to coating were done at 37 °C except with substrate which was left at room temperature. After coating the plates were washed and then blocked with 200 µl 0.5 % (w/v) BSA-PBS per well and incubated for 1 hour. After a wash step the plates were incubated for 2 hours with 100 µl of the antigen-specific primary antibody and washed again. They were then incubated with 120 µl of the rabbit-anti-chicken HRPO antibody diluted 1/15000 for 1 hour and washed. All antibody solutions were prepared in 0.5 % (w/v) BSA-PBS. Finally the plates were incubated with 150 µl substrate (0.05 % (w/v) ABTS; 0.0015 % (v/v) $H_2O_2$) prepared in a 0.15 M citrate phosphate buffer at pH 5.0 per well and left to develop in the dark at room temperature for 30 min. The plates were then read immediately in an ELISA-plate reader at 405 nm. Background controls included: no antigen (or no coat), no primary antibody and no detection antibody. All results were corrected for background. Positive controls included a no blocking control. Additional controls were stated in text where applicable.

#### 2.5.4.2 Double antibody sandwich ELISA method

Plates were coated with 150 µl of an antigen-specific capture antibody at a concentration of 1 µg / ml prepared in PBS and incubated overnight at 4 °C. All other antibody solutions were prepared in 0.5 % (w/v) BSA-PBS As in the direct ELISA method, all subsequent incubation steps were done at 37 °C and all wash steps were repeated 3 times with 0.1 % (v/v) PBS-Tween 20. After coating plates were washed and incubated with 0.5 % (w/v) BSA-PBS for 1 hour and washed. 150 µl of the antigen-containing sample was then loaded per well at the desired concentration which had to be optimised to avoid the prozone effect. Recombinant protein solutions were prepared in 0.5 % (w/v) BSA-PBS and used to prepare antigen standard curves. Plates were incubated for 2 hours, washed and then incubated with 150 µl of a detection antigen-specific antibody linked to HRPO diluted 1/200 for 2 hours and washed again. 150 µl substrate solution was added per well and the plates were incubated in the dark for 30 min at room temperature, after which they were immediately read in an ELISA-plate reader at 405 nm. Background controls included: no antigen, no capture antibody and no

detection antibody. All results were corrected for background. Positive controls included a no blocking control. Additional controls were stated in text where applicable.

### 2.5.5 Coupling peptides to rabbit albumin

Four milligrams of the target peptide was dissolved in 50 µl DMSO and made up to 500 µl in reducing buffer (100 mM Tris; 1 mM EDTA; 0.02 % (w/v) $NaN_3$ at pH 8.0), after which 500 µl 10 mM DTT solution (10 mM DTT in reducing buffer) was added and the solution was mixed and incubated at 37 °C in a water bath for 90 min.

The ratio of peptide to carrier is 40:1, therefore the mass of rabbit albumin (RA) required for coupling was calculated as follows, where the molar mass of rabbit albumin is 68.2 kD:

$$68200 \times \frac{1}{40} \times \frac{4 \times 10^{-3} \text{ g } \textit{(peptide)}}{\textit{Mr peptide}} \times 1000 = \textit{carrier (mg)}$$

The ratio of carrier to MBS is 1:40, therefore the mass of MBS required for coupling was calculated as follows, where the molar mass of MBS is 314.26 g / mol.

$$314.26 \times 40 \times \frac{\textit{carrier (mg)}}{68200} \times 1000 = \textit{MBS (mg)}$$

The calculated amounts of RA were dissolved in 500 µl PBS and the MBS was dissolved in 200 µl Dimethyl formazan (DMF) and 300 µl PBS. Once dissolved the two solutions were combined and left to stand at room temperature for 30 min. This incubation was timed to start 30 min into the peptide incubation.

Two MEC columns were equilibrated with MEC buffer (100 mM $NaH_2PO_4$; 0.02 % (w/v) $NaN_3$ at pH 7.0). A Sephadex G-10 column was used to separate the reduced peptide from DTT, and the eluted 1 ml fractions were assessed for reduced peptide by adding 10 µl eluent to 10 µl Ellman's reagent (4 mg/ml) prepared fresh in Ellman's buffer (100 mM Tris; 1 mM EDTA; 0.1 % (w/v) SDS at pH 8.0). Yellow reactions indicated reduced peptide eluents. These were retained and used for coupling to the MBS activated RA carrier. The activated RA carrier was prepared by running it over a Sephadex G-25 column after the 30 min incubation

at room temperature with MBS as explained above. 1 ml fractions were collected and by measuring $A_{280}$ values those fractions with $A_{280}$ values greater than 0.3 were pooled and combined with the reduced peptide fractions eluted off the Sephadex G-10 column. This mixture was then left to stand at room temperature for 3 hours with gentle stirring. The resulting peptide-carrier conjugate solution was then split into 4 aliquots and stored at -20 °C until required for immunisation.

### 2.5.6 Chicken immunisation

(Ethics number 36/11 Animal)

Fifty micrograms recombinant protein was used per immunisation per chicken. Alternatively 4 mg of a prepared peptide conjugate sample was used for the whole immunisation schedule for one chicken, the sample was split into 4 aliquots that is. The samples for immunisation were prepared in PBS and were mixed 1:1 with the respective adjuvant used either Freund's or Pheroids™. In the case of Freund's adjuvant, the complete adjuvant (FCA) containing heat killed *Mycobacterium* was used for primary immunisations and the incomplete adjuvant (FIA) without *Mycobacterium* was used for booster immunisations. All samples were prepared by trituration with a syringe, where the Freund's adjuvant samples eventually formed water in oil emulsions. In the case of using Pheroids™ as the adjuvant, the samples were triturated for the same time it took for the Freund's samples to be prepared. Chickens were given intramuscular immunisations into each chest muscle, where the immunisation sites were sterilised with 70 % (v/v) ethanol prior to immunisation.

### 2.5.7 IgY isolation

The method for isolation of chicken antibodies (IgY) was followed as described by Polson *et al*., (1985).

Chicken eggs were collected on a daily basis and stored at 4 °C until use. They were cracked and the yolk was retained while washing the egg white off under running water to remove all the albumin. The yolk sac was then pierced with a needle and the yolk was collected into a measuring cylinder to determine the volume. Two volumes of isolation buffer (100 mM $NaH_2PO_4$; 0.02 % (w/v) $NaN_3$ at pH 7.6) were then added to increase the sample volume to

three times the initial yolk volume. PEG (Mr 6000) was then added to a final concentration of 3.5 % (w/v) and the solution was stirred gently until the PEG dissolved completely. The solution was then centrifuged (4420 x *g*, 4 °C, 30 min), which removed the precipitated vitellin fraction and the supernatant was decanted and filtered through cotton wool. The PEG concentration of the supernatant was then increased to 12 % (w/v) and stirred gently until completely dissolved. In this case the sample was centrifuged (12000 x *g*, 4 °C, 10 min) and the precipitate was retained and dissolved in a volume of isolation buffer equal to that of the filtrate. The PEG concentration was again brought to 12 % (w/v) and allowed to dissolve completely with gentle stirring. The sample was then centrifuged (12000 x *g*, 4 °C, 10 min) and the final pellet was dissolved in 1/6 of the initial yolk volume in storage buffer and stored at 4 °C.

### 2.5.8 Preparation of affinity matrices for antibody purification

#### 2.5.8.1 AminoLink™

AminoLink™ was used when whole protein antigens were to be used for preparation of affinity columns, as outlined below.

Five milligrams of the protein to be coupled was dialysed against coupling buffer (100mM $NaH_2PO_4$; 0.05 % (w/v) $NaN_3$ at pH7.2). The AminoLink™ resin was poured into a mini-column and the storage buffer was drained after the resin had settled. The resin was then equilibrated with 6 ml coupling buffer and drained. The dialysed protein solution was then added (2-4 ml) and 0.1 ml was retained to determine the coupling efficiency of the protein to the column. Forty microliters cyanoborohydride solution (5M $NaCNBH_3$; 1M NaOH) was added, and the column was mixed end-over-end for 6 hours at room temperature. The column was then drained of buffer and an eluent sample was retained to determine the coupling efficiency of the protein to the column. The column was then washed with 4 ml coupling buffer after which 2 ml quenching buffer (1M Tris-HCl at pH 7.4) was added with 40µl cyanoborohydride and mixed on an end-over-end mixer for 30 min. The column was then drained again and washed with 10 ml wash solution (100mM $NaH_2PO_4$; 0.2% (w/v) $NaN_3$ at pH 6.5) and stored at 4 °C until required.

### 2.5.8.2 SulfoLink™

SulfoLink™ resin was used for producing peptide-linked affinity columns, linking the peptides via terminal Cysteine residues.

Five milligrams of the peptide to be coupled was dissolved in 100 µl DMSO and 400 µl general buffer (50 mM Tris-HCl; 50 mM EDTA at pH 8.5), to which 500 µl DTT was added and the sample was then incubated for 1.5 hours at 37 °C (water bath). A Sephadex G-10 column equilibrated with general buffer was used to separate the reduced peptide from the DTT. This was done by collecting 1ml eluents off the column and combining 10 µl of each eluent separately with 10 µl Ellmans reagent as described in 2.5.5. The reduced peptides reacted with the Ellmans reagent to give a yellow solution. The eluents containing the reduced peptide were pooled and added immediately to 1 ml prepared SulfoLink™ resin and mixed for 15 min after which the resin was allowed to stand for 30 min. After 3 washes with general buffer (1 column volume each) 1 ml of a 50 mM L-Cysteine solution was added to the resin, mixed for 15 min on an end over end mixer and then left to stand for 30 min. The column was then drained and washed with 16 column volumes washing buffer followed by 2 column volumes of a 0.1 M phosphate buffer at pH 7.6 and stored at 4 °C until use.

### 2.5.9 IgY affinity purification

Crude IgY was isolated from single eggs collected at the end of each week after immunisation. Weeks showing high antibody titres were pooled and used for affinity purification. The crude IgY was circulated over the column overnight at room temperature. The column was then washed with PBS until the $A_{280}$ of eluting samples dropped down to between 0.01-0.02. Eppendorfs were prepared for collection of eluent samples by adding 50 µl neutralisation buffer (1 M $NaH_2PO_4$; 0.02 % (w/v) $NaN_3$ at pH 8.5) to each tube. The specific antibodies bound to the antigen on the column were then eluted with a change in pH by adding 8 ml elution buffer (100 mM glycine; 0.02 % (w/v) $NaN_3$ at pH 2.8) to the column and collection 1 ml eluents. The IgY concentration was then determined by measuring the $A_{280}$ values of the samples and calculated using the extinction coefficient of IgY ($\varepsilon$ = 1.25) (Coetzer, 1985). Affinity purified samples with $A_{280}$ values greater than 0.2 were pooled and kept at 4 °C, and the remainder was discarded.

### 2.5.10 Conjugation of horse radish peroxidase to IgY antibodies

Eight milligrams of horse radish peroxidase (HRPO) (1360 Units) was dissolved in $dH_2O$. Two hundred microliters 0.1 M sodium periodate was added and the solution turned from brown to a greenish brown and was stirred gently for 20 min at room temperature. The solution was then dialysed overnight (16 hours) at 4 °C against sodium acetate buffer (0.1 M sodium acetate; 0.22 % (v/v) acetic acid at pH 4.4), after which 20 µl sodium carbonate buffer (13 ml of a 0.2 M sodium carbonate solution and 37 ml of a 0.2 M sodium hydrogen carbonate solution were made up to 200 ml at pH 9.5) was added to raise the pH of the solution to between 9-9.5 and 1 ml (8 mg) of the IgY sample to be conjugated was added immediately. The antibody-HRPO mixture was inverted every 15 min and left at room temperature for a total of 2 hours. Finally 100 µl sodium borohydride solution (4 mg/ml) was added to reduce any unbound HRPO and the solution was left to stand for 2 hours at 4 °C. The IgY-HRPO solution was then dialysed against a 0.1 M borate buffer at pH 7.4 after which an equal volume of 60% (v/v) glycerol solution (prepared in borate buffer) was added and the samples were stored at 4 °C.

# Chapter 3

# Expression and characterisation of recombinant *Pf*LDH and *Pf*GAPDH

## 3.1 Introduction

Current rapid diagnostic tests (RDTs) are based on three malarial proteins found in the parasite cytoplasm. These include histidine-rich protein 2 (HRP-2), lactate dehydrogenase (LDH) and aldolase (Murray *et al*., 2008, Murray and Bennett, 2009). HRP-2 is used for the detection of *Plasmodium falciparum* infection as it is only expressed by this species (Murray *et al*., 2008). Tests that use HRP-2 exclusively include Paracheck Pf®; ParaHIT *f*® and *Para*Sight-F for example (Murray *et al*., 2008).

There are currently 5 malaria species that infect humans including *P. falciparum*, *P. vivax*, *P. ovale*, *P. malariae* and *P. knowlesi*. *P. knowlesi* was recently added as a recognised human infective species, transmitted by the mosquito vector *Anopheles latens* which is parasitic to both humans and monkeys (Anderios, 2009, Daneshvar *et al.*, 2009, Lee *et al.*, 2009, Sabbatani *et al.*, 2010, Van den Eede *et al.*, 2010, van Hellemond *et al.*, 2009). Due to co-infections with *P. falciparum* and other malaria species RDTs have to be able to detect and differentiate between these species. With co-infections, drug therapies are required to target each infecting malarial species and to avoid relapse (Chuangchaiya *et al.*, 2009; Murray *et al*., 2008). Alternate protein targets to HRP-2, such as the glycolytic enzymes LDH and aldolase, which are common to all malaria species, are therefore used for diagnosis to detect mixed infections (Murray *et al.*, 2008). RDTs either target LDH alone (OptiMAL® or OptiMAL-IT® tests), or HRP-2 in combination with either LDH (CARESTART™), or with aldolase (BinaxNOW® test) to detect mixed infections (Ashley *et al*., 2009; Khairnar, 2009; Murray *et al.*, 2008).

HRP-2 is secreted and is also found in knob-like protrusions present on the parasitized red blood cell membrane (Howard *et al*., 1986). There have been reports of false negative diagnoses of *P. falciparum* infection using HRP-2 as a target due to HRP-2 gene deletions. Isolates in Peru have been shown to have the HRP-2 gene deleted (Gamboa *et al*., 2010). Variation in amino acid composition of HRP-2 (known as antigenic variation) has also been reported to affect detection (Baker *et al*., 2010, Lee *et al*., 2006a). Sequence analysis of LDH and aldolase from malaria field isolates has shown that the amino acid sequence in these

proteins does not undergo antigenic variation, unlike HRP-2 (Lee *et al*., 2006b) which should allow for a more consistent detection of infections.

Another aim for RDTs is to monitor treatment, allowing clinicians to adjust or alter drug treatments based on the efficacy of the drug. This is hampered for tests based on HRP-2 as the protein persists in serum for 14 to 28 days after the parasitemia is cleared (Iqbal *et al*., 2004; Kodisinghe *et al*., 1997; Murray *et al*., 2008; Tjitra *et al*., 2001). This is not the case with LDH and aldolase due to their short half-life. Both LDH and aldolase are involved in metabolism and are thus associated with living parasites (Iqbal *et al*., 2004, Murray *et al*., 2008). LDH based tests (CareStart™ and OptiMAL-IT®) reverted back to negative within 2 and 7 days respectively after drug clearance of infection (Ashley *et al*., 2009). The only possible drawback is that all 3 antigens are also produced in the gametocyte stage of the parasite, however due to the low gametocyte numbers in comparison to the asexual stages, parasite clearance could still be monitored using LDH and aldolase (Murray *et al*., 2008, Tjitra *et al*., 2001).

Tracking the clearance of infection has become an important factor for the treatment of malaria as well as other tropical diseases. The early symptoms of malaria infections overlap with those of other tropical diseases and therefore these infections are often mistaken for malaria and treated as such (Gwer *et al*., 2007, Källander *et al*., 2004). An estimated one third of children displaying malaria-like symptoms end up testing negative for malaria and misdiagnoses are often fatal due to incorrect treatment. Outlines for clinicians have been provided by the centre for disease control (Lalloo *et al*., 2007) encouraging diagnosis before treatment (Lalloo *et al*., 2007). Confidence in malaria RDTs is still lacking however, as argued by Bisoffi *et al*., (2009) with clinicians reverting to presumptive treatment of malaria in the case of a negative test.

To improve confidence in RDTs, quality assurance is very important and has also been recommended by the WHO (WHO, 2008). These measures include buying RDTs from manufacturers with evidence of good manufacturing practice as well as "in the field testing" of RDTs. One of the methods for testing RDTs in the field was by inclusion of a positive control. This would entail the use of recombinant antigens or peptides reconstituted in uninfected blood (Lon *et al*., 2005, Murray *et al*., 2008). Alternatively Versteeg and Mens in 2009 used dried infected blood spots as positive controls, where they found this format to work best for HRP-2 based tests due to the stability of the antigen, but to be less effective for

LDH and aldolase based tests. Further work has to be done on the heat stability of positive controls and on optimisation of antigen concentrations that will allow for exclusion of RDTs that lack appropriate sensitivity (Lon *et al*., 2005).

Two malarial metabolic proteins were selected for studying as diagnostic targets. The proteins were *Plasmodial* LDH and glyceraldehyde-3-phosphate dehydrogenase (GAPDH). Both LDH and GAPDH are key conserved metabolic enzymes, making them ideal targets for diagnostics (Daubenberger *et al*., 2000; Lee *et al*., 2006b). Both *P. falciparum* proteins were recombinantly expressed and the recombinant proteins were characterised using SDS-PAGE, Western blotting and molecular exclusion chromatography. The purified recombinant proteins were used for raising antibodies in chickens.

## 3.2 Results

### 3.2.1 Confirmation of the identity of the coding sequences cloned for the expression of *P. falciparum* LDH and GAPDH

*E. coli* BL21(DE3) cells were transformed with either a pKK223-3 vector containing the coding gene for *Pf*LDH (*Pf*(K1) strain), or with a pET-15b vector containing the coding gene for *Pf*GAPDH ( *Pf*(3D7) strain). These were kindly provided by Professor R.L. Brady (University of Bristol, UK) and Professor L. Tilley (Satchell *et al.,* 2005) respectively.

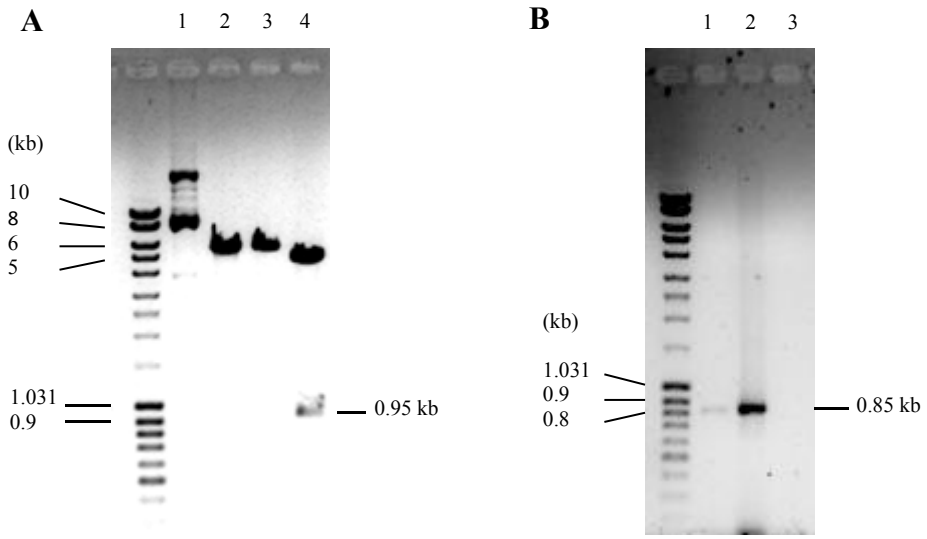


**Figure 3.1 Confirmation of the r*Pf*LDH gene insert in the pKK223-3 plasmid by EcoRI and PstI restriction digestion and PCR amplification.**
Samples were run on 1% (w/v) agarose gels in the presence of ethidium bromide with the co-migrating DNA ladder sizes labelled on the left in kilo base pairs (kb) and bands of interest on the right. EcoRI and PstI digests of purified r*Pf*LDH plasmid DNA (pKK223-3 vector) were shown in (A) and the samples were run as follows: lane 1 undigested; lane 2 EcoRI digest; lane 3 PstI digest; lane 4 EcoRI and PstI double digest. PCR products were run in (B) as follows: lane 1 colony PCR; lane 2 PCR with purified plasmid and lane 3 no template control.

Figure 3.1 (A) shows results for the digestion of the pKK223-3 vector containing the LDH gene with EcoRI and PstI restriction endonucleases alone or together. The size of the insert was estimated at 950 bp. The vector alone was estimated to be 4.8 kb and to be 5.8 kb with the insert. A single 850 bp amplicon was obtained for PCR amplification (Figure 3.1 (B)) as expected of the plasmodial LDH.

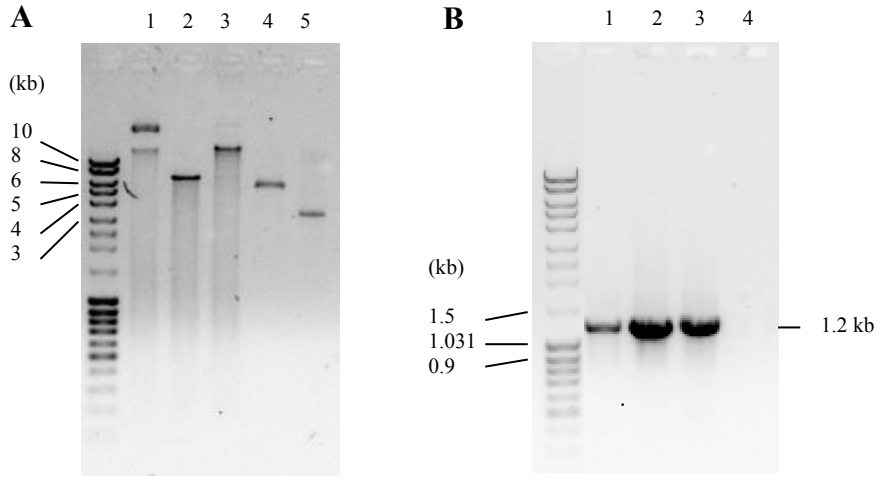


**Figure 3.2 Confirmation of the r*Pf*GAPDH gene insert in the pET-15b plasmid by XhoI and NdeI restriction digestion and PCR amplification.**
Samples were run on 1% (w/v) agarose gels in the presence of ethidium bromide, with the co-migrating DNA ladder sizes labelled in kb on the left of each gel and bands of interest on the right. XhoI and NdeI digests of the purified r*Pf*GAPDH plasmid DNA (pET-15b vector) were shown in (A) and the samples were run as follows: lane 1 undigested; lane 2 XhoI and lane 3 NdeI digest. Lane 4 NdeI digest of pET-28a; lane 5 undigested pET-28a. PCR products were run in (B) as follows: lane 1 colony PCR r*Pf*GAPDH; lane 2 colony PCR r*P.yoelii* GAPDH; lane 3 PCR of purified r*Pf*GAPDH plasmid; lane 4 no template control.

A double digest of the r*Pf*GAPDH plasmid was unsuccessful as NdeI failed to digest the plasmid (Figure 3.2 (A)). To verify NdeI activity, a single digest of a separate plasmid pET-28a was performed and was successful as shown in lane 4 of the same gel. XhoI digested the plasmid and the linearized plasmid was approximately 1000 bp larger than the vector alone. The PCR results (Figure 3.2 (B)) showed a n amplicon of around 1.2 kb. Both sizes corresponded well to that predicted from the base sequence. PET specific primers were used, which amplify an additional 322 bp outside the expected 1014 bp of the insert DNA. A *P. yoelii* GAPDH insert was amplified from a pET-15b plasmid with the same pET specific primers and run in lane 3 (Figure 3.2 (B)) producing an amplicon of around 1.2 kb.

The inserts were sequenced using both forward and reverse primers, where the same primers were used for the LDH sequencing and PCR reactions. For the GAPDH sequencing T7 forward and reverse primers were used. Consensus sequences were identified and aligned with the respective *Pf*(3D7) coding sequences (Figures 3.3 and 3.4). BLASTn searches showed 98% and 96% homology for the *Pf*LDH and *Pf*GAPDH consensus sequences respectively (http://www.ncbi.nlm.nih.gov/BLAST/, accessed 15.09.2011).

```
PfLDH           ATGGCACCAAAAGCAAAAATCGTTTTAGTTGGCTCAGGTATGATTGGAGGAGTAATGGCT 60
Consensus       ATGGCACCAAAAGCAAAAATCGTTTTAGTTGGCTCAGGTATGATTGGTGGTGTAATGGCT 60
                ********************************************** ** *********

PfLDH           ACCTTAATTGTTCAGAAAAATTTAGGAGATGTAGTTTTGTTCGATATTGTAAAGAACATG 120
Consensus       ACTTTAATTGTTCAGAAAAATTTAGGAGATGTAGTTTTGTTCGATATTGTAAAGAACATG 120
                ** ************************************************************

PfLDH           CCACATGGAAAAGCTTTAGATACATCTCATACTAATGTTATGGCATATTCAAATTGCAAA 180
Consensus       CCACATGGAAAAGCTTTAGATACATCTCATACTAATGTTATGGCATATTCAAATTGCAAA 180
                ************************************************************

PfLDH           GTAAGTGGTTCAAACACTTATGACGATTTGGCTGGAGCAGATGTAGTAATAGTAACAGCT 240
Consensus       GTAAGTGGTTCAAACACTTATGACGATTTGGCTGGAGCAGATGTAGTAATAGTAACAGCT 240
                ************************************************************

PfLDH           GGATTTACCAAGGCCCCAGGAAAGAGTGACAAAGAATGGAATAGAGATGATTTATTACCA 300
Consensus       GGATTTACCAAGGCCCCAGGAAAGAGTGACAAAGAATGGAATAGAGATGATTTATTACCA 300
                ************************************************************

PfLDH           TTAAACAACAAGATTATGATTGAAATTGGTGGTCATATTAAGAAGAATTGTCCAAATGCT 360
Consensus       TTAAACAACAAGATTATGATTGAAATTGGTGGTCATATTAAGAAGAATTGTCCAAATGCT 360
                ************************************************************

PfLDH           TTTATTATTGTTGTAACAAACCCAGTAGATGTTATGGTACAATTATTACATCAACATTCA 420
Consensus       TTTATTATTGTTGTAACAAACCCAGTAGATGTTATGGTACAATTATTACATCAACATTCA 420
                ************************************************************

PfLDH           GGTGTTCCTAAAAACAAGATTATTGGTTTAGGTGGTGTATTAGATACATCAAGATTGAAG 480
Consensus       GGTGTTCCTAAAAACAAGATTATTGGTCTAGGTGGTGTATTAGATACATCAAGATTGAAG 480
                *************************** ********************************

PfLDH           TATTACATATCTCAGAAATTAAATGTATGCCCAAGAGATGTAAATGCACACATTGTAGGT 540
Consensus       TATTACATATCTCAGAAATTAAATGTATGCCCAAGAGATGTAAATGCACACATTGTAGGT 540
                ************************************************************

PfLDH           GCTCATGGAAATAAAATGGTTCTTTTAAAAAGATACATTACTGTAGGTGGTATCCCTTTA 600
Consensus       GCTCATGGAAATAAAATGGTTCTTTTAAAAAGATACATTACTGTAGGTGGTATCCCTTTA 600
                ************************************************************

PfLDH           CAAGAATTTATTAATAACAAGTTAATTTCTGATGCTGAATTAGAAGCTATATTTGATAGA 660
Consensus       CAAGAATTTATTAATAACAAGTTAATTTCTGATGCTGAATTAGAAGCTATATTTGATAGA 660
                ************************************************************

PfLDH           ACTGTTAATACTGCATTAGAAATTGTAAACTTACATGCATCACCATATGTTGCACCAGCT 720
Consensus       ACTGTTAATACTGCATTAGAAATTGTAAACTTACATGCATCACCATATGTTGCACCAGCT 720
                ************************************************************

PfLDH           GCTGCTATTATCGAAATGGCTGAATCCTACTTAAAAGATTTGAAAAAAGTATTAATTT-G 779
Consensus       GCTGCTATTATCGAAATGGCTGAATCCTACTTAAAAGATTTGAAAAAAGTATTAATTTTG 780
                ************************************************************ *

PfLDH           CTCAACCTTGTTAGAAGGACAATATGGACACTCCGATATATTCGGTGGTACACCTG-TTG 838
Consensus       CTCAACCTTGTTAGAAGGACAATATGGACACTCCGATATATTCCGTGGTACACCTGGTTG 840
                ****************************************** ************ ***

PfLDH           TTTTAGGTGCTAATGGTGTTGAACAAGTTATCGAATTACAATTAAATAGTGAGGAAAAAG 898
Consensus       TYTTAGGTGCTAATGGYGTTGAACAAGTTATTCGAATACNATTAAATAGYGAGGAAAAAN 900
                * ************** **************   * *** ********* *********

PfLDH           CTAAATTTGATGAAGCCATAGCT-GAAACTAAGAGAATGAAGGCATTAGCTTAA 951
Consensus       CTAAATTTGATGAANCCNTAGCTCAANACTNAGAGAATGAAGGCATTAGCTCAT 954
                ************** ** *****  * *** ******************** *
```

**Figure 3.3 Alignment of the *Pf*LDH DNA sequence with the LDH coding sequence from the *Pf*(K1) strain.**

Multiple sequence alignment of the *Pf*LDH DNA sequence and the LDH coding sequence from the *Pf*(K1) strain (NCBI ID: DQ198261). Sequence identity was annotated with "*" representing identical residues and blank spaces representing no identity. The overall percentage identity between the two sequences was 98 % (http://www.ncbi.nlm.nih.gov/BLAST/, accessed 10.01.2012). The symbols "N" and "Y" denote incompletely specified bases.

```
PfGAPDH         ATGGCAGTAACAAAACTTGGAATTAATGGATTTGGTCGTATCGGACGTTTAGTATTTAGA 60
Consensus       ATGGCAGTAACAAAACTTGGAATTAATGGATTTGGTCGTATCGGACGTTTAGTATTTAGA 60
                ************************************************************

PfGAPDH         GCAGCCTTTGGAAGGAAAGATATCGAAGTAGTTGCTATTAACGACCCATTTATGGACCTT 120
Consensus       GCAGCCTTTGGAAGGAAAGATATCGAAGTAGTTGCTATTAACGACCCATTTATGGACCTT 120
                ************************************************************

PfGAPDH         AACCACTTATGCTATCTCTTGAAATACGATTCAGTACATGGTCAATTTCCATGTGAGGTA 180
Consensus       AACCACTTATGCTATCTCTTGAAATACGATTCAGTACATGGTCAATTTCCATGTGAGGTA 180
                ************************************************************

PfGAPDH         ACCCACGCTGATGGATTTTTATTAATCGGAGAAAAGAAAGTCAGTGTTTTTGCTGAAAAG 240
Consensus       ACCCACGCTGATGGATTTTTATTAATCGGAGAAAAGAAAGTCAGTGTTTTTGCTGAAAAG 240
                ************************************************************

PfGAPDH         GATCCATCTCAAATTCCTTGGGGAAAATGCCAAGTAGATGTTGTATGTGAATCAACTGGT 300
Consensus       GATCCATCTCAAATTCCTTGGGGAAAATGCCAAGTAGATGTTGTATGTGAATCAACTGGT 300
                ************************************************************

PfGAPDH         GTATTTTTAACCAAAGAATTAGCTAGCAGTCACCTTAAGGGAGGAGCCAAGAAGGTTATT 360
Consensus       GTATTTTTAACCAAAGAATTAGCTAGCAGTCACCTTAAGGGAGGAGCCAAGAAGGTTATT 360
                ************************************************************

PfGAPDH         ATGTCCGCCCCACCAAAGGATGACACCCCAATTTATGTTATGGGTATTAACCACCACCAA 420
Consensus       ATGTCCGCCCCACCAAAGGATGACACCCCAATTTATGTTATGGGTATTAACCACCACCAA 420
                ************************************************************

PfGAPDH         TATGATACCAAACAACTTATTGTTTCCAATGCATCATGTACCACAAACTGCTTAGCTCCA 480
Consensus       TATGATACCAAACAACTTATTGTTTCCAATGCATCATGTACCACAAACTGCTTAGCTCCR 480
                ************************************************************

PfGAPDH         TTAGCTAAAGTTATTAATGATCGTTTTGGAATTGTT-GAAGGTTTAATGACCACCGTTCA 539
Consensus       TTAGCTAAAGTTATTAATGATCGTTTTGGAATTGKTTGAAGGTTTARTGACCACCGTTCA 540
                ********************************** * ********* **************

PfGAPDH         TGCATCCACTGCTAACCAATTAGTTGTTGATGGTCCATCAAA-GGGTGGTAAGGACTGGA 598
Consensus       TGCATCCACTGCTAACCAATTAGTTGTTGATGGTCCATCARAAGGGTGGTAAGGACTGGA 600
                ****************************************** * ******************

PfGAPDH         GAGCAGGTAGATGTGCATTATCCAACATTATTCCAGCTTCCACTGGTGCAGCTAAAGCTG 658
Consensus       KAGCAGGTAGATGTSCATTATCCRACATTATTCCR-CTTCCACWGGTGCARCTAAAGCTG 659
                 ************* ******** **********  ******* ****** *********

PfGAPDH         TAGGTAAAGTTTTACCTGAACTTAATGGAAAATTAACAGGTGTAGCTTT-CAGA-GTACC 716
Consensus       TAGGTAAAGTTTTACCTGAACTTAATGGAAA-TTARCAGGTKTAGCTTTTCAGAAGTACC 718
                ******************************** *** ***** ******* **** *****

PfGAPDH         AATTGGAAC-TGTATCAGTTG-TTGATTTAGTTTGCAGATTAC--AAAAACCAGCAAAAT 772
Consensus       AATTGGAAMCTGTATYARTTGRTTSATTTASTTTGCARAATAACAAWAARCCAGCAAAAT 778
                ********  ***** * *** ** ***** ****** * **   * ** **********

PfGAPDH         ATGAAGAAG-TTGCTTTAGAAATTAAAAAAGCTGCTGAAGGTCCACTTAAAGGAATCTTA 831
Consensus       AKGAAGAAGGTTGCTTTAGAAATTWAAAAAGCTGCTGAAGGTCCACTTAAAGGAATCTCA 838
                * ******* ************** ********************************** *

PfGAPDH         GGATACACTGAAGATGAAGTTGTTTCTCAAGATTTCGTTCATGATAACAGATCATCAATC 891
Consensus       GGATACACYGAAGATGAAGTTGTTTCTCAAGATTTCGTTCATGATAACAGATCATCAATC 898
                ******** ************************************************

PfGAPDH         TTTGACATGAAAGCTGGTTTAGCCTTAAACGACAATTTCTTCAAATTAGTTTCATGGTAC 951
Consensus       TTYGACATGAAAGCTGGTTTAGCCTTAAACGACAATTTCTTCAAATTAGTTTCATGGTRC 958
                ** ********************************************************* *

PfGAPDH         GATAATGAATGGGGATACTCAAACCGTGTTCTTGATTTAGCCGTACACATTACTAACAAC 1011
Consensus       GATAATGAATGGGGATACTCAAMCCGTGTTCTYGATT-AGCCGTACACATTACTAACAAM 1017
                ********************** ********* **** ********************

PfGAPDH         TAA 1014
Consensus       TAA 1020
                ***
```

**Figure 3.4 Alignment of the *Pf*GAPDH DNA sequence with the GAPDH coding sequence from the *Pf*(3D7) strain.**

Multiple sequence alignment of the *Pf*GAPDH DNA sequence and the GAPDH coding sequence from the *Pf*(3D7) strain (PlasmoDB ID: PF14_0598). Sequence identity was annotated with "*" representing identical residues and blank spaces representing no identity. The overall percentage identity between the two sequences was 96 % (http://www.ncbi.nlm.nih.gov/BLAST/, accessed 10.01.2012). The symbols "M", "W", "R" and "Y" denote incompletely specified bases.

There were a few nucleotides with no identity between the consensus and coding sequences for both *Pf*LDH and *Pf*GAPDH. With the *Pf*GAPDH alignment there were a few insertions as well, with the longest being two nucleotides. BLASTp searches of the amino acid sequences of LDH and GAPDH orthologs from all the *P. falciparum* strains revealed 99 % identity between the respective orthologs, suggesting that the differences in the nucleotide sequences had little effect on the homology between the orthologs.

### 3.2.2 Optimisation of incubation temperature during expression and buffer pH for affinity purification of recombinant *Pf*LDH and *Pf*GAPDH

Different *E. coli* culture incubation temperatures were tested for protein expression. An overnight culture was grown at 37 ºC and used for the inoculation of fresh broth. These cultures were then grown at either 30 or 37 ºC for protein expression. Protein solubility and overall charge are dependent on ionic strength and pH of the buffer respectively, and so purification conditions compared pH 7.0 and pH 8.0 (50 mM $NaH_2PO_4$; 300 mM NaCl). The data was recorded in Table 3.1 and showed that the highest protein yields, with a combination of incubation temperature and pH for both proteins were obtained at 30 ºC and using isolation buffers at pH 8.0.

**Table 3.1 The effect of incubation temperature during expression and buffer pH for affinity purification r*Pf*LDH and r*Pf*GAPDH.**

| | Yield (µg) | |
|---|---|---|
| Sample name | r*Pf*LDH | r*Pf*GAPDH |
| 30 ºC at pH 7.0 | 97.9 | 32.8 |
| 37 ºC at pH 7.0 | 68.1 | 36.5 |
| 30 ºC at pH 8.0 | 114.5 | 69.5 |
| 37 ºC at pH 8.0 | 48.1 | 46.1 |

Data represent average values from duplicate experiments using 10 ml LB cultures.

A range of different ionic strengths in the buffer was tested from 50 mM NaCl to 300 mM with no significant effect observed (data not shown).

### 3.2.2.1 Expression and affinity purification of recombinant *Pf*LDH

The expression of r*Pf*LDH from 200 ml cultures was used and high yields of recombinant proteins were obtained (Figure 3.5).

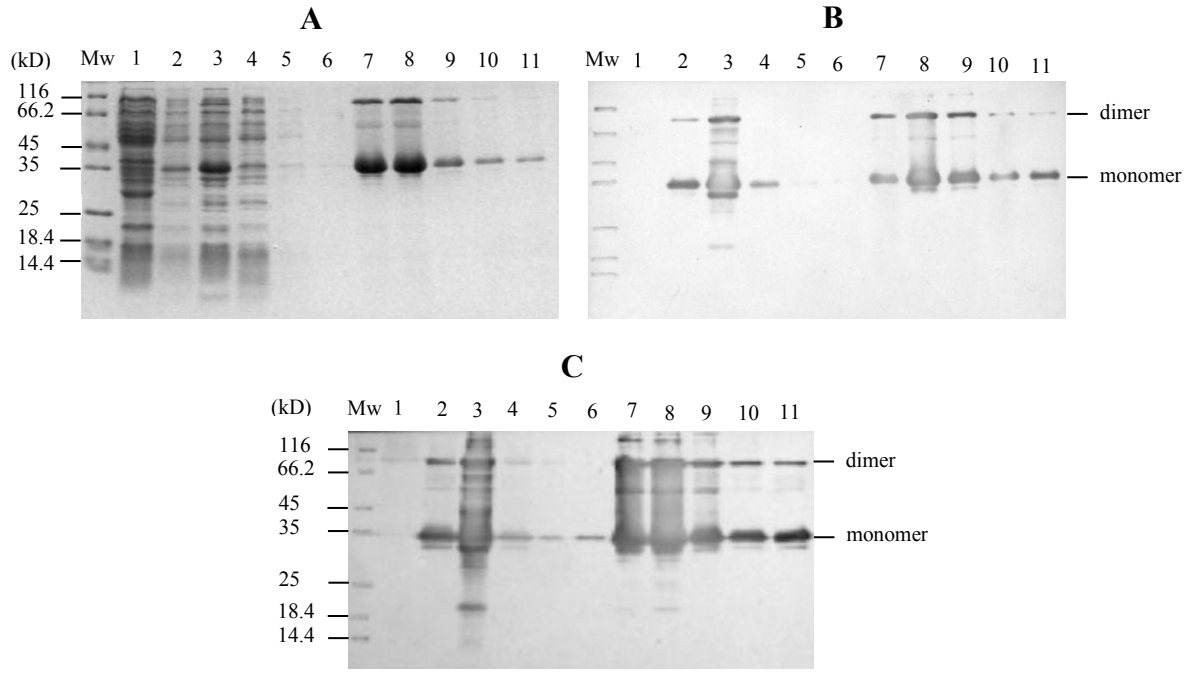


**Figure 3.5 Expression, purification and detection of r *Pf*LDH with anti-His and anti-r*Pf*LDH antibodies.**
Recombinant *Pf*LDH was expressed at 30ºC and induced with IPTG, and affinity purified with a TALON ($Co^{2+}$) resin in phosphate buffer pH 8.0. Protein samples were evaluated on reducing 12.5% SDS-PAGE gels. The samples were run as follows: lane 1 untransformed *E. coli* BL21(DE3); lane 2 un-induced and lane 3 induced; lane 4 unbound; lane 5-6 washes; lane 7-11 affinity purified r*Pf*LDH eluents; Mw (Molecular weight markers). Panels (B) and (C) are Western blots of the Coomassie R-250 stained reference gel (A). (B) was probed with anti His-HRPO mouse monoclonal antibody at 1/5000 dilution and (C) with an anti-r*Pf*LDH IgY primary (1 µg/ml) and detected with a rabbit-anti-chicken IgY-HRPO secondary antibody at 1/12000. A monomeric as well as a dimeric form of r*Pf*LDH was detected as labelled along-side the Western blots.

No r*Pf*LDH was detected in the untransformed BL21(DE3) control (Figure 3.5). There was "leaky" protein expression observed in the un-induced samples as protein was detected in lane 2 of panels 3.3B and C. Protein expression increased with induction (lane 3), as shown by the increased intensity of the band at around 36 kD. The additional band at around 75 kD was detected in (B) and (C) with the most prominent being the 36 kD band. In lanes 7, 8 and 9 there was also detection of a doublet of 36 kD and 33 kD, which was possibly a truncated

form of r*Pf*LDH. Lower molecular weight products were also detected in (C) which was not as evident in (B).

### 3.2.2.2 Expression and affinity purification of recombinant *Pf*GAPDH

The expression of r*Pf*GAPDH from 200 ml cultures was used and high yields of recombinant proteins were obtained (Figure 3.6).

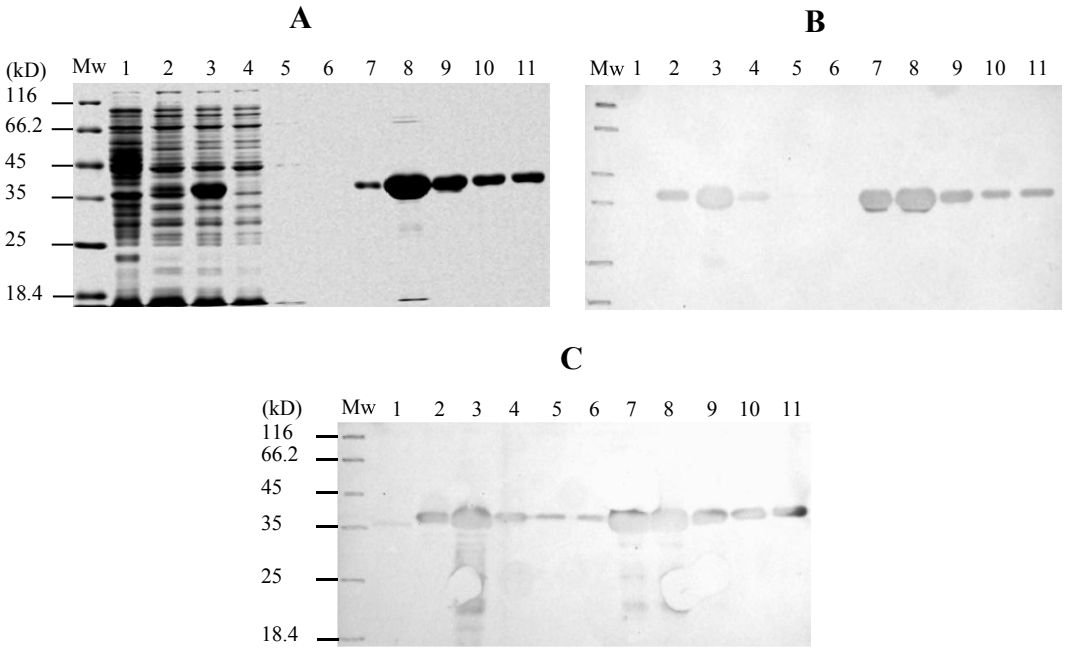


**Figure 3.6 Expression, purification and detection of r*Pf*GAPDH with anti-His and anti-r*Pf*GAPDH antibodies.**
Recombinant *Pf*GAPDH was expressed at 30ºC and induced with IPTG, and affinity purified with a TALON (Co2+) resin in phosphate buffer pH 8.0. Protein samples were evaluated on reducing 12.5% SDS-PAGE gels. The samples were run as follows: lane 1 untransformed E. coli BL21(DE3); lane 2 un-induced and lane 3 induced; lane 4 unbound; lane 5-6 washes; lane 7-11 affinity purified rPfLDH eluents; Mw (Molecular weight markers). Panels (B) and (C) are Western blots of the Coomassie R-250 stained reference gel (A). (B) was probed with anti His-HRPO mouse monoclonal antibody at 1/5000 dilution and (C) with an anti-r*Pf*GAPDH IgY primary (1 µg/ml) and detected with a rabbit-anti-chicken IgY-HRPO secondary antibody at 1/12000.

Examination of r*Pf*GAPDH purification steps in Figure 3.6, showed r*Pf*GAPDH was not expressed in the untransformed BL21(DE3) control run in lane 1. A band was detected around 39 kD in lane 2 (B and C). This was suggestive of "leaky" protein expression. There was a clear increased intensity of this band in lane 3, after expression was induced. There was a faint band around 80 kD in lane 8 in (A) which was not detected in the blots. Smaller bands were detected in (C) with the anti-r*Pf*GAPDH IgY antibodies which were not detected in the anti-His tag Western blot in (B).

### 3.2.3 Assessing tetramer formation of the recombinant *Pf*LDH and *Pf*GAPDH proteins by molecular exclusion chromatography

Both LDH and GAPDH proteins form tetramers in their native state (Berwal *et al*., 2008; Daubenberger *et al*., 2003). To evaluate the quaternary structure of both recombinant His-tag proteins, they were subjected to molecular exclusion (gel filtration chromatography) on a Sephacryl S200 column (Figures 3.8 and 3.9). The calibration of the Sephacryl S200 column was shown in Figure 3.7.

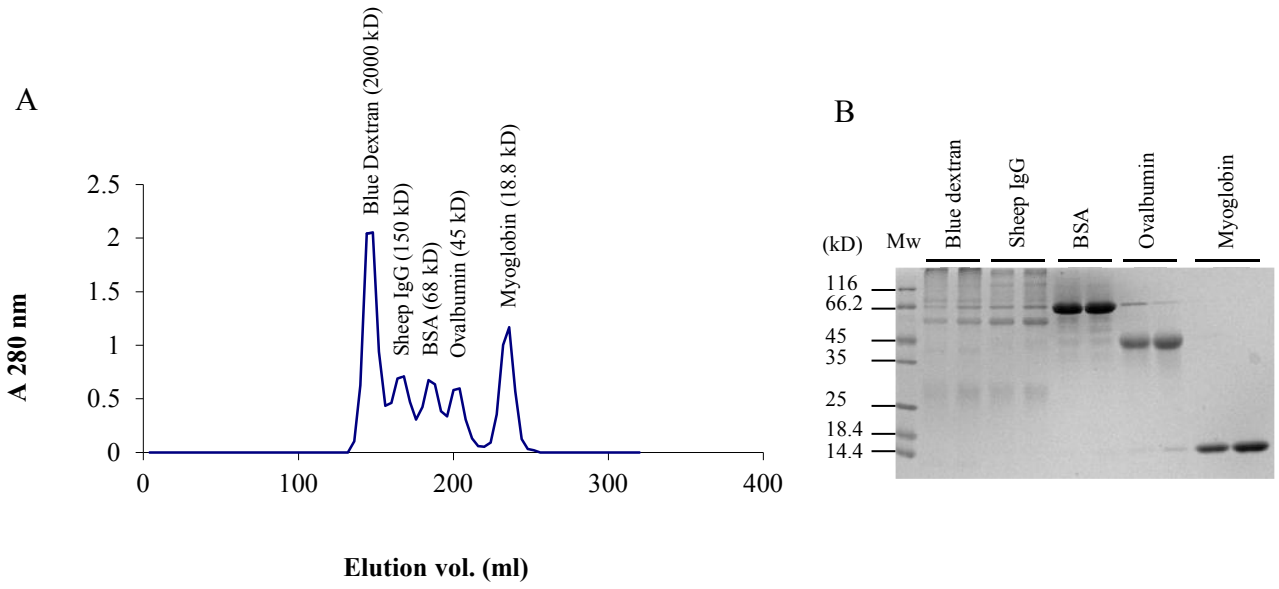


**Figure 3.7 Sephacryl S200 column calibration profile using five molecular weight standards.**
The Sephacryl S200 column was calibrated with: Blue dextran (2000 kD); sheep IgG (150 kD); bovine serum albumin (BSA) (68 kD); ovalbumin (45 kD) and myoglobin (18.8 kD). The column volume was 319 ml and was run at a flow rate of 1 ml/min and 80 fractions of 4 ml each were collected. The calibration profile was shown in (A). The elution peaks were run on a reducing 12.5 % SDS-PAGE gel stained with Coomassie R-250 shown alongside in (B). The void volume ($V_o$) was calculated as 144 ml at the elution peak of blue dextran.

There was a minor overlap of the higher molecular weight protein standards as seen in the SDS-PAGE gel in Figure 3.7(B), where the prominent bands were of the expected sizes. The Sheep IgG standard showed dissociation of the heavy and light chains of the IgG molecule under reducing conditions. The resulting major protein bands ran at approximately 50 kD and 27 kD for the heavy and light chains respectively, with incomplete reduction yielding 127 kD; 100 kD and 77 kD products. The recombinant *Pf*LDH and *Pf*GAPDH protein samples were

run over the molecular exclusion chromatography column and the elution profiles were shown in Figures 3.8 and 3.9 respectively.

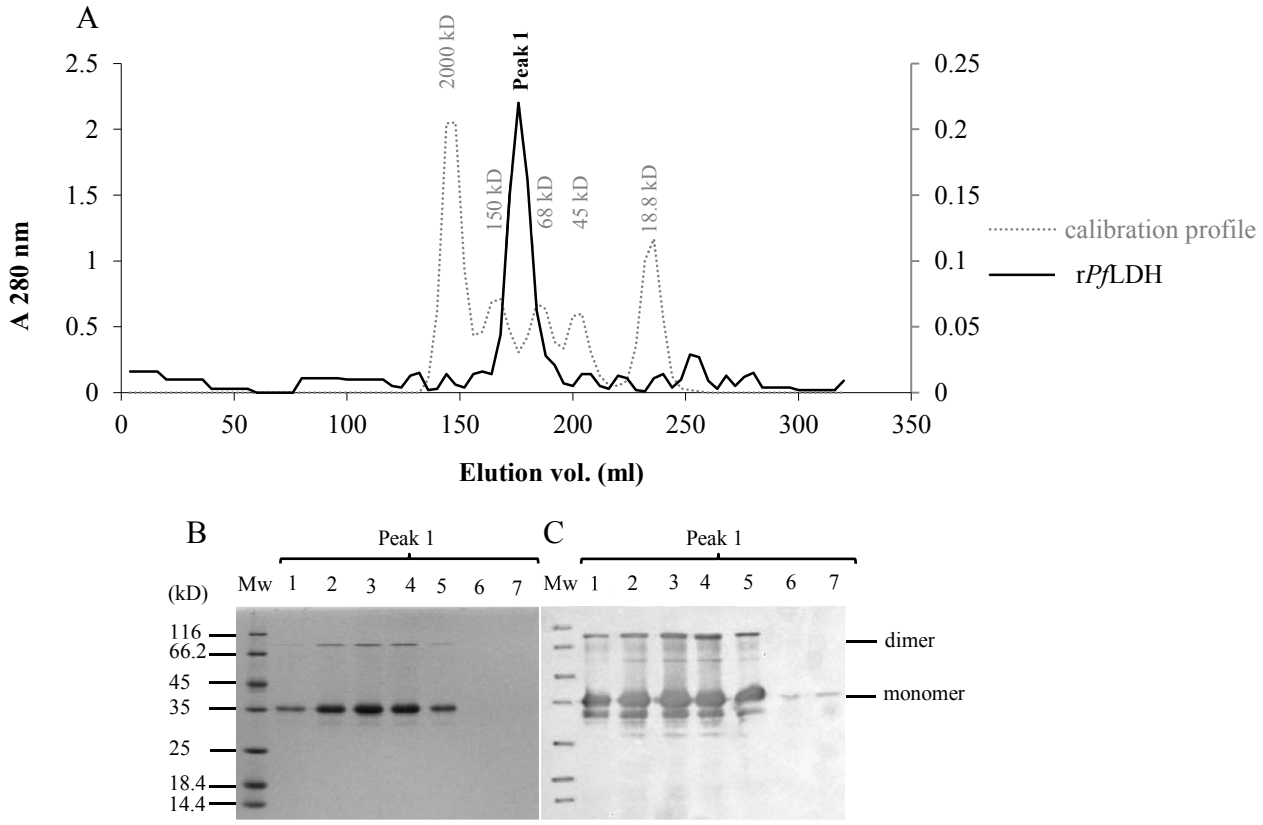


**Figure 3.8 rPfLDH forms tetramers in solution as shown by Sephacryl S200 gel filtration.**
Affinity purified r*Pf*LDH was run over a Sephacryl S200 column. The r*Pf*LDH elution profile was plotted in (A), where the column calibration profile was plotted on the primary y-axis. The sizes of the standard proteins used for the column calibration were labelled above their respective peaks. The eluents comprising peak 1 in (A) were run on a reducing 12.5 % SDS-PAGE gel (B) and detected on a Western blot with anti-r*Pf*LDH IgY and secondary rabbit-anti-chicken HRPO antibody at 1/12000 (C). The molecular weight standards (Mw) used were labelled on the left of the gels in kilo Daltons (kD).

Recombinant *Pf*LDH (Figure 3.8 (A)) eluted from the Sephacryl S200 column as a large sharp peak estimated to be 140 kD in size. Berwal *et al.,* (2008) obtained a peak of around 145 kD. Peak 1 had a shoulder which may have been the dimeric form of the protein which would have eluted at around 70 kD. The remainder of the peaks are minor and were not evaluated. Peak 1 was run on an SDS-PAGE gel and blotted as shown in the same figure (B and C respectively). The major bands ran at around 36 kD and 75 kD. A minor band was also detected just below the 35 kD marker (approximately 33 kD) as seen in the previous blots in Figure 3.5.

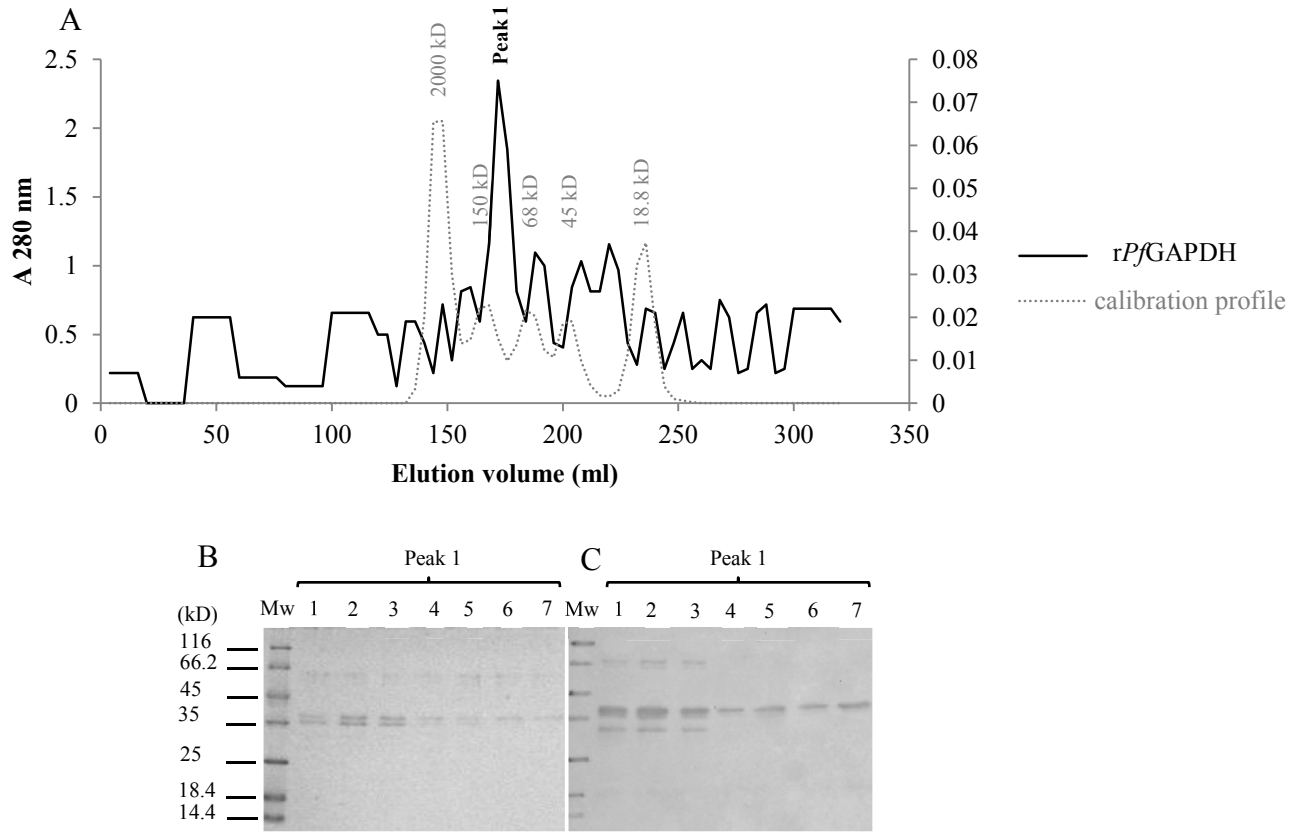


**Figure 3.9 rPfGAPDH forms tetramers in solution as shown by Sephacryl S200 gel filtration.**
Affinity purified r*Pf*GAPDH was run over a Sephacryl S200 column. The elution profile was plotted in (A), where the column calibration profile was plotted on the primary y-axis. The sizes of the standard proteins used for the column calibration were labelled above their respective peaks. The eluents comprising peak 1 in (A) were run on a reducing 12.5 % SDS-PAGE gel (B) and detected on a Western blot with anti-r*Pf*GAPDH IgY and secondary rabbit-anti-chicken HRPO at 1/12000 (C). The molecular weight standards (Mw) used were labelled on the left hand side of the gels in kilo Daltons (kD).

Recombinant *Pf*GAPDH (Figure 3.9 (A)) eluted from the Sephacryl S200 column as a large sharp peak estimated to be 140 kD in size. Satchell *et al.,* (2005) obtained a tetramer form of around 130 kD. Peak 1 was run on an SDS-PAGE gel and blotted as shown in the same figure (B and C respectively). The major bands ran at around 39 kD and 70 kD. A second band was detected just below the 35 kD marker at around 33 kD.

### 3.3 Discussion

Since the expression plasmids were provided, both plasmids were tested to ensure they contained the correct coding sequences. The coding sequence for *Pf*LDH is 951 bp in length and that of *Pf*GAPDH is 1014 bp (PlasmoDB). The *Pf*LDH insert was approximately 950 bp in size, as determined by double restriction digestion, where the PCR amplicon was around 850 bp. The reason was that the primers used were generic/control primers for *Plasmodium* LDH and this size amplicon was expected after analysis of where they annealed within the coding sequence. Following unsuccessful restriction digestion of the *Pf*GAPDH plasmid with NdeI due to an apparent loss of the NdeI restriction site, an amplicon of around 1.2 kb was obtained for the PCR. This was larger than the literature value for the *Pf*GAPDH coding sequence, but was expected, however, as the pET primers should amplify an additional 322 bp outside of the coding region of the insert.

The gene inserts were then sequenced and showed high homology to the coding sequences of the respective proteins. Slight variation of the sequences may have been due to sequencing error. Single nucleotide errors within the Genbank database were assessed by Wesche *et al*., in 2004 who found there to be only approximately 0.1 % (SE 0.012%) error for coding DNA entries. Studies by Hill *et al*., 2000; Kristensen *et al*., 1992 and Lamperti *et al*., 1992 found errors between 3.1 to 3.6 %. Our sequencing results varied between 2 to 4 % from the coding sequences in PlasmoDB and NCBI. Comparison of the amino acid sequences of the different *P. falciparum* LDH and GAPDH orthologs revealed 99 % sequence identity. This supported results found by Lee *et al.,* in 2006 who reported that LDH from field isolates had conserved amino acid sequences and did not undergo antigenic variation.

Some expression parameters were assessed including the temperatures of the bacterial growth cultures as well as the pH and ionic strength of the protein isolation buffer. Lower incubation temperature of 30°C compared to 37°C produced more protein, similar to the result found by Schein and Noteborn in 1988, where Berwal *et al*., (2008) obtained the highest soluble yield of r*Pf*LDH using a 15°C culture incubation temperature. A further aspect of recombinant expression that can be optimised, which was not done in this study, is the media. Different proteins are expressed at different levels dependent on the media used and this can be assessed using a screen as described by Broedel *et al.,* in 2001. The solubility of proteins is dependent on their overall charge, which is affected by the pH of the buffer. The pI of *Pf*GAPDH is around pH 8.99 and that of *Pf*LDH around pH 8.5 (NCBI; Nirmalan *et al*,

2004), thus at pH 7.0 or 8.0 both proteins would have overall positive charges keeping them in solution in a low ionic strength buffer (Voet and Voet, 2004). At the same time for purification of His-tag proteins the pKa of imidazole, the side chain of histidine, is important as this interacts with the cobalt ion ($Co^{2+}$) on the affinity resin. The approximate pKa of imidazole is 6.04 (Voet and Voet, 2004). Therefore at a pH of 8.0 it will be neutral and have a higher affinity for the positive $Co^{2+}$ ion than at pH 7.0. This explained the larger purification yields for both proteins at pH 8.0 as opposed to pH 7.0. The improved solubility of both proteins when dialysed against a higher ionic strength buffer made use of the principle of "salting in" of proteins (Voet and Voet, 2004).

The *E. coli* BL21(DE3) expression host has several advantages. The *E. coli* BL21 strain is non-pathogenic and does not express ompT and lon proteases, which may digest the recombinant protein being expressed. Zymograms testing for protease activity of *E. coli* BL21(DE3) culture lysates were carried out by others in the lab and showed no activity. The (DE3) nomenclature means that the T7 RNA polymerase gene was lysogenized into the host *E. coli* BL21 genome (Sorensen and Mortensen, 2005).

"Leaky" expression was observed with both r*Pf*LDH and r*Pf*GAPDH proteins. This is a common phenomenon and is dependent on the promoters in the plasmid as well as the composition of the media. The plasmids here make use of either the *lac* promoter (pET-15b) or the *tac* promoter (pKK223-3), which is a hybrid of the *lac* and *trp* promoters (de Boer *et al.*, 1983). Both systems require the use of a lysogenized *E. coli* host strain, such as the BL21(DE3) strain used here. Transcription is inhibited in the absence of lactose by the LacI repressor, which binds the *lac/tac* operator. Low levels of glucose increase levels of cyclic adenosine monophosphate (cAMP) which also aids in *lac/tac* promoter repression (Sorensen and Mortensen, 2004). As IPTG, a metabolite of lactose, is added, it binds LacI allowing expression of T7 RNA polymerase from the *E. coli* BL21(DE3) genome and hence expression of the recombinant protein (Schumann and Ferreira, 2004; Sorensen and Mortensen, 2004). Alternate promoters such as $lacI^q$ and $lacI^{qI}$ have been used in the pET expression system, which result in higher LacI levels and thus reduce "leaky" expression (Schumann and Ferreira, 2004).

Native *Pf*LDH is around 34.4 kD in size (PlasmoDB). Berwal *et al.*, (2008) expressed *Pf*LDH with a single $His_6$-tag and found it to be approximately 36.3 kD in size. Hurdayal *et al.*, (2010) found that r*Pf*LDH expressed with 2 $His_6$-tags to be approximately 39 kD in size.

Western blots using both anti-r*Pf*LDH as well as anti-His-tag antibodies detected a major band of approximately 36 kD in this study. A second minor band of around 75 kD was also detected which may have been as a result of dimer formation. Zocher *et al*., (2012) observed dimers of recombinant *P. falciparum* glutamate dehydrogenase 1 on reducing SDS-PAGE gels which were detected by Western blotting, similar to what was seen here with r*Pf*LDH.

Detection of a second band just below the 35 kD band in the *Pf*LDH Western blots was similar to the result found by Berwal *et al.,* (2008); Hurdayal *et al.,* (2010) and Turgut-Balik *et al.,* (2004) and is thought to be a truncated form of the protein. This was due to an internal Shine Dalgarno sequence (GGAGGA) between bases 46 to 51 in the coding sequence for r*Pf*LDH. The reason it was also detected in the anti-His blots was as the r*Pf*LDH was expressed with two $His_6$ tags, thus the C-terminal $His_6$-tag would still have been detected.

A major band around 39 kD was detected on the r*Pf*GAPDH Western blots with both the anti-r*Pf*GAPDH and anti-His-tag antibodies. Both Satchell *et al.,* (2005) and Daubenberger *et al.,* (2003) expressed recombinant forms of around 36.6 kD in size.

Both recombinant proteins were shown to form tetramers in solution, despite the additional $His_6$-tags, estimated to be around 140 kD in size. This was similar to the results found by Satchell *et al.,* (2005) who estimated the tetramer for r*Pf*GAPDH to be approximately130 kD in size. The $His_6$-tag did have an effect on the quality of crystal in their study, however enzyme activity was not affected in a study by Daubenberger *et al.,* (2000). Similarly Berwal *et al.,* (2008) found r*Pf*LDH with a single $His_6$-tag to be approximately 145 kD in size and also enzymatically active.

In conclusion the coding sequences for both proteins were of the expected sizes and the sequence identity was confirmed by sequencing. The expressed proteins were detected by specific antibodies against the whole recombinant antigens as well as with anti-$His_6$-tag antibodies. An additional control for identification of the recombinant proteins would be to do N-terminal sequencing. Both proteins formed tetramers without removal of the $His_6$-tags being required, however to further assess the overall conformations of GAPDH and LDH, enzyme activity could be assessed as described by (Daubenberger *et al.*, 2000; Ferdinand, 1964) for GAPDH and (Berwal *et al.*, 2008; Gomez *et al.*, 1997) for LDH respectively.

# Chapter 4

# Identifying malarial peptide epitopes on lactate dehydrogenase and glyceraldehyde-3-phosphate dehydrogenase, and assessing Pheroids™ as an adjuvant in chickens

## 4.1 Introduction

Rapid diagnostic tests (RDTs) are lateral flow immunochromatographic tests which make use of monoclonal antibodies for diagnosis. The monoclonal antibodies are typically selected rather than starting with a unique epitope. As a result epitope mapping is done to determine the epitope target (Saravanan and Kumar., 2009). Knowing the target epitope is useful as often antigenic variation may affect detection of certain antigens. Histidine rich protein 2 (HRP2) is a common RDT target for diagnosis of *Plasmodium falciparum* malaria (Baker *et al*., 2010, Lee *et al*., 2006) and the target protein undergoes antigenic variation leading to false negative results. An alternative approach to monoclonal antibodies, and employed here, was to raise polyclonal antibodies against specific peptides from the target protein.

Tomar *et al.*, (2006) have validated the use of polyclonal antibodies raised against the peptides of malarial target proteins for diagnosis, and Hurdayal *et al*., (2010) demonstrated this for differentiation between malarial lactate dehydrogenases. Peptides used in diagnostics are typically 12 to 15 amino acids in length and are not large enough to elicit an immune response by themselves and so are coupled to a carrier protein such as rabbit albumin. Alternatively multiple antigenic peptides (MAPs) have been used. MAPs consist of an amino acid, usually alanine, linked to a resin bead, followed by several layers of lysine residues. The lysines then facilitate binding of multiple peptides and as a result coupling of peptides to carrier proteins is not required (Saravanan and Kumar 2009).

In a normal infection the malaria pathogen would provide various co-stimulatory signals such as pathogen associated molecular patterns (PAMPs) which promote the immunogenicity of antigenic proteins or peptides usually via Toll like receptors (De Gregorio *et al.*, 2009; Morein *et al.*, 2004; Palm and Medzhitov, 2009; Reed *et al.*, 2008). In the absence of the pathogen the individual proteins are not as immunogenic and an additional stimulant is required for the host to produce sufficiently high yields/titres of antibodies. For this purpose adjuvants are added to the antigens for immunisation.

Adjuvants are immune-enhancing substances, meaning that they promote an immune response to a particular antigen but don't have any antigenic effect themselves. There are 3 basic mechanisms by which adjuvants function, the first being by a depot effect (Reed *et al*., 2008). This describes the slow release of antigen from the immunisation site (Herbert, 1968) as adjuvants usually consist of a poorly degradable substance such as mineral oil in the case of Freund's adjuvant. The second function is to stimulate antigen uptake by antigen presenting cells (APCs) by providing stimulatory signals such as PAMPs which stimulate phagocytosis. The third mechanism is to promote the immune bias caused by the antigen alone, that is either humoral or cell mediated immunity (Wilson-Welder *et al*., 2009).

Two of the most common adjuvants used for raising antibodies are Freund's adjuvant, first described in 1937 (Gupta and Siber, 1995), and alum first described in 1926 (Glenny *et al.*, 1926). Freund's adjuvant has become a popular choice for use in research, as unlike alum, it is able to induce an immune response against peptide antigens coupled to protein carriers (Johansson *et al.*, 2004) making it ideal for this study. The antigen is encapsulated into the mineral oil component of the adjuvant via a surfactant mannide mono-oleate (Arlacel A). This makes up the incomplete adjuvant (FIA), where a second form, complete adjuvant (FCA), combines heat-killed *Mycobacterium* in the formulation (Gupta and Siber, 1995). Freund's falls under the vehicle type adjuvants as described by Reed *et al*., (2008), promoting either cellular or humoral immunity, depending on whether or not the *Mycobacterium* component is present (Johansson *et al.*, 2004). Due to the low purity mineral oil and emulsifier used in Freund's adjuvant, as well as the presence of *Mycobacterium* in the complete adjuvant formulation, site-specific hypersensitivity and granuloma formation are often observed. This makes it an unsuitable adjuvant for use in humans and it is being withdrawn for use in animals. Use of purer mineral and biodegradable oils such as squalenes and plant oils have been tested and showed reduced hypersensitivity (Johansson *et al.*, 2004; Reed *et al.*, 2008; Wilson-Welder *et al.*, 2009).

For a long time alum was the only adjuvant certified for use in humans (Lindblad, 2004), and a standard research formulation, Alhydrogel$^{TM}$, was chosen in 1988 (Gregoriadis *et al.*, 1989). Alum's ability to induce a strong humoral immune response as opposed to cell mediated immunity made it favourable for use in humans as it did not cause tissue hypersensitivity reactions. However, recent recordings of hypersensitivity reactions have been made (Gupta and Siber, 1995; Rimaniol *et al.*, 2004; Goldman and Lambert, 2004). Another drawback of

alum is that it is ineffective for use with peptide antigens, as well as DNA based vaccines (Wilson-Welder *et al.*, 2009). This has therefore placed pressure on finding better adjuvant formulations for use in humans as well as in experimental animals.

This chapter describes the selection of specific peptide epitopes of target proteins that were identified for malaria diagnosis, namely glyceraldehyde-3-phosphate dehydrogenase (GAPDH) and lactate dehydrogenase (LDH). The target proteins are conserved in all malarial species and epitopes were selected to be either a shared epitope (pan-malarial) or a species-specific epitope. Antibodies were raised in chickens against both whole recombinant proteins to evaluate the antibody responses using a potential new adjuvant called Pheroids™ compared to Freund's. Pheroids™ was developed by the University of the North West and is a liposome type delivery system composed of fatty acids, using nitrous oxide as an active ingredient (US Patent Application number 12280880).

## 4.2 Results

### 4.2.1 Peptide selection for raising species-specific and pan-malarial IgY

Two malarial proteins lactate dehydrogenase (LDH) and glyceraldehyde-3-phosphate dehydrogenase (GAPDH) were chosen as target antigens for malaria diagnosis. Alignments of the amino acid sequences were used to identify any potential peptides that could be used as target epitopes and included the *P. falciparum*, *P. vivax* and *P. yoelii* sequences as shown in Figures 4.1 and 4.4. To ensure that these sequences were unique to malaria, human (*Homo sapiens*) and mouse (*Mus musculus*) GAPDH and LDH were included. As the anti-peptide antibodies were to be raised in chickens, chicken GAPDH and LDH (*Gallus gallus*) were also included.

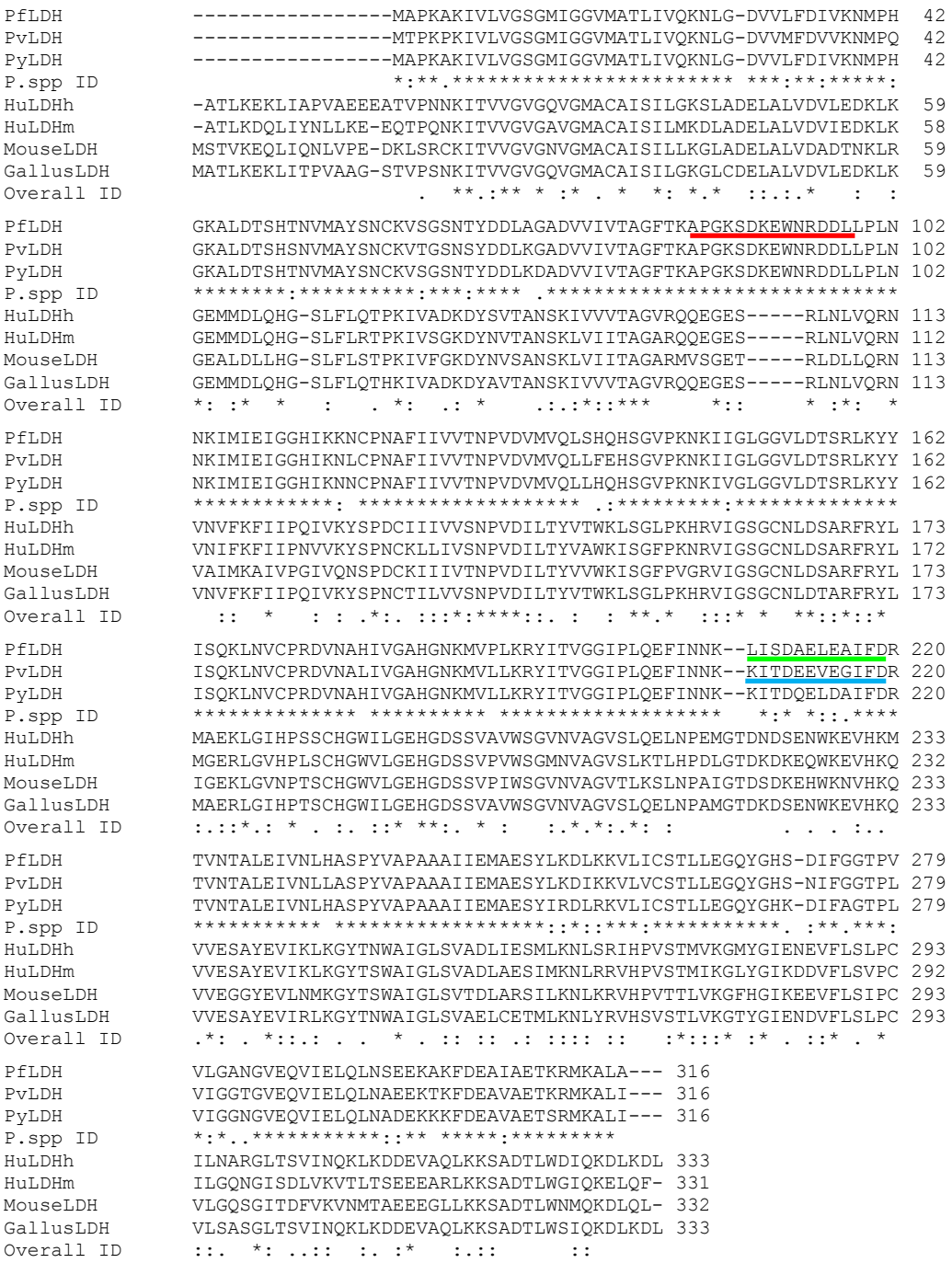


**Figure 4.1 Alignment of LDH amino acid sequences to select peptides for raising species-specific and pan-malarial antibodies in chickens.**

A multiple sequence alignment of the *P. falciparum* (PfLDH); *P. vivax* (PvLDH); *P. yoelii* (PyLDH), human heart (HuLDHh), human muscle (HuLDHm), chicken (GallusLDH) and mouse (MouseLDH) LDH amino acid sequences was done using ClustalW. Percentage identity (ID) was the first criterion for peptide selection and residues were annotated as follows: "*" identical residues; ":" conserved residues; "." semi-conserved residues and blank spaces represented no identity between the sequences. Percentage identity was assessed between the 3 malaria sequences (P. spp ID) and between all 7 LDH sequences (Overall ID). Specific peptides were selected based on lowest percentage identity and common peptides on 100 % identity between the malaria sequences. The three peptide sequences of interest were underlined in green and blue for the specific peptides and red for the common peptide. Sequence accession numbers are *Pf*LDH: PlasmoDB ID: PF13_0141; *Pv*LDH: PlasmoDB ID: PVX_116630; *Py*LDH: PlasmoDB ID: PY03885; Human heart LDH and muscle LDH respectively: NCBI ID: 1IOZ_B and 1 I1O_H; Chicken (*Gallus gallus*) LDH: NCBI ID: NP_989508.1; Mouse LDH: NCBI ID: NP_038608.1.

Based on the data in Figure 4.1 a species-specific peptide sequence was identified (amino acids 208 to 219) for both *P. falciparum* and *P. vivax* LDH. These were highlighted in green and blue in the figure respectively. The common sequence was underlined in red (amino acids 85 to 98) and was 100% conserved across all the malaria sequences. A BLASTp search in PlasmoDB with the peptide sequence also confirmed its conserved sequence across all 3 additional species of malaria affecting man, namely *P. ovale*, *P. malariae* and *P. knowlesi*, where the only difference was in the *P. malariae* sequence with the alanine residue being replaced by a valine which is a semi-conservative substitution (Table 4.1). The peptide included a 5 amino acid insert that was unique to the malarial LDH sequences, with a low overall identity with the rest of the non-malarial sequences shown. BLASTp searches in PlasmoDB revealed that the *P. vivax* peptide had 91 % identity with a *P. knowlesi* sequence, where the rest of the species-specific peptides had no identity with other human malaria species.

In addition to sequence alignment, the amino acids of the chosen peptide sequences were evaluated in an epitope prediction program Predict7$^{TM}$ to assess hydrophilicity, surface probability, antigenicity and flexibility as shown in Figure 4.2. All three peptides were synthesised with an additional cysteine residue at the C-terminus (as indicated by "C" in the figure) to facilitate coupling to rabbit albumin via M-maleimidobenzoil acid N-hydroxy succinimide ester (MBS).

The common APGKSDKEWNRDDL peptide with an identical sequence in all *Plasmodial* LDH proteins (Figure 4.2 (A)) showed good hydrophilicity and surface probability as the majority of the plots were above 0, with the highest values toward the N-terminal end of the peptide. As a result the cysteine was added to the C-terminus. The flexibility plot was poor with all values being $\leq 0$, where the antigenicity prediction had the majority of values just above 0, with a slight peak toward the C-terminus of the peptide.

The *P. vivax* specific peptide KITDEEVEGIFD showed an increase toward the N-terminus for all plots except flexibility, therefore the cysteine was added to the C-terminus. The hydrophilicity and surface probability plots were similar with the majority of values above 0. Antigenicity had no residues above 0 where flexibility values remained around 0 with a slight dip toward the middle of the sequence.

**Table 4.1 Alignments of the selected *Plasmodium* LDH and GAPDH sequences.**

| | Peptide name | | | | |
|---|---|---|---|---|---|
| ***Plasmodium* species** | **LDH specific** | **LDH common** | **GAPDH specific 1** | **GAPDH specific 2** | **GAPDH common** |
| *falciparum* | LISDAELEAIFD | APGKSDKEWNRDDL | ADGFLLIGEKKVSVFA | AEKDPSQIPWGKCQV | KDDTPIYVMGINH |
| *vivax* | KITDEEVEGIFD | APGKSDKEWNRDDL | GDGCFTVGNKKIFVHS | SEKDPAQIPWGKYEI | KDDTPIYVMGINH |
| *malariae* | KITDAELDAIFD | VPGKSDKEWNRDDL | GDGKIIVGNKTINIHN | NEKEPSQIPWGKYGI | KDDTPIYVMGINH |
| *ovale* | KITDAELDAIFD | APGKSDKEWNRDDL | – | – | – |
| *knowlesi* | KITDEEVEAIFD | APGKSDKEWNRDDL | GDGFFTIGNKKIFVHH | HEKDPANIPWGKYGI | KDDTPIYVMGINH |
| Percentage identity | *:* *::.*** | .********** | .** : :*:*.: :. | **:*::***** : | ********** |

A multiple sequence alignment of the *P. falciparum*; *P. vivax*; *P. malariae*; *P. ovale* and *P. knowlesi* LDH amino acid sequences was done using ClustalW. Percentage identity (ID) was annotated as follows: "*" identical residues; ":" conserved residues; "." semi-conserved residues and blank spaces represented no identity between the sequences. Sequence accession numbers are as follows: *Pf*LDH: ABH03417.1; *Pv*LDH: EDL45893.1; *Pm*LDH: AAS77572.1; *Po*LDH: AAS77571.1; *Pk*LDH: XP_002260092.1; *Pf*GAPDH: XP_001348772.1; *Pv*GAPDH: ABU50378.1; *Pm*GAPDH: ABU50375.1; *Pk*GAPDH: ABU50374.1; *Po*GAPDH: sequence was not yet available on NCBI or PlasmoDB (accessed 15.05.2012).

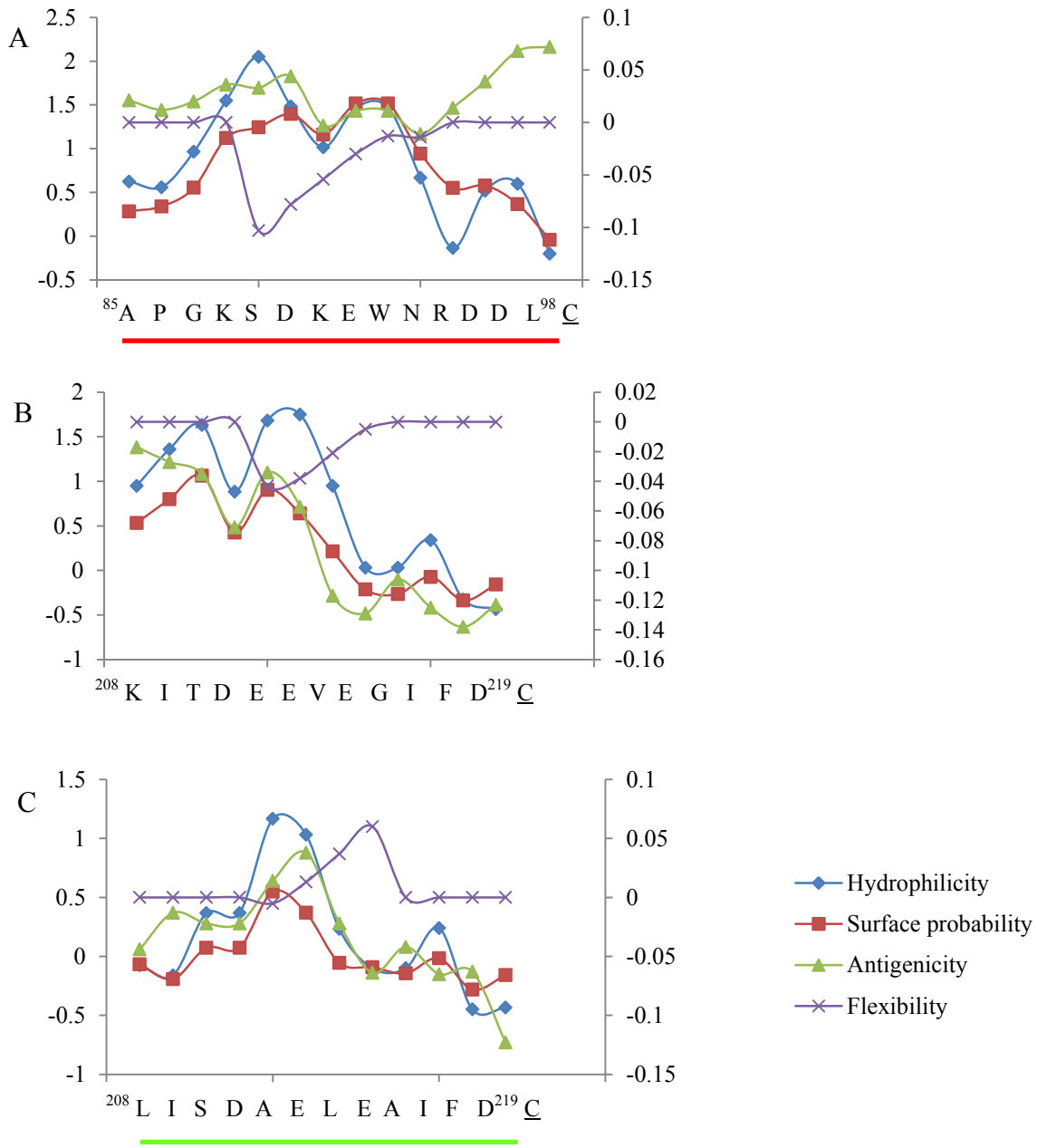


**Figure 4.2 Predict7$^{TM}$ analysis of three selected malaria LDH peptides.**
Predict7$^{TM}$ plots of the three LDH peptides illustrating hydrofilicity, surface probability, flexibility and antigenicity (key in the bottom right). The common peptide was plotted in (A), the *P. vivax* specific peptide in (B) and the *P. falciparum* specific peptide in (C). Flexibility and antigenicity were plotted on the secondary axes in each graph. The amino acid sequences were shown along the bottom of the graphs, with the first and last amino acid residues shown in superscript and the addition of a C-terminal cysteine was indicated with a "C" in each case.

The *P. vivax* specific peptide (Figure 4.2 (B)) and the *P. falciparum* specific peptide LISDAELEAIFD (Figure 4.2(C)) had very similar plots. This was expected due to the sequence similarity shared between these two peptides. The *P. falciparum* specific peptide had flexibility values around 0 and a slight peak toward the middle of the sequence. The other

three plots decreased toward the C-terminus, thus the cysteine was added to this end of the peptide. Hydrophilicity and surface probability plots had values above 0 for the majority of the sequence, whereas antigenicity was below 0.

The pan-malarial (APGKSDKEWNRDDL) and *P. falciparum* specific (LISDAELEAIFD) peptides (Figure 4.2 (A and C) respectively) were located on the surface of the 3D crystal structure model of *Pf*LDH published by (Dunn *et al*., 1996) as shown in Figure 4.3 and are therefore expected to be available for interaction with antibodies.

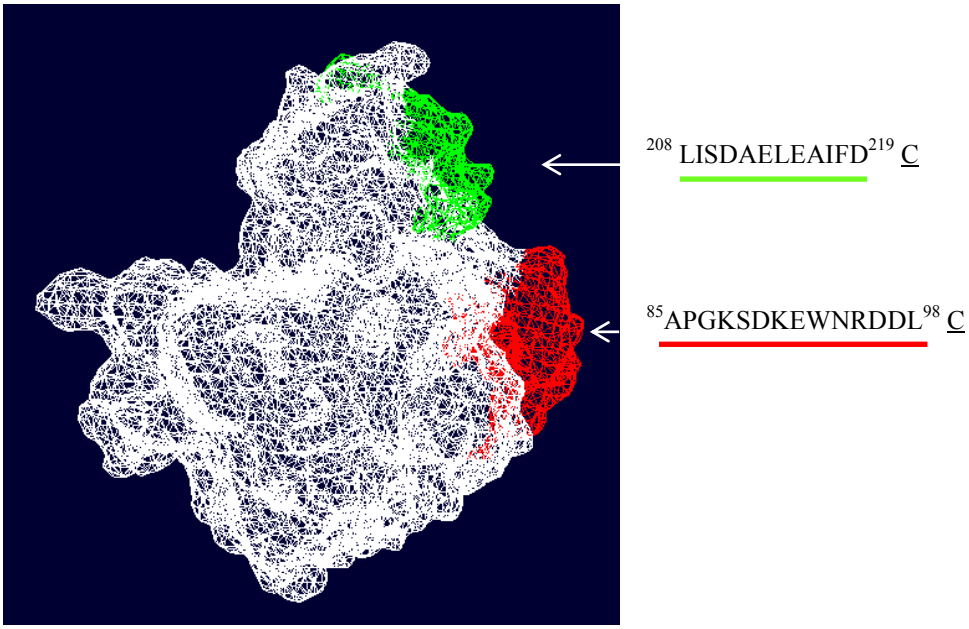


**Figure 4.3 Location of the *P. falciparum* specific and the pan-malarial epitopes on the 3D crystal structure model of *Pf*LDH.**
The selected peptide sequences were located on the surface of the 3D structure of *Pf*LDH (monomer) and highlighted in their corresponding colours (specific peptide in green and the pan-malarial peptide in red) on the structure using Swiss-Pdb viewer 4.0.1 (http://www.expasy.org.spdbv/). The amino acid sequences were shown alongside of the structure, with the first and last amino acid residues shown in superscript and the addition of a C-terminal cysteine indicated with a "C" in each case. Structural data (1t2d) obtained from swiss pdb.

The selection of common and specific peptides from the GAPDH sequence was shown in Figures 4.4 to 4.6 starting with the alignment of the sequences. Based on the data in Figure 4.4 two *P. falciparum* specific peptide sequences were identified, the first (amino acids 63 to 78), underlined in green and the second (amino acids 78 to 92) underlined in blue. The specific peptides showed no identity with any other human malaria species using a BLASTp search in PlasmoDB, where the pan-malarial peptide (amino acids 126 to 138) was common to all malaria sequences (Table 4.1).

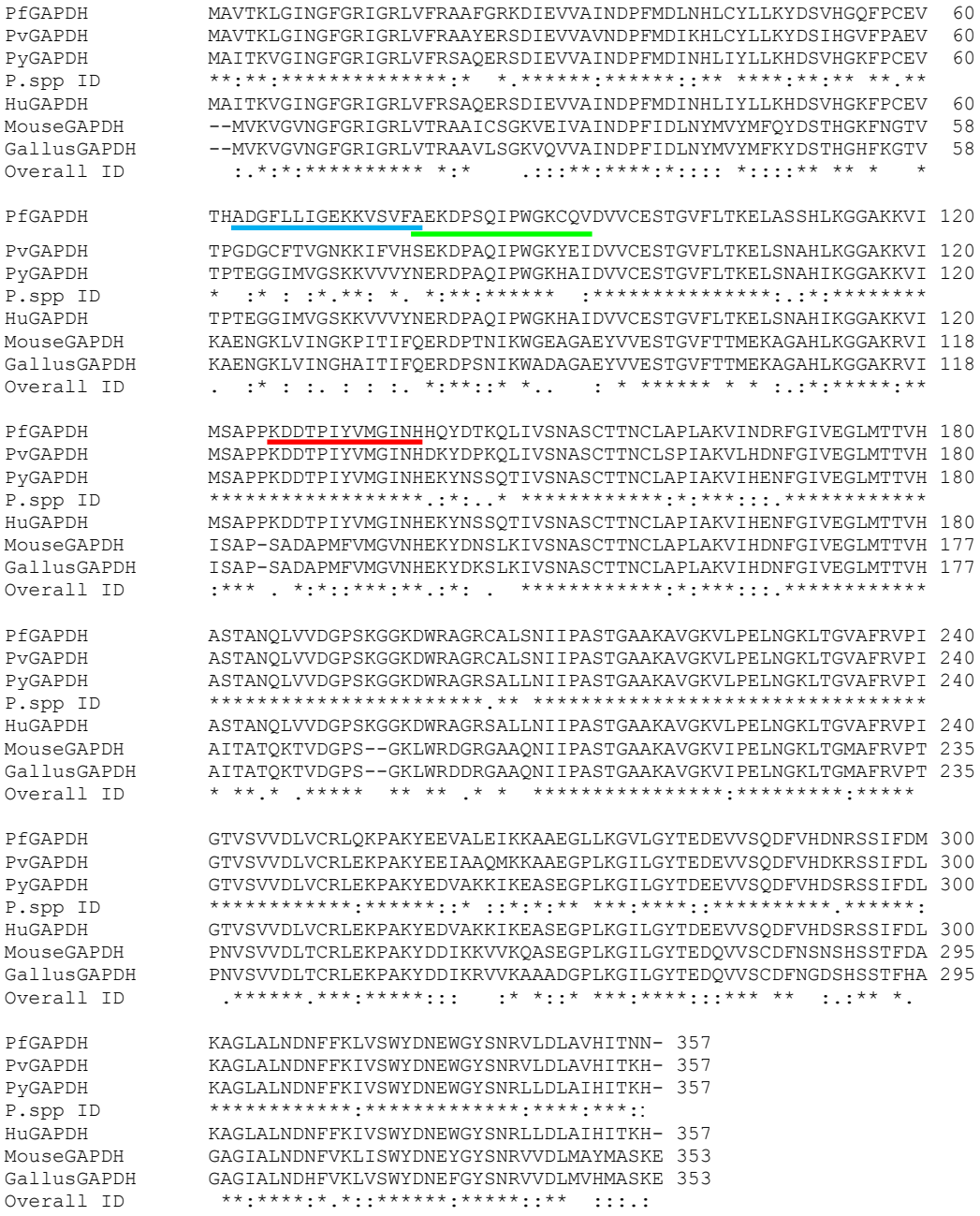


**Figure 4.4 Alignment of GAPDH amino acid sequences to select peptides for raising species-specific and pan-malarial antibodies in chickens.**

A multiple sequence alignment of the *P. falciparum* (PfGAPDH); *P. vivax* (PvGAPDH); *P. yoelii* (PyGAPDH), human (HuGAPDH), chicken (GallusGAPDH) and mouse (MouseGAPDH) GAPDH amino acid sequences was done using ClustalW. Percentage identity (ID) was the first criterion for selection and residues were annotated as follows: "*" identical residues; ":" conserved residues; "." semi-conserved r esidues and b lank s paces represented n o id entity b etween th e sequences. Percentage id entity was as sessed b etween t he 3 malaria sequences (P. spp ID) and between all 6 GAPDH sequences (Overall ID). Specific peptides were selected based on lowest percentage identity and common peptides on 100% identity between the malaria sequences. The three peptide sequences of interest were underlined in green and blue for the specific peptides and red for the common peptide. Sequence ac cession n umbers ar e *Pf*GAPDH: PlasmoDB I D: P F14_0598; *Pv*GAPDH: NCBI I D: ABU50378.1; *Py*GAPDH: PlasmoDB I D: P Y03280; Human GAPDH: NCBI I D: C AA25833.1; Chicken (*Gallus gallus*) GAPDH: NCBI ID: AAA48774.1; Mouse GAPDH: NCBI ID: NP_032110.1.

The GA PDH pe ptides were a nalyzed usin g P redict7™ as shown in Figure 4.5. All the peptides were synthesized with an additional cysteine residue at the N-terminus (as annotated with "C" in the figure) to facilitate coupling to rabbit albumin via MBS.

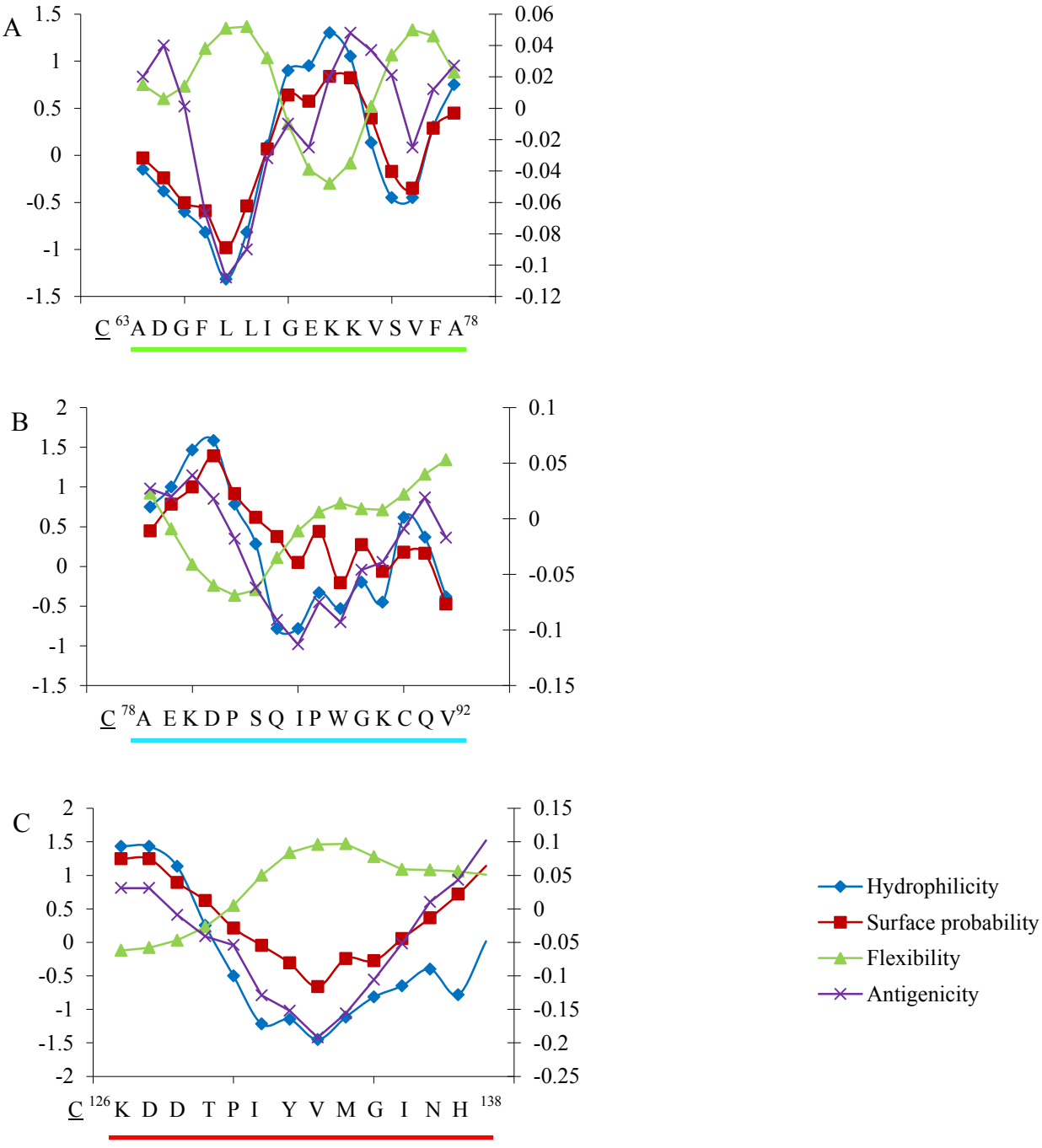


**Figure 4.5 Predict7™ analysis of three selected malaria GAPDH peptides.**
Predict7™ plots o f the th ree GAPDH p eptides illustrating h ydrofilicity, s urface probability, f lexibility an d antigenicity (key in the bottom right). The two *P. falciparum* specific peptides were plotted in (A and B) with the common p eptide plotted in ( C). Flexibility a nd a ntigenicity were p lotted o n t he s econdary a xes in ea ch graph. The amino acid sequences were shown along the bottom of the graphs, with the first and last amino acid residues shown in superscript and the addition of an N-terminal cysteine was indicated with a "C" in each case.

The first *P. falciparum* specific peptide ADGFLLIGEKKVSVFA (Figure 4.5 (A)) had similar flexibility at both ends. The hydrophilicity and surface probability plots increased toward the C-terminus however, with most points above 0 and therefore coupling to the N-terminus was chosen. The antigenicity plot had a similar trend, however, most values were below 0.

The second *P. falciparum* specific peptide AEKDPSQIPWGKCQV (Figure 4.5 (B)) had similar plots for all parameters except flexibility, with values around 0 throughout. Hydrofilicity and surface probability showed minor peaks toward the N-terminus, however flexibility was greatest toward the C-terminus, thus coupling to the N-terminus was chosen.

The pan-malarial peptide KDDTPIYVMGINH (Figure 4.5 (C)) showed high hydrophilicity and surface probability values toward the N-terminus. The antigenicity plot showed the majority of values below 0, whereas the flexibility had an increasing trend toward the C-terminus with the majority of values above 0, thus coupling to the N-terminus was chosen.

All 3 peptide sequences were located on the surface of the 3D crystal structure model of *Pf*GAPDH published by (Satchell *et al*., 2005) as shown in Figure 4.6 and are therefore expected to be available for interaction with antibodies.

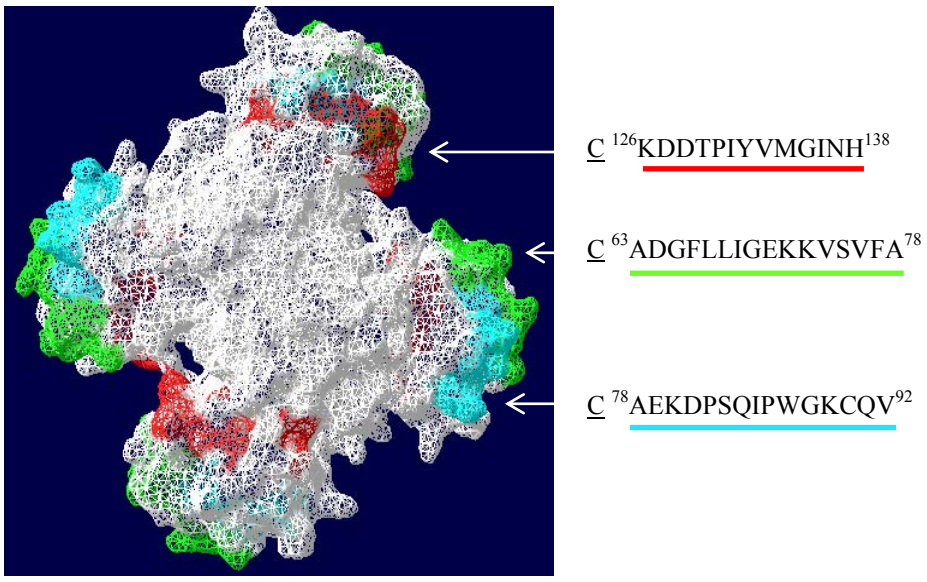


**Figure 4.6 Location of the *P. falciparum* specific and the pan-malarial epitopes on the 3D crystal structure of *Pf*GAPDH.**
The selected peptide sequences were located on the surface of the 3D structure of *Pf*GAPDH (tetramer) and highlighted in their corresponding colours on the structure using Swiss-Pdb viewer 4.0.1 (http://www.expasy.org.spdbv/). The amino acid sequences were shown alongside of the structure, with the first and last amino acid residues shown in superscript and the addition of an N-terminal cysteine indicated with a "C" in each case. Structural data (1ywg) obtained from swiss pdb.

### 4.2.2 Anti-LDH peptide antibody production and final yields of affinity-purified IgY

Antibodies against the malaria LDH peptides coupled to rabbit albumin (RA) were raised in chickens using Freund's adjuvant. Antibody production against the peptides was measured and shown in Figure 4.7, followed by affinity purification of the respective anti-peptide antibodies shown in Figure 4.8. The chickens immunised with the *P. falciparum* specific peptide were named FDC1 and 2. Those immunised with the pan-malarial peptide were named APG 1 and 2 and those immunised with the *P. vivax* specific peptide were named KIT 1 and 2. Chicken APG2 stopped laying eggs completely and FDC2 stopped laying eggs from week 4 to 8. The chicken names and their respective anti-LDH peptides were shown in Table 4.2.

**Table 4.2 Chickens immunised with the respective anti-LDH peptides.**

| Chicken names | Peptide sequence | Peptide description |
|---|---|---|
| FDC 1 and 2 | $^{208}$LISDAELEAIFD$^{219}$ C | *P. falciparum* specific |
| APG 1 and 2 | $^{85}$APGKSDKEWNRDDL$^{98}$ C | Pan-malarial |
| KIT 1 and 2 | $^{208}$KITDEEVEGIFD$^{219}$ C | *P. vivax* specific |

In Figure 4.7 antibody titres against the carrier rabbit albumin was followed as a control. The titre of anti-albumin IgY followed a similar trend to the anti-peptide IgY titres for the 3 experiments except in the case of the APG group, where the anti-albumin antibody titres increased before the anti-peptide IgY titres. Anti-peptide IgY titres seemed to rise latest in the APG 1 chicken in comparison to all other groups, with a peak observed as late as week 8. In comparison the KIT 1 and 2 chickens produced anti-peptide antibodies the earliest of the groups, with initial peaks observed at weeks 6 and 4 for the two chickens respectively. The FDC1 chicken showed an initial anti-peptide IgY peak at week 6, where FDC2 only started laying eggs again at week 9, and showed high antibody production through to week 12. IgY isolated between weeks 4 to 12 were pooled and affinity purified using the specific peptide-coupled SulfoLink® affinity matrix.

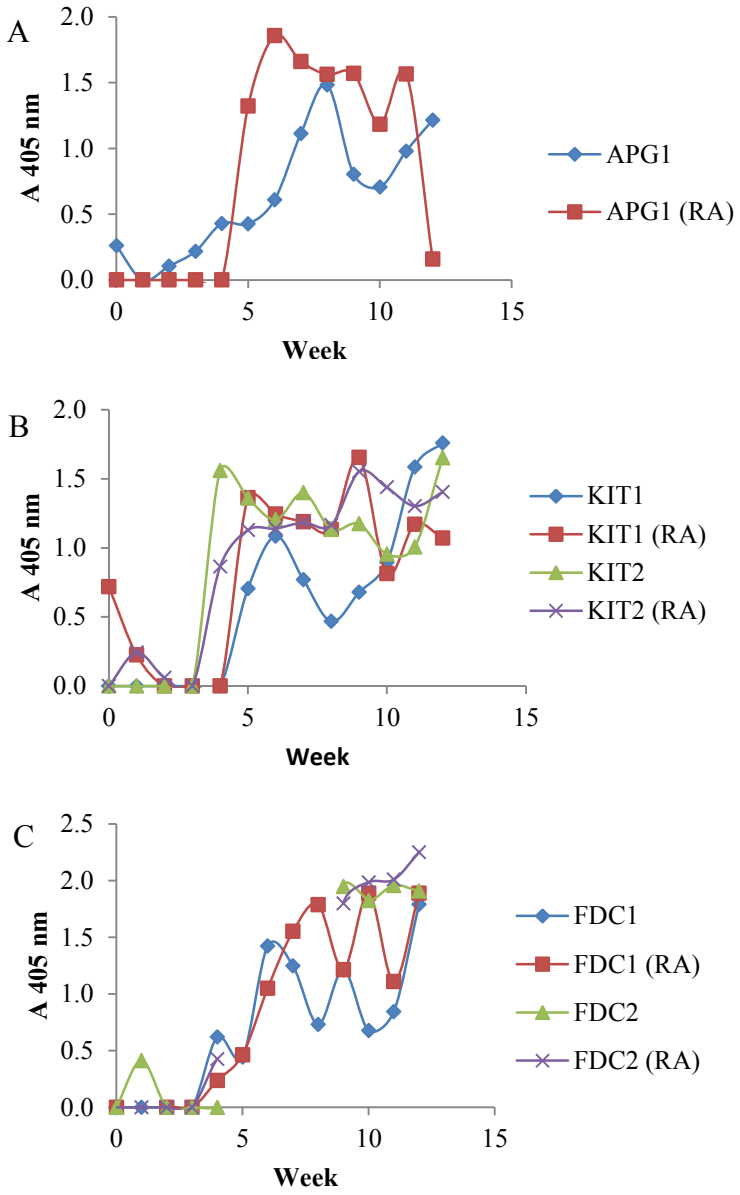


**Figure 4.7 Measuring anti-LDH peptide and anti-RA carrier antibody production in chickens.** Peptides were coupled to rabbit albumin (RA) for immunisation and two chickens were immunised per peptide on weeks 0, 2, 4 and 6 using Freund's adjuvant. Crude IgY was isolated from each from weeks 0 to 12. Titres of specific anti-peptide IgY was measured by direct ELISA. Plates were coated with the respective peptides at 1 µg/ml and rabbit albumin at the same concentration as a control (RA). Crude primary IgY samples were added at 100 µg/ml and detected with a rabbit-anti-chicken-IgY-HRPO secondary antibody at 1/15000 dilution. Weeks showing high antibody titres against the peptide were pooled for affinity purification. The titres shown in (A) were for chicken APG 1; (B) was for chickens KIT 1 and 2 and (C) was for chickens FDC 1 and 2.

The elution profiles were shown in Figure 4.8 and the overall yields were recorded in Table 4.3.

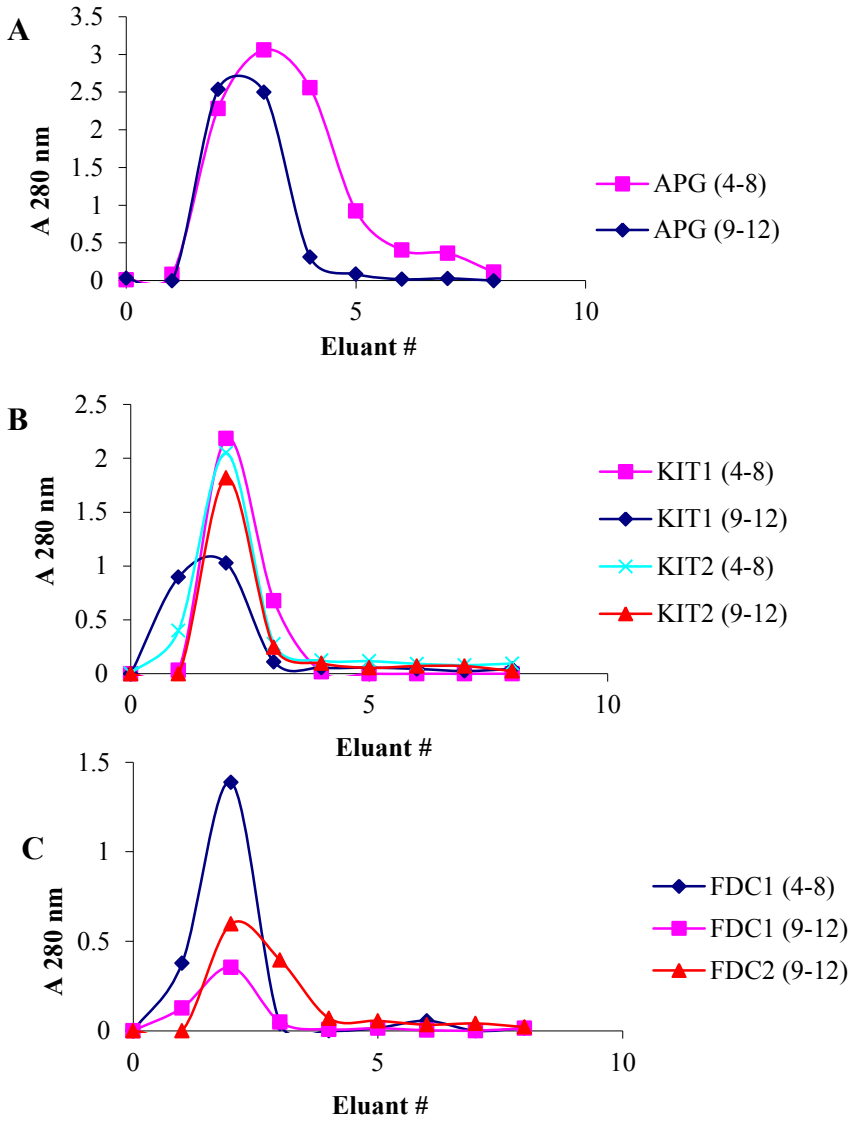


**Figure 4.8 Elution profiles after affinity purification of anti-LDH peptide antibodies (IgY).** Crude IgY was isolated from weeks showing high specific antibody titres. Pooled IgY from weeks 4 to 12 post immunisation were affinity purified by passing over peptide-linked SulfoLink® columns. The elution profile in (A) was for the pan-malarial (APGKSDKEWNRDDL) peptide; (B) was for the *P. viva x*-specific (KITDEEVEGIFD) peptide and (C) was for the *P. falciparum*-specific (LISDAELEAIFD) peptide.

A high yield of 18.1 mg was obtained for the anti-APGKSDKEWNRDDL IgY (Figure 4.8 (A)), followed by the anti-KITDEEVEGIFD IgY (Figure 4.8 (B)) with 11.4 mg and the anti-LISDAELEAIFD specific IgY (Figure 4.8(C)) with a yield of 2.6 mg as recorded in Table 4.2.

**Table 4.3: Yields of affinity purified IgY raised against the selected LDH peptides.**

| LDH sequence origin | Accession number (PlasmoDB) | Peptide sequence | Yield of affinity purified IgY (mg) |
|---|---|---|---|
| *P. falciparum* (3D7) | PF13_0141 | $^{208}$ LISDAELEAIFD$^{219}$ C | 2.6 |
| *P. vivax* (Sal1) | PVX_116630 | $^{208}$ KITDEEVEGIFD$^{219}$ C | 11.4 |
| Pan-malarial | | $^{85}$APGKSDKEWNRDDL$^{98}$ C | 18.1 |

The antibodies against the selected GAPDH peptides were raised previously and for that reason the data was omitted. However antibodies against the C$^{63}$ADGFLLIGEKKVSVFA$^{78}$ peptide have not been raised and will be raised and affinity purified in future work.

### 4.2.3 Comparison of Pheroids$^{TM}$ and Freund's adjuvants

Pheroids$^{TM}$ and Freund's adjuvants were compared and to do this, chickens were immunised with recombinant *Pf*LDH or *Pf*GAPDH (r*Pf*LDH or r*Pf*GAPDH). From the alignments of the respective amino acid sequences in Figures 4.1 and 4.4 the GAPDH sequences were more conserved than the LDH sequences sharing 64 % identity, whereas the LDH sequences shared only 32 % identity with the chicken sequences.

The resulting antibody titres in chickens following immunisation with the respective recombinant proteins and adjuvant were shown in Figure 4.9 and 4.10. Chicken 2 in the Freund's + r*Pf*LDH group stopped laying eggs from week 3 to 9, and chicken 3 in the PBS + r*Pf*GAPDH control group stopped laying eggs from week 3 onwards.

All the immunised chickens with antigen-adjuvant preparations showed an earlier initial rise in antibody titres in comparison to the antigen alone (Figure 4.9). The initial peaks reading were observed around weeks 2 to 4. The highest titres were observed for the Freund's + r*Pf*LDH group, with the titres ranging from 0.8 to 1.4. This was followed by the PBS + r*Pf*LDH control group with peaks ranging from 0.8 to 1.2 and then the Pheroids$^{TM}$ + r*Pf*LDH group with the majority of the values ranging from 0.4 to 0.7. The chickens immunised with antigen-adjuvant preparations had sustained antibody titres over the 12 week period, compared to those immunised with antigen alone.

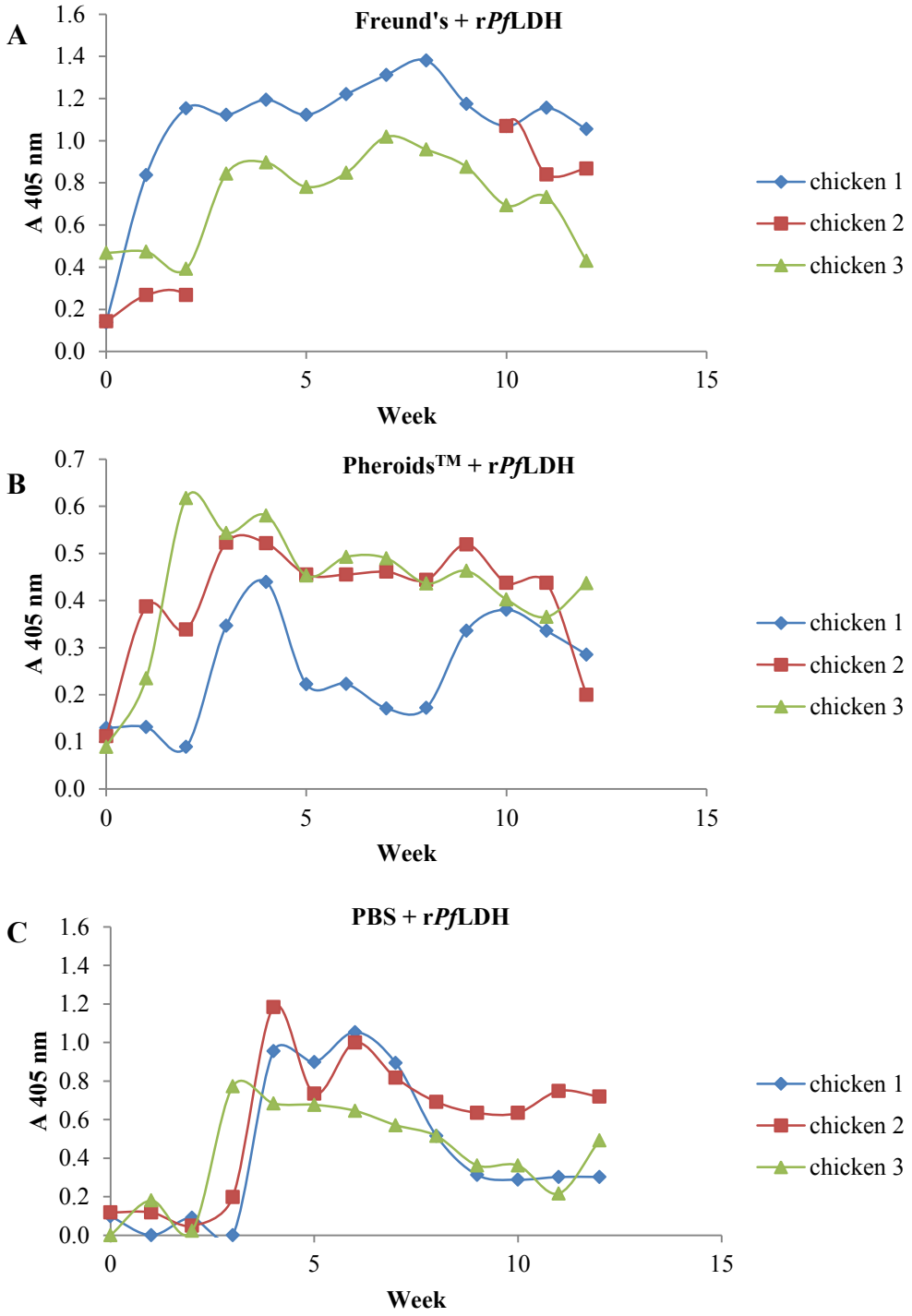


**Figure 4.9 Antibody titres in eggs from chickens immunised with r*Pf*LDH using either Freund's or Pheroids™ as adjuvant, or the recombinant protein alone in PBS.**
All chickens were immunised on the same day (week 0) and antibody titres were measured post immunisation. Three chickens were immunised per group and booster immunisations were given on weeks 2, 4 and 6. All groups were immunised with r*Pf*LDH as the antigen, and the groups were based on the adjuvant used, showing (A) the Freund's adjuvant group, (B) the Pheroids™ group and (C) the PBS group. Chickens immunised with Freund's adjuvant were immunised with the complete adjuvant for primary immunisations and the incomplete adjuvant for booster immunisations. Crude IgY was isolated from eggs at the end of each week from weeks 0 to 12. IgY titres against r*Pf*LDH were measured by direct ELISA using a rabbit-anti-chicken-IgY-HRPO secondary antibody at 1/15000 dilution.

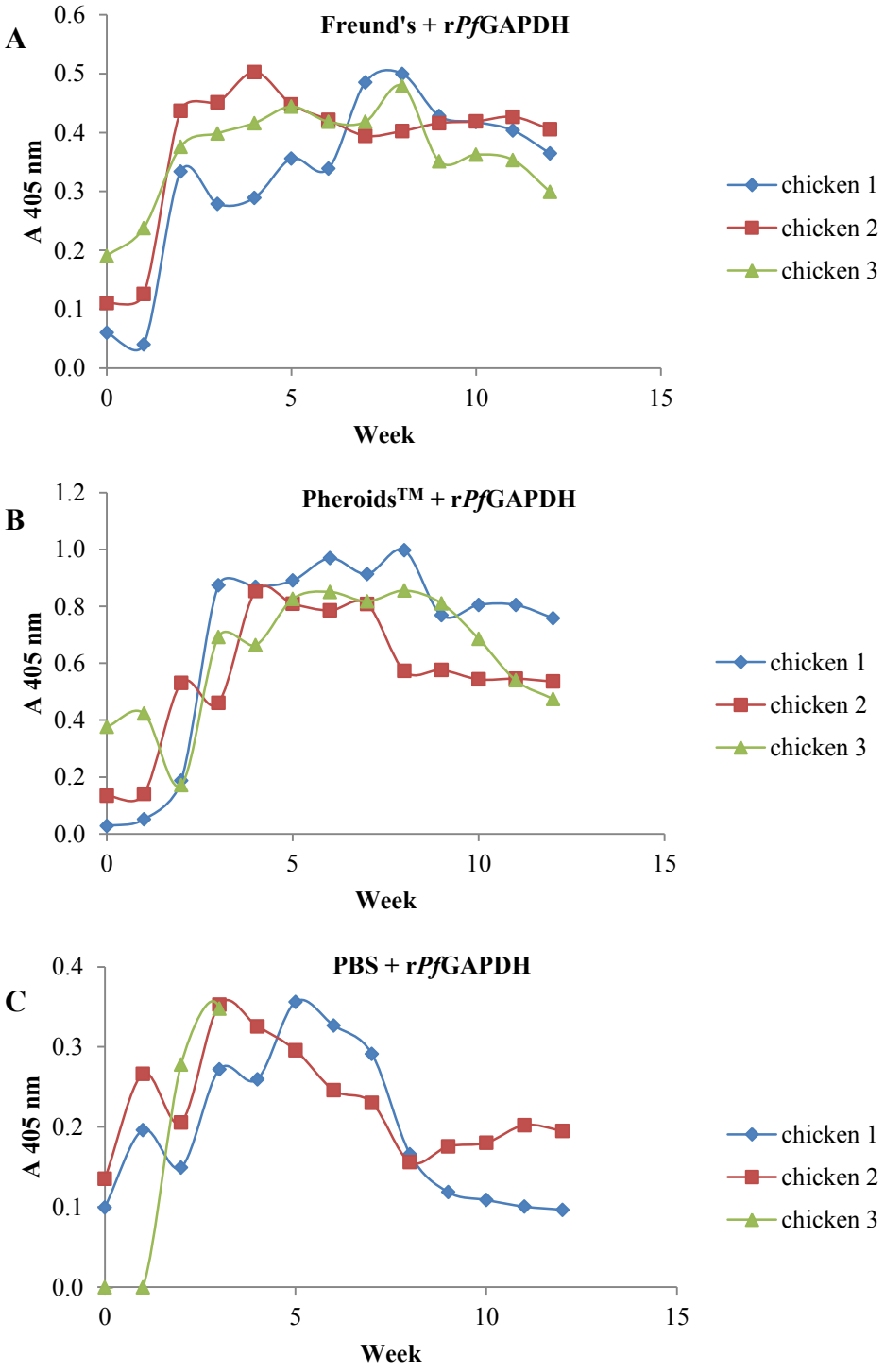


**Figure 4.10 Antibody titres in eggs from chickens immunised with r*Pf*GAPDH using either Freund's or Pheroids™ as adjuvant, or the recombinant protein alone in PBS.**
All chickens were immunised on the same day (week 0) and antibody titres were measured post immunisation. Three chickens were immunised per group and booster immunisations were given on weeks 2, 4 and 6. All groups were immunised with r*Pf*GAPDH as the antigen, and the groups were based on the adjuvant used, showing (A) the Freund's adjuvant group, (B) the Pheroids™ group and (C) the PBS group. Chickens immunised with Freund's adjuvant were immunised with the complete adjuvant for primary immunisations and the incomplete adjuvant for booster immunisations. Crude IgY was isolated from eggs at the end of each week from weeks 0 to 12. IgY titres against r*Pf*GAPDH were measured by direct ELISA using a rabbit-anti-chicken-IgY-HRPO secondary antibody at 1/15000 dilution.

The resulting titres for chickens immunised with the r*Pf*GAPDH antigen followed a similar trend to r*Pf*LDH (Figure 4.10). All chickens showed rapid increase in antibody titres with an initial peak between weeks 2 to 3. The $A_{405}$ values were highest for the chickens immunised with Pheroids™ + r*Pf*GAPDH (0.6 to 1.0). This was followed by the group immunised with Freund's + r*Pf*GAPDH (0.3 to 0.5) and finally the PBS + r*Pf*GAPDH control group (0.3 to 0.4). The PBS + r*Pf*GAPDH control group again showed a decrease antibody titre earlier in the experiment than the adjuvant-antigen groups.

Antibodies isolated from eggs for weeks 3 to 7 and 8 to 12 were pooled for affinity purification of the anti-r*Pf*LDH and anti-r*Pf*GAPDH antibodies. The elution profiles of the specific anti-recombinant antibodies off their respective AminoLink® affinity columns were shown in Figures 4.11 and 4.12.

Elution peaks within the group of chickens immunised with r*Pf*LDH were highest for the chickens immunised with Freund's, followed by the Pheroids™ and the control group (Figure 4.11).

Chickens immunised with r*Pf*GAPDH (Figure 4.12) also showed highest elution peaks when immunised with Freund's, followed by the Pheroids™ and the antigen control group respectively.

To compare total antibody yields, eluents from the affinity matrix with $A_{280}$ values greater than 0.1 were pooled and the final IgY yield was determined per chicken and evaluated against initial yolk volume, since the number of eggs laid per chicken varied, the yields were expressed as mg IgY / ml yolk and the results shown in Figure 4.13. As a control an ELISA was performed with the unbound samples after affinity purification and showed little or no $A_{405}$ above background (data not shown).

Chickens in each group showed varied IgY responses. Chickens immunised with Freund's adjuvant showed a significant difference in IgY yields compared to the control group immunised with antigen alone. There was an increased IgY yield for the chickens immunised with Pheroids™, however this was not statistically different to the response in the control group.

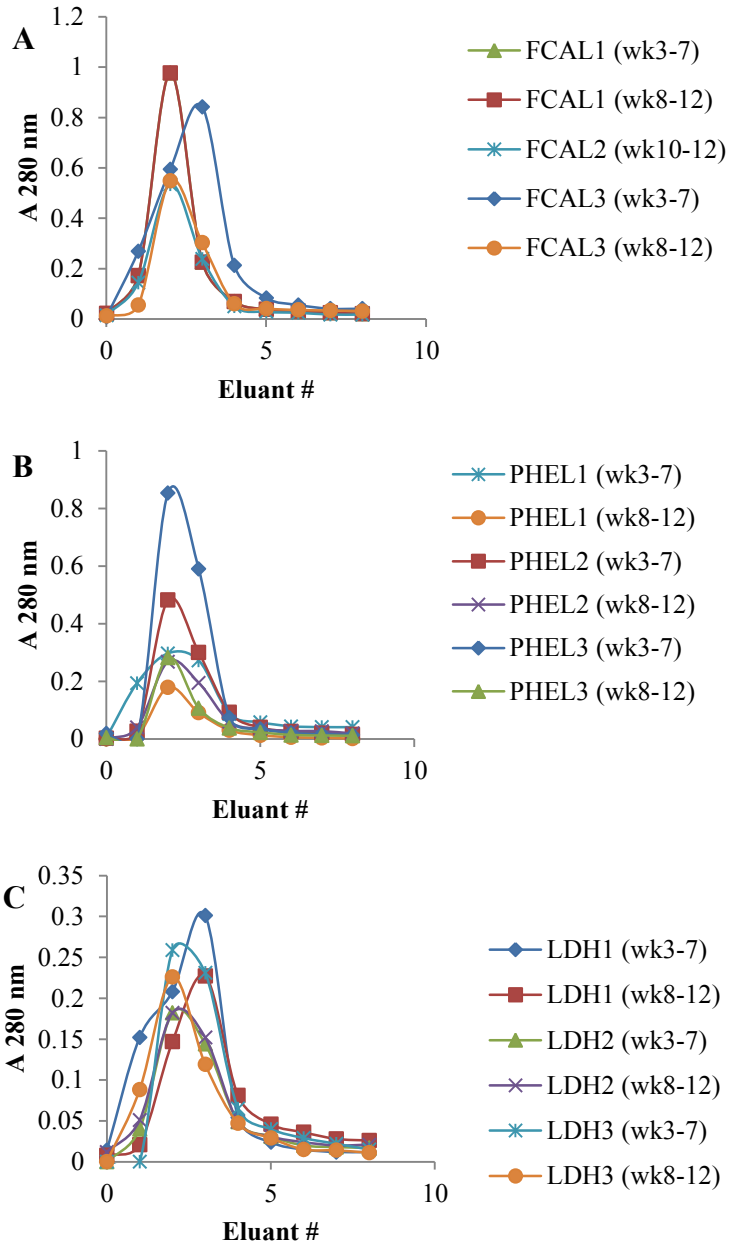


**Figure 4.11 Affinity purification of anti-r*Pf*LDH IgY from chickens immunised with Freund's, Pheroids™ or antigen alone.**
Crude IgY isolated from eggs collected between weeks 3-7 and 8-12 were pooled and circulated over a recombinant *Pf*LDH AminoLink® matrix overnight. The columns were then washed with PBS until $A_{280}$ values of the eluents were between 0.01-0.02, at which point the bound anti-r*Pf*LDH-IgY was eluted using Glycine HCl at pH 2.8, and fractions were collected. (A to C) show antibodies raised using Freund's or Pheroids™ as adjuvant or r*Pf*LDH alone for immunisation respectively.

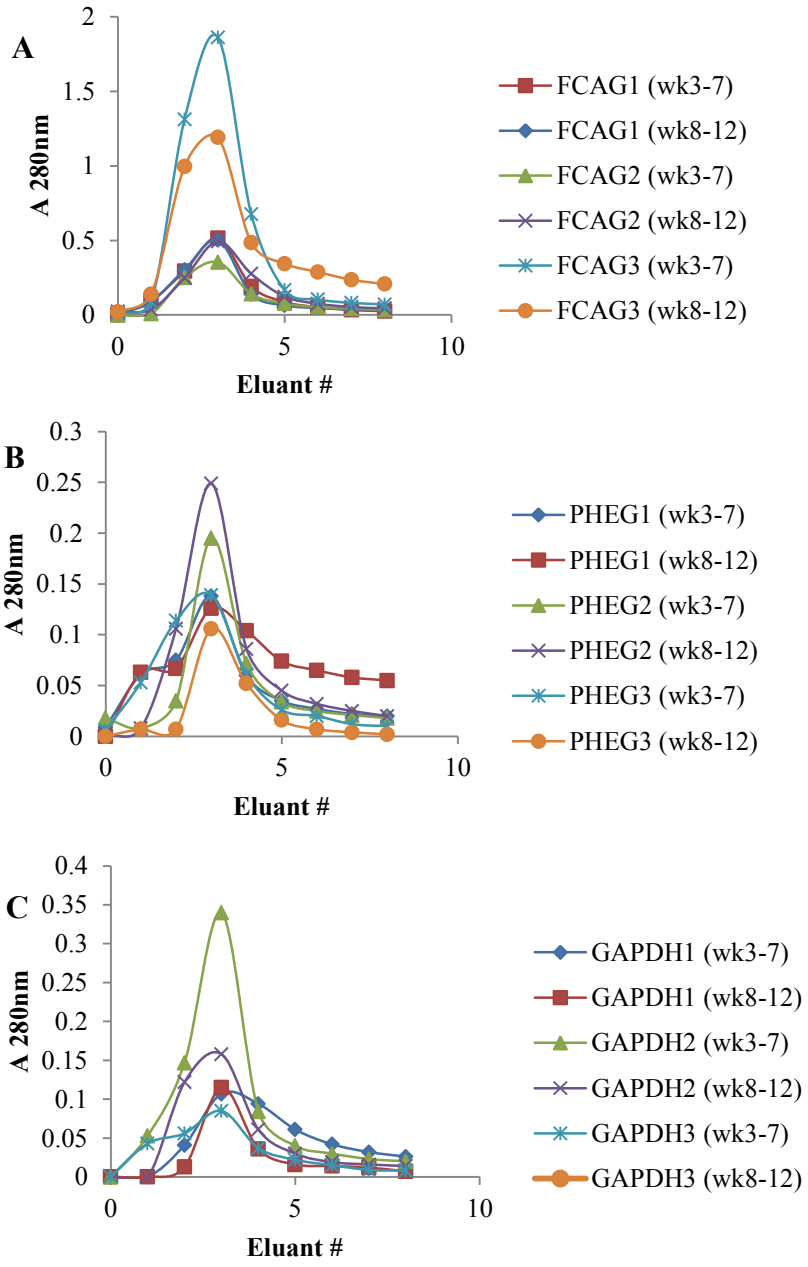


**Figure 4.12 Affinity purification of anti-recombinant GAPDH IgY from chickens immunised with Freund's, Pheroids™ or antigen alone.**
Crude Ig Y isolated from eggs collected between weeks 3 -7 and 8 -12 were pooled and circulated over a recombinant *Pf*GAPDH AminoLink® matrix overnight. The columns were then washed with PBS until $A_{280}$ values of the eluents were between 0.01-0.02, at which point the bound anti-r*Pf*GAPDH-IgY was eluted using Glycine HCl at pH 2.8, and fractions were collected. (A to C) show antibodies raised using Freund's or Pheroids™ as adjuvant or with r*Pf*GAPDH alone for immunisation respectively.

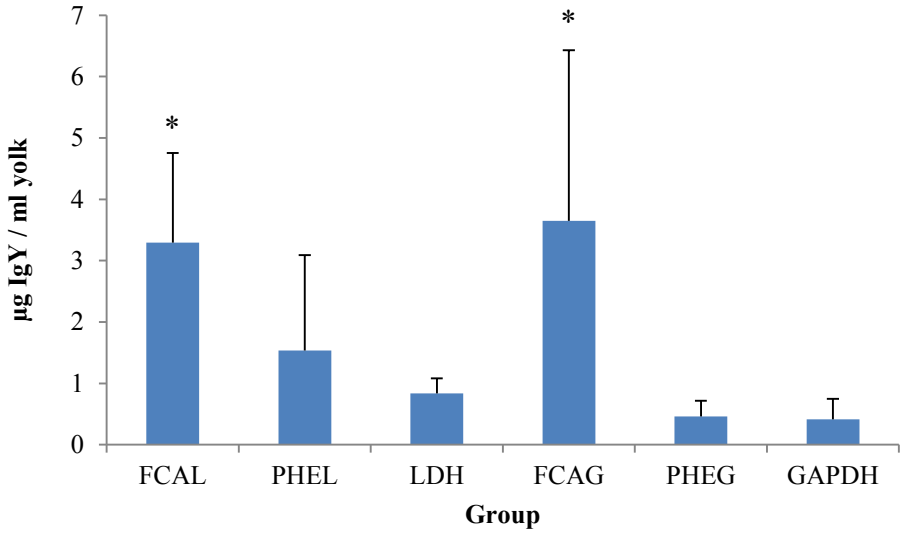


**Figure 4.13 Final yields of affinity purified IgY raised against r*Pf*LDH or r*Pf*GAPDH as antigens, from chickens immunised with Freund's, Pheroids™ or PBS.**
Chickens were immunised with either r*Pf*LDH or r*Pf*GAPDH and were separated into groups of 3 depending on whether they were immunised with Freund's adjuvant (FCAL/G) or Pheroids™ (PHEL/G) or antigen alone (LDH/GAPDH). Final affinity purified IgY yields against the respective antigens were presented as mg IgY / ml yolk due to a variation in egg production per chicken. A significant increase in yield with respect to the control group ($p < 0.05$) was annotated with "*".

Antibodies were raised against recombinant *P. falciparum* heat shock protein 70 (*Pf*Hsp70) for use as a loading control in enhanced chemiluminescence work. The antibody production was measured (Figure 4.15 (A)) and the resulting elution profile of affinity purified anti-r*Pf*Hsp70 IgY was shown in (B) of the same figure. The overall yield of affinity purified anti-r*Pf*Hsp70 IgY was 7.17 mg of affinity purified anti-r*Pf*Hsp70 IgY from two chickens.

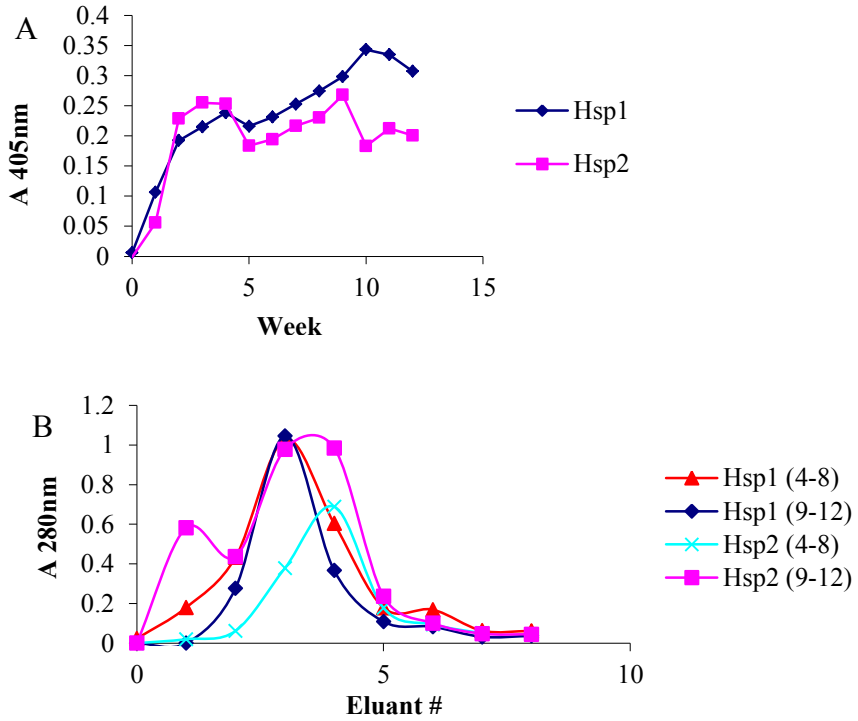


**Figure 4.14 Measure of anti-r*Pf*Hsp70 IgY titres and affinity purification of anti-r*Pf*Hsp70 IgY.** Two chickens were immunised with r*Pf*Hsp70 on weeks 0, 2, 4 and 6 using Freund's complete and incomplete adjuvant. Crude IgY was then isolated from single eggs at the end of each week from weeks 0 to 12. Specific IgY responses were measured by direct ELISA and plotted in (A). Plates were coated with recombinant *Pf*Hsp70 at 1µg/ml. Crude primary IgY samples were added at 100µg/ml and detected with a rabbit-anti-chicken-IgY-HRPO secondary antibody at 1/15000 dilution. Weeks showing specific antibody production were then pooled and affinity purified on a recombinant *Pf*Hsp70 AminoLink® matrix. The elution profile was plotted in (B).

## 4.3 Discussion

In this chapter both anti-peptide as well as anti-recombinant (whole protein) chicken antibodies were raised against *Pf*LDH and *Pf*GAPDH. Antibodies were raised against recombinant proteins for use as the capture antibody in diagnostics, and to compare a new adjuvant, called Pheroids™.

To identify appropriate peptide targets, multiple sequence alignments, an epitope prediction program (Predict7™) and the 3D crystallographic data of both target proteins were used. From the sequence alignments, regions of conserved amino acids were identified between the *Plasmodium* species which would allow detection of all *Plasmodium* orthologs of the target proteins. These were designated pan- or common peptides. Alternatively regions of variable amino acid sequences, which were not conserved between the *Plasmodium* species, were identified as species-specific peptides. The chosen peptides ranged in size from 13 to 17 amino acids including the additional cysteine residues added during synthesis.

The potential peptide targets were then analysed using Predict7™. This program overlaps 7 amino acids of the protein primary sequence at a time. Each amino acid side chain has unique properties and these are compared in an algorithm in the Predict7™ program (Cármenes *et al*., 1989). The algorithm predicts secondary structure, such as alpha-helix or beta-sheet (Chou and Fasman, 1978); surface probability (Kyte and Doolittle, 1982; Emini *et al.*, 1985); hydrophilicity (Hopp and Woods, 1981) and antigenicity (Jameson and Wolf, 1988).

Hydrophilicity and surface probability are indicators of likely peptide location within the overall protein structure. All peptides had values above 0 for these two parameters indicating that they were likely to be located on the surface and are also likely to be soluble for use in an ELISA. Surface location of the peptides is essential in order for antibodies to easily recognise and bind their epitopes on the native proteins in solution (Saravanan *et al.*, 2009). The Predict7™ results were also used to decide on the orientation of coupling, either N- or C-terminal to rabbit albumin. This was done with the aim of exposing the end of the peptide with highest antigenicity to the immune system. To support the Predict7™ data all the *P. falciparum* peptides were found to be on the surface of the 3D crystal structure models of their respective proteins. Experimental confirmation of the surface antigenicity of the peptide antigens is shown in chapter 5.

Overall the polarity of the peptide structures seemed to correlate with the antibody yields, where the order was APGKSDKEWNRDDL > KITDEEVEGIFD > LISDAELEAIFD. The

APGKSDKEWNRDDL peptide had 7 charged polar amino acid side chains, followed by KIT with 6 and FDC with 4.

The LDH amino acid sequence contained a 5 amino acid insert which was not found in the non-malarial sequences in the alignment, but was conserved across all human malarial species as confirmed using a BLASTp search. This sequence is found within the active site of *Plasmodial* LDH and affects the substrate and cofactor specificity of the enzyme (Gomez *et al.*, 1997). BLASTp searches in PlasmoDB with the *P. falciparum* LDH specific peptide (LISDAELEAIFD) showed no identity with other human malaria species, where the *P. vivax* sequence (KITDEEVEGIFD) showed 91 % identity with the *P. knowlesi* sequence, suggesting cross reactivity may occur and will have to be assessed. *P. knowlesi* infections have been detected with LDH and aldolase based RDTs (Kawai *et al.*, 2009; van Hellemond *et al.*, 2009). BLASTp searches with the GAPDH peptides showed the common *Plasmodial* GAPDH peptide to be 100 % conserved, within the *Plasmodium* sequences sequenced to date. The *P. falciparum* sequences showed no identity with any other human malaria sequences. *P. vivax* specific sequences can be identified as the corresponding sequence to the *P. falciparum* specific peptides in the GAPDH alignment, however they should still be assessed using Predict7™.

The European Centre for the Validation of Alternative Methods in 1993 outlined the 3 R's associated with the use of experimental animals in research, these are: refine, reduce and replace. Choosing the chicken as the experimental animal for antibody production has an advantage due to the higher yields of antibody, with approximately 7 times greater yields from egg yolk in comparison to rabbit serum for example (Schade *et al.*, 1991). This also eliminates the need to bleed the animals. Finding an alternative to Freund's adjuvant would address the hypersensitivity reactions associated with its use (Wilson-Welder *et al.*, 2009). Freund's is often associated with granuloma formation at the site of immunisations and these have been recorded to last up to 2 years in humans (Chapel and August, 1976). Granulomas were also observed in this study within the Freund's groups, with none observed in the Pheroids™ and no-antigen control groups, but these disappeared over the course of the experiment.

Sustained antibody titres were observed in chickens immunised with Freund's and Pheroids™ where, in comparison, titres in the control groups decreased rapidly. This was suggestive of the depot effect for both adjuvants which is a function of adjuvants (Reed *et al.*,

2008). The depot effect was first described as a possible mode of action for Freund's adjuvant by Herbert in 1968, who observed the slow and sustained release of ovalbumin from the site of immunisation in mice. These findings were similar to those seen in a study by Sun *et al.,* in 2008 between adjuvant and no-adjuvant control groups. In the same study Sun *et al.,* observed a one week lag in specific IgY production, where our results showed similar trends between weeks 2 and 3.

The final antibody yields against the whole recombinant proteins showed Freund's to be superior to Pheroids™. Yields were expressed in relation to egg yolk volume as yolk volume has been shown to be directly proportional to antibody yield (Li *et al.*, 1998). There was a statistically significant difference between the yields for the chickens immunised with Freund's adjuvant and the control groups. The results for the chickens immunised with Pheroids™ were slightly higher than those for antigen alone, but were not statistically significant. This showed that Freund's stimulated a more aggressive humoral immune response than Pheroids™. This may be due to the strong initial stimulation caused by the Freund's complete adjuvant due to the presence of the heat killed *Mycobacterium*. To improve the immune stimulation by Pheroids™ alternate methods may be used such as mannosylation. This has been used in conjunction with similar microsphere delivery systems to target mannose receptors in macrophages (Jiang *et al.*, 2007). Another alternative may be the addition of a saponin such as Quil A (Demana *et al.*, 2004).

Pheroids™ has been used as a drug delivery system, similar to other liposome or lipid based systems that have been used as adjuvants such as immunostimulatory complexes (ISCOMs) (Demana *et al.*, 2004; Fernando *et al.*, 1995; Reed *et al.*, 2008; Wilson-Welder *et al.*, 2009). Liposome delivery systems function by fusing with the host cell membrane after phagocytosis and releasing the antigen into the cell cytoplasm. Particle size is important as it affects phagocytosis and antigen delivery (Demana *et al.*, 2004). This may have had an effect in this study and alternate methods of preparation as opposed to trituration may result in increased antibody yields.

The method of antigen delivery is important as it determines the presentation pathway used by antigen presenting cells. Internal antigens are processed and presented by the major histocompatibility complex I (MHC I), whereas external antigens are presented by MHC II. This in turn affects the host immune response bias. The delivery mechanism employed by Pheroids™ suggests an MHC I biased response whereas Freund's should promote an MHC II

response. Presentation with MHC I promotes a cell mediated immune response where presentation with MHC II promotes a humoral immune response (Delves *et al*., 2006; McNeela and Mills, 2001; Reed *et al.*, 2008; Wilson-Welder *et al*., 2009). Cross-presentation is where an MHC I presentation may result in humoral and an MHC II in cell mediated immunity responses are also possible (Guermonprez *et al.,* 2003; Houde *et al.,* 2003). Future studies could thus focus on the effect of Pheroids™ on cytokine expression by monocytes and perhaps inclusion of additional stimulatory substances such as quil A or mannose. Assessing possible differences in affinities between antibodies raised using the two adjuvants should also be done.

Although not suited to antibody production, comparison of Pheroids™ to other lipid-based adjuvants such as ISCOMs may be warranted as these can potentially be used in oral vaccines (Demana *et al.*, 2004; Reed *et al.*, 2008). In developing a malaria vaccine, a school of thought is to elicit a cell mediated immune response as opposed to a humoral-dominated response (Friesen *et al.*, 2010). Pheroids™ may offer an alternative adjuvant in such an instance. Further comparison and characterisation of the anti-recombinant and anti-peptide antibodies raised would also be of interest. In the following chapter both antibodies are used for detection and quantification of the malaria diagnostic target *Pf*LDH compared to *Pf*GAPDH.

# Chapter 5

# Detection and quantitation of native *Pf*GAPDH and *Pf*LDH using both anti-peptide and anti-recombinant chicken antibodies

## 5.1 Introduction

Throughout its lifecycle the malaria parasite requires different proteins in order to carry out various functions. According to the central dogma of molecular biology (Crick, 1970), genes are transcribed into messenger RNA (mRNA) and then translated into protein. Various studies have been performed on the malaria transcriptome (Bozdech *et al.*, 2003; Le Roch *et al.*, 2003), and the data has been used to identify protein targets for drug assays, vaccine development and molecular markers.

According to Bozdech *et al.*, (2003), the majority of *Plasmodium* proteins are instantly translated from their respective transcripts. It has since been shown that parasite mRNA levels are not always directly proportional to protein levels due to posttranscriptional and posttranslational regulation of gene expression (Foth *et al.*, 2008; Hall *et al.*, 2010; Jackson *et al.*, 2011; Nirmalan *et al.*, 2004). A study by Mackinnon *et al.,* in 2009 showed that there were variations between levels of gene expression in long-term laboratory cultured *Plasmodium* isolates compared to field isolates (Mackinnon *et al.*, 2009). The studies by Le Roch *et al.,* and Bozdech *et al.,* in 2003 were both done using the *P. falciparum* 3D7 and HB3 strains laboratory isolates respectively. As a result the transcriptional data are used as a starting point for identifying target genes. *Plasmodium falciparum* glyceraldehyde-3-phosphate dehydrogenase (*Pf*GAPDH) was chosen as a potential new target for malaria diagnosis as it was shown to be between 2.4 to 8 times more abundant than *Plasmodium falciparum* lactate dehydrogenase (*Pf*LDH) from transcription data (Le Roch *et al.,* 2003).

The *Plasmodium* proteome has been studied using semi-quantitative protein analyses involving two-dimensional gel electrophoresis and mass spectrometry (Aebersold and Mann, 2003; Lasonder *et al.*, 2002; Nirmalan *et al.*, 2004; Smit *et al.*, 2009). These methods allow for the quantification of relative amounts of protein, usually with respect to the initial ring stage of the parasite and thus give an idea of up- or down-regulation of protein levels throughout the life cycle. This can be compared to mRNA levels and gives an idea as to whether the gene is regulated after transcription. In the case of *Pf*GAPDH and *Pf*LDH, both transcript and protein expression levels showed increasing trends from the ring to

trophozoite stages of the parasite life cycle (Smit S. *et al*., 2009, Nirmalan *et al*., 2004) supporting the initial transcription data from Le Roch *et al*., (2003).

Quantitation of individual proteins still relies on specific methods. A popular strategy uses antibodies for the detection of antigens, in an ELISA assay (van Weemen and Schuurs, 1971). The antibodies have to be characterised to establish affinities or avidities for target antigens (Pereira Arias-Bouda *et al*., 2003; Ferreira and Katzin, 1995).

An antigen generally contains a number of potential epitopes which are each recognised by an individual B-cell clone. Each B-cell clone in turn produces an epitope specific antibody, hence the name monoclonal antibody (Pluschke *et al*., 1998). The strength of the interaction between a single antibody and its specific epitope is defined as its affinity, which is also used to describe the strength of a monoclonal antibody binding its epitope. Alternatively polyclonal antibodies are raised from an entire subset of B-cells (hence the term polyclonal). As a result the polyclonal antibodies produced may all be specific to the same antigen, but recognise different epitopes and therefore have different individual affinities for the same antigen. The sum of the individual affinities of a group of polyclonal antibodies for the same antigen is defined as avidity (Delves *et al*., 2006; Ferreira and Katzin, 1995; Pereira Arias-Bouda *et al.*, 2003).

A typical IgG antibody molecule is divalent and has the ability to bind two epitope regions on an antigen and can, in theory, bind two antigen molecules or alternatively bind strongly to a single antigen if the epitope is repeated. As a result the antigen binding capacity of an antibody in solution is dependent on the antibody concentration and the binding efficiency is dependent on the affinity/avidity of that antibody as well as its valence (Delves *et al.*, 2006). Malaria rapid diagnostic tests (RDTs) capture and detect malarial antigens from infected blood lysates using antibodies (Murray and Bennett, 2009; Murray *et al*., 2008). As a result RDT sensitivity is a function of: 1) antibody affinity/avidity for its target antigen; 2) antibody valence and 3) the concentration of the target antigen within the test sample.

As with any antibody based test, however, RDTs also have limits of detection. HRP-2 based tests have been shown to be affected by a phenomenon called the prozone effect (Gillet *et al.*, 2009), where LDH and aldolase based tests were unaffected. The prozone effect describes the appearance of faint positive or even false negative results due to high antigen concentration within hyper-parasitemia samples for example, as shown in Figure 5.1.

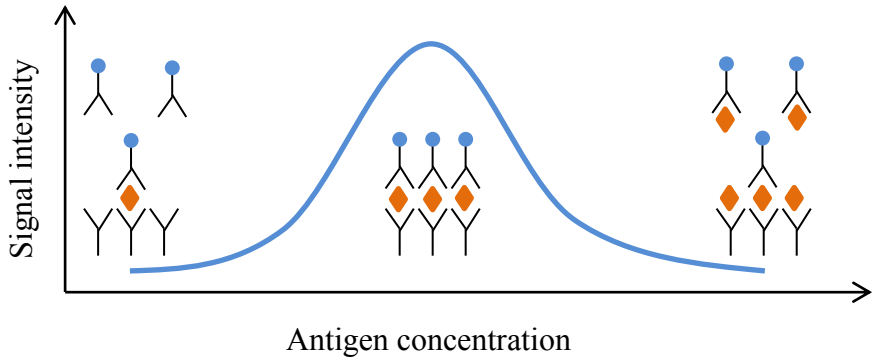


**Figure 5.1 A simplistic representation of the prozone effect on antibody-based antigen capture and detection assays.**
A defined concentration of capture antibody ( ) and detection antibody ( ) are used to detect antigen ( ). Signal intensity is represented by the blue line and is dependent on the ratio of antigen to antibody concentrations.

From Figure 5.1 too little antigen (far left) gives a faint signal and equal concentrations of antigen to antibody gives the strongest signal (middle). As the antigen becomes excessive, the detection antibody-antigen ratio becomes diluted and a faint signal results (far right). This phenomenon (far right) is known as the prozone effect (Gillet *et al.*, 2009). The concentration of HRP-2 to LDH has been quantified as approximately 6:1 (Martin *et al.*, 2009), explaining the sensitivity of the HRP-2 based tests to the prozone effect, which is easily rectified by simple dilution of test samples.

Direct quantitation and comparison of *Pf*LDH and *Pf*GAPDH proteins have not been made to date. The aim in this section was to compare their concentrations in parasite lysate material using antibody based detection methods. Such detection would mimic that of a malarial RDT format and would allow for more accurate conclusions about *Pf*GAPDH as a new RDT target in comparison to *Pf*LDH.

## 5.2 Results

*Pf*GAPDH and *Pf*LDH both have similar molecular masses of around 35 kD therefore not allowing for their differentiation based on size on reducing SDS-PAGE gels. Since the aim was to compare the concentrations of both native proteins in *P. falciparum* lysate samples, it had to be ensured that the antibodies used were not cross-reactive. Control Western blots were therefore run using both anti-peptide and anti-recombinant whole protein antibodies raised previously.

### 5.2.1 Characterising antibodies

Both anti-recombinant as well as anti-peptide antibodies were tested for cross-reactivity against r*Pf*GAPDH and r*Pf*LDH (Figure 5.2).

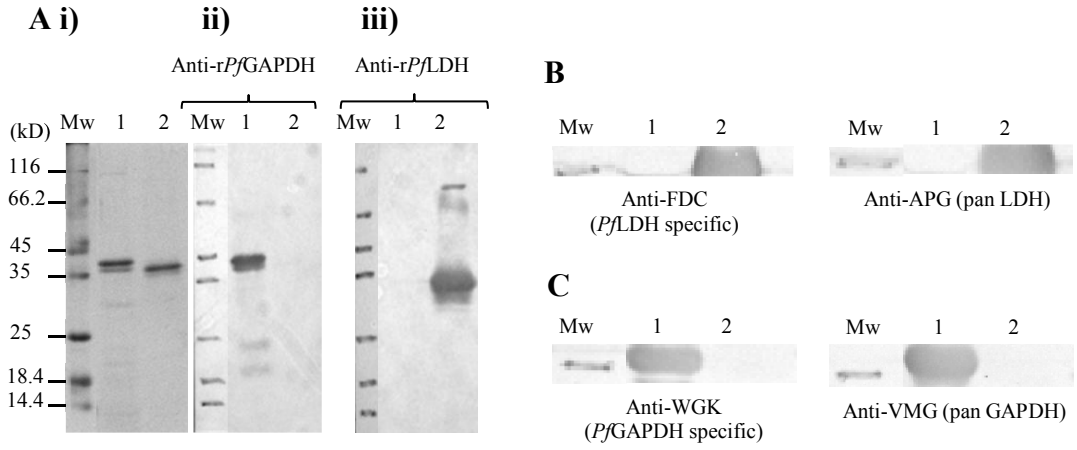


**Figure 5.2 Anti-recombinant protein and anti-peptide antibodies detected the respective recombinant proteins on Western blots.**
Affinity purified r*Pf*GAPDH or r*Pf*LDH were run in lanes 1 and 2 respectively, on 12.5 % SDS-PAGE gels. Panel (A i)) was a reference gel stained with Coomassie R-250 with molecular weight markers (Mw). Recombinant *Pf*GAPDH or r*Pf*LDH were detected by Western blotting using anti-recombinant whole protein antibodies (1 µg/ml) in (A ii)) and iii)) respectively; or using anti-peptide antibodies (5 µg/ml) as indicated in (B) and (C). The molecular weight marker (Mw) in (B and C) was the 35 kD marker. A rabbit anti-chicken-HRPO secondary antibody at 1/12000 dilution was used for all sets of Western blots.

The result in Figure 5.2 showed the specificities of the anti-recombinant antibodies for their respective antigens. Recombinant *Pf*GAPDH was detected by the anti-r*Pf*GAPDH antibodies as a major band around 39 kD with minor products smaller than 35 kD. The anti-r*Pf*LDH antibodies detected a minor band around 75 kD as well as a major band of approximately 36 kD as expected for r*Pf*LDH. These patterns were similar to those detected in chapter 3 for both anti-recombinant and anti-$His_6$-tag Western blots (Figures 3.5 and 3.6). The anti-peptide

antibodies also showed specificity for their respective antigens as shown in (B) of the same figure, detecting major bands just above the 35 kD molecular weight marker as expected.

The anti-recombinant antibodies were then used to detect *Pf*GAPDH and *Pf*LDH on Western blots of *P. falciparum* (D10) culture (*Pf*(D10)) lysate samples as shown in Figure 5.3.

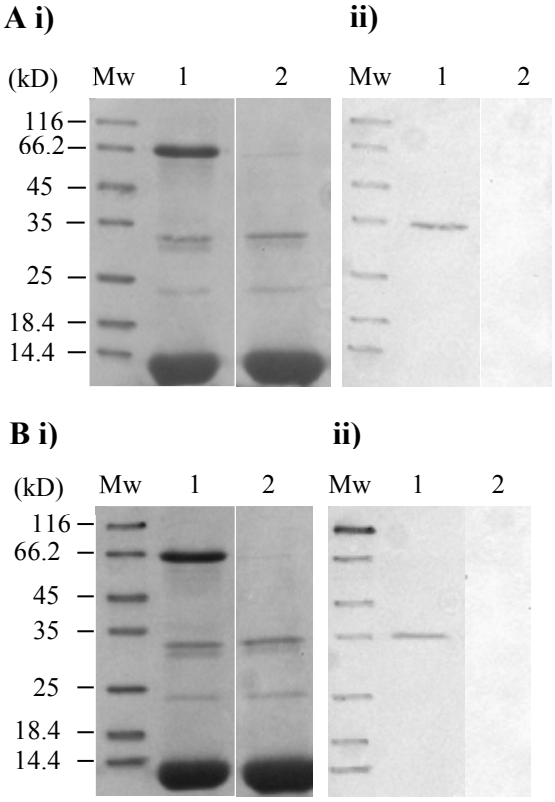


**Figure 5.3 Detection of *Pf*LDH and *Pf*GAPDH in *in vitro P. falciparum* (D10) culture lysates using anti-r*Pf*LDH or anti-r*Pf*GAPDH IgY.**
Infected human red blood cell lysates were run on a 12.5% SDS-PAGE gel, transferred to nitrocellulose and stained with Ponceau S (A i)) and (B i)) or probed with anti-r*Pf*LDH (A ii)) or anti-r*Pf*GAPDH (B ii)) IgY and detected with a rabbit anti-chicken-HRPO secondary at 1/12000 dilution. Lane 1 contained the lysate of a *P. falciparum* (D10) culture at 15 % parasitemia; lane 2 contained uninfected human type "O" blood and molecular weight markers were run in the (Mw) lane.

Both anti-recombinant antibodies detected their respective antigens on Western blots of *Pf*(D10) lysate samples and did not cross react with any human red blood cell proteins. The native proteins both had similar molecular weights of around 35 kD, with native *Pf*LDH at around 34 kD and native *Pf*GAPDH around 36 kD.

Anti-recombinant *Pf*Hsp70 IgY antibodies were also tested and showed specificity for a major protein around 73 kD within a *Pf*(D10) lysate sample as shown in Figure 5.4, with no cross-reactivity with human red blood cell proteins.

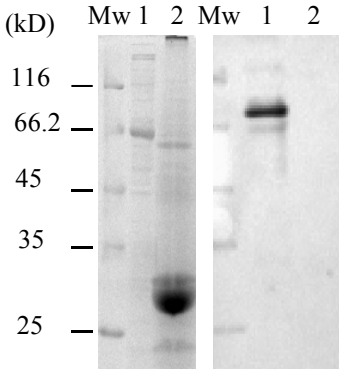


**Figure 5.4 Detection of *Pf*Hsp70 on a Western blot of *in vitro* *Plasmodium falciparum* (*Pf*(D10)) lysate with anti-r*Pf*Hsp70 IgY.**
Samples were run on a 12.5% SDS-PAGE gel. Lane 1 *Pf*(D10) lysate at 15 % parasitemia, lane 2 uninfected lysed human type "O" blood. The gel on the left was stained with Coomassie R250 and served as a reference for the Western blot on the right. *Pf*Hsp70 was detected with an anti-r*Pf*Hsp70 IgY primary (1 µg/ml) and a rabbit anti-chicken-HRPO secondary antibody at 1/12000 dilution.

All three anti-recombinant antibodies were tested in an enhanced chemiluminescence format and each antibody detected a band at the expected sizes (Figure 5.5). Uninfected red blood cell lysates were excluded as haemoglobin gives false signals on film paper when reacted with the chemiluminescence substrate.

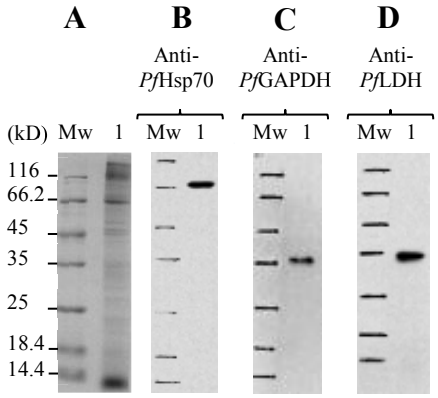


**Figure 5.5 Detection of native *Pf*GAPDH, *Pf*LDH and *Pf*Hsp70 in *Pf*(D10) lysate with anti-recombinant antibodies.**
Lysate samples (20 µg) of *Pf*(D10) infected human red blood cell lysates were run on 12.5 % SDS-PAGE gels as shown in the reference gel stained with Coomassie R-250 (A). Molecular weight markers (Mw) were labelled alongside in kilo Daltons (kD). ECL blots were probed with anti-r*Pf*Hsp70 (B); anti-r*Pf*GAPDH (C) or anti-r*Pf*LDH (D), all using primary antibody concentrations of 1 µg/ml and a rabbit anti-IgY-HRPO secondary antibody at 1/8000 dilution.

### 5.2.2 Immunoprecipitation of native proteins

The next approach was to "pull down" or immunoprecipitate native *Pf*GAPDH and *Pf*LDH from a *Pf*(D10) culture lysates using the anti-recombinant IgY antibodies (Figure 5.6).

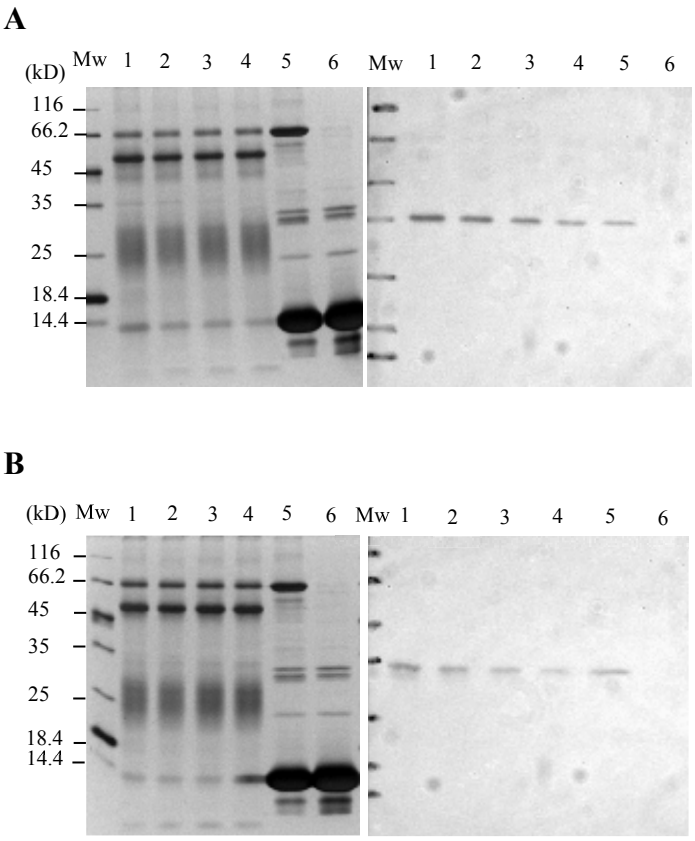


**Figure 5.6 Immunoprecipitation of native *Pf*GAPDH and *Pf*LDH from *Pf*(D10) lysates.**
All samples were run on 12.5 % SDS-PAGE gels. A lysate protein concentration range of 5 mg/ml (lane 1); 2.5 mg/ml (lane 2); 1.25 mg/ml (lane 3) and 0.625 mg/ml (lane 4) were precipitated with 25ug anti-r*Pf*GAPDH or anti-r*Pf*LDH IgY, 10ug secondary rabbit anti-IgY antibodies and protein G. A scontrols non-immunoprecipitated parasite lysate (5 mg/ml) as well as uninfected red blood cell lysate (5 mg/ml) were run in lanes 5 and 6 respectively. Silver stained reference gels were shown on the left with the respective anti-r*Pf*GAPDH (A) or anti-r*Pf*LDH (B) Western blots on the right. Western blots were probed with anti-r*Pf*GAPDH or anti-r*Pf*LDH IgY antibodies at 1 µg/ml and a rabbit anti-IgY-HRPO secondary antibody at 1/12000 dilution.

Both native proteins were detected at around 35 kD as was expected, but what was interesting was a second minor band just below the 35 kD band detected in the 5 mg/ml *Pf*(D10) lysate sample precipitated with anti-r*Pf*LDH antibodies. This was similar to the doublet obtained in the r*Pf*LDH samples seen previously (Figure 3.5). The intensity of the bands decreased with a decrease in the lysate concentration.

In a second immunoprecipitate experiment, the native proteins were detected using anti-peptide IgY antibodies (Figure 5.7) for both proteins.

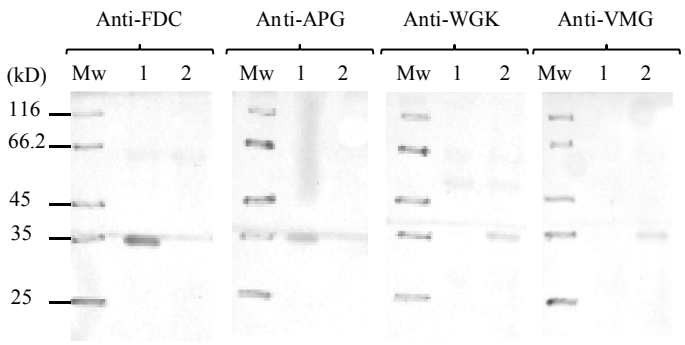


**Figure 5.7 Native *Pf*LDH and *Pf*GAPDH precipitated from *Pf*(D10) lysate with anti-recombinant protein IgY were detected with specific anti-peptide IgY antibodies on Western blots.**
Native *Pf*LDH and *Pf*GAPDH were precipitated from *Pf*(D10) lysate material at 5 mg/ml using anti-recombinant IgY at 25 µg/ml, 10 µg/ml secondary rabbit anti-IgY antibodies and protein G. Samples precipitated using anti-r*Pf*LDH IgY were run in lane 1 and those precipitated with anti-r*Pf*GAPDH IgY in lane 2 on 12.5 % reducing SDS-PAGE gels. These were then probed with anti-peptide IgY at 5 µg/ml, where anti-FDC and anti-APG are *Pf*LDH specific and common peptides respectively and anti-WGK and anti-VMG are *Pf*GAPDH specific and common peptides respectively. A rabbit anti-IgY-HRPO secondary antibody was used at 1/12000 dilution throughout.

The anti-FDC (*Pf*LDH specific) and anti-APG (pan LDH) peptide antibodies only detected the proteins precipitated using the anti-r*Pf*LDH antibodies (Figure 5.7), both also detecting a band of approximately 34 kD. Similarly the anti-WGK (*Pf*GAPDH specific) and anti-VMG (pan GAPDH) peptide antibodies only detected the proteins precipitated with the anti-r*Pf*GAPDH antibodies, again around 36 kD as expected. The smear in lane one of the anti-APG Western blot and the horizontal line across the anti-FDC and anti-APG Western blots were Ponceau S stain and were not as a result of antibody detection.

Sequential precipitation of both native *Pf*GAPDH and *Pf*LDH was also performed using the anti-recombinant IgY antibodies. First *Pf*GAPDH was precipitated, followed by *Pf*LDH from the same *Pf*(D10) lysate. Then *Pf*LDH, followed by *Pf*GAPDH from a separate *Pf*(D10) lysate. The resulting Western blots were shown in Figure 5.8.

This result (Figure 5.8) served as a control for antibody specificity again showing that the anti-recombinant antibodies each bound and precipitated a separate antigen of approximately 35 kD within the same lysate sample. Dilutions of parasite lysates were made, while the antibody concentrations used remained the same for each dilution. This ensured that the antibody concentration was not limiting, therefore the proteins "pulled down" in the sequential immunoprecipitation were likely to be separate proteins and not the same 35 kD protein.

**A** i) Precipitated and probed with anti-r*Pf*GAPDH

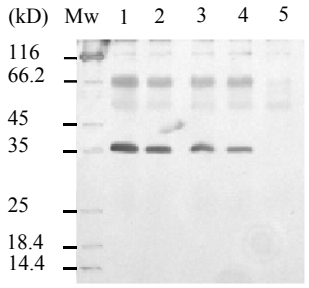


ii) Sequentially precipitated and probed with anti-r*Pf*LDH

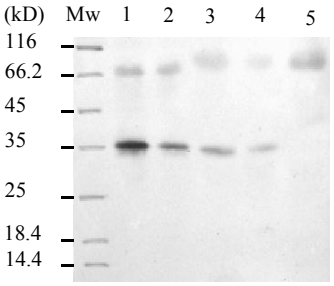


**B** i) Precipitated and probed with anti-r*Pf*LDH

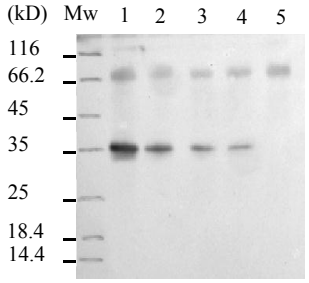


ii) Sequentially precipitated and probed with anti-r*Pf*GAPDH

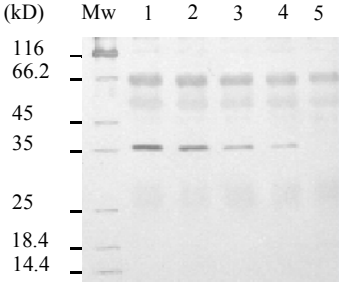


**Figure 5.8 Sequential immunoprecipitation of native *Pf*GAPDH and *Pf*LDH from *Pf*(D10) lysate samples.**
All samples were run on 12.5 % SDS-PAGE gels. Lysates were prepared to give a total protein concentration range of 5 mg/ml (lane 1); 2.5 mg/ml (lane 2); 1.25 mg/ml (lane 3) and 0.625 mg/ml (lane 4) and were precipitated with 25 µg/ml anti-r*Pf*GAPDH or anti-r*Pf*LDH IgY, 10 µg/ml secondary rabbit anti-IgY antibodies and protein G. The lysates were retained and a sequential round of precipitations was performed. Samples incubated with anti-r*Pf*GAPDH (A i)) were then incubated with anti-r*Pf*LDH (A ii)) and *vice versa*. In lane 5 uninfected human blood lysate (5 mg/ml) replaced the infected parasite lysate. Western blots were probed with either an anti-r*Pf*GAPDH or anti-r*Pf*LDH IgY (1 µg/ml) as shown in the figure and a rabbit anti-IgY-HRPO secondary antibody at 1/12000 dilution.

The immunoprecipitation experiments using the anti-recombinant antibodies were repeated in triplicate. Using densitometry the band intensities observed for native *Pf*GAPDH and *Pf*LDH on Western blots were compared and summarised in Figure 5.8.

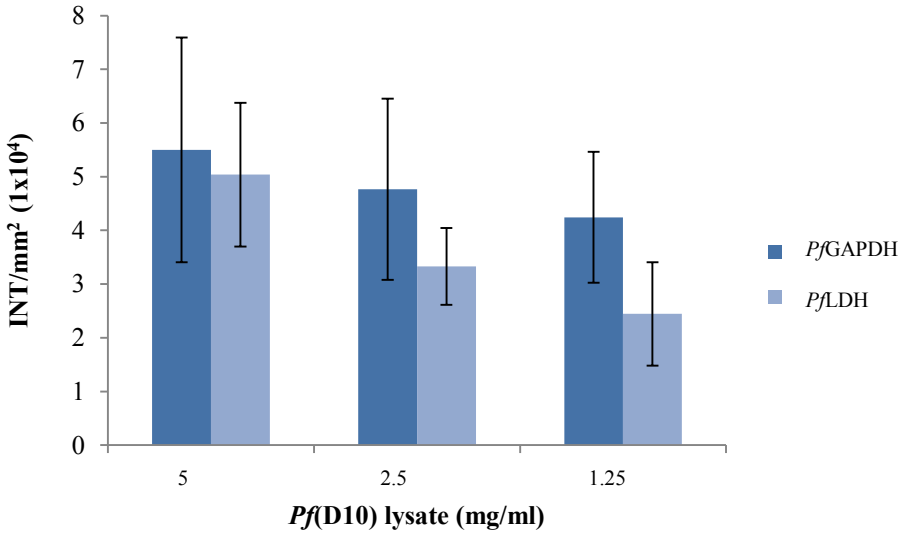


**Figure 5.9 Densitometry analysis of the immunoprecipitation results for *Pf*GAPDH and *Pf*LDH from *Pf*(D10) lysate samples.**
Lysate samples were diluted to give protein concentrations of 5; 2.5 and 1.25 mg/ml and were incubated with 25ug anti-r*Pf*GAPDH or anti-r*Pf*LDH IgY; 10ug secondary rabbit anti-IgY antibodies and protein G. After separation on 12.5 % SDS-PAGE gels, samples were assessed by Western blotting with the respective anti-r*Pf*GAPDH or anti-r*Pf*LDH antibodies at 1 µg/ml and detected with a rabbit anti-IgY-HRPO secondary at 1/12000 dilution. The blots were analysed using Quantity One® Version 4.6.0 (Bio-Rad Laboratories © 2005) and densitometric values were assigned to the bands detected as intensity (INT) per $mm^2$. The results show the mean values of experiments done in triplicate (n = 3), with standard deviations.

Band intensities are subject to the polyclonal antibody avidities and antigen concentration, so without a standard curve to associate band intensity with approximate protein concentration, the results in Figure 5.8 may be misleading. The results suggest a higher concentration of native *Pf*GAPDH to *Pf*LDH within the lysate samples. The increasing absorbance values for all three samples suggest that the antibody concentrations were in excess, as increasing protein levels were detected with each increase in lysate concentration, with the same antibody concentration used throughout.

### 5.2.3 Detection of native proteins using a direct ELISA

A direct ELISA with parasite lysate was used to coat the wells and *Pf*LDH or *Pf*GAPDH were detected using the respective anti-recombinant IgY antibodies. Since separate antibodies were used for each protein, standard curves had to be prepared which would allow for quantitation of the proteins. These were shown in Figure 5.10 and were prepared using the respective recombinant proteins.

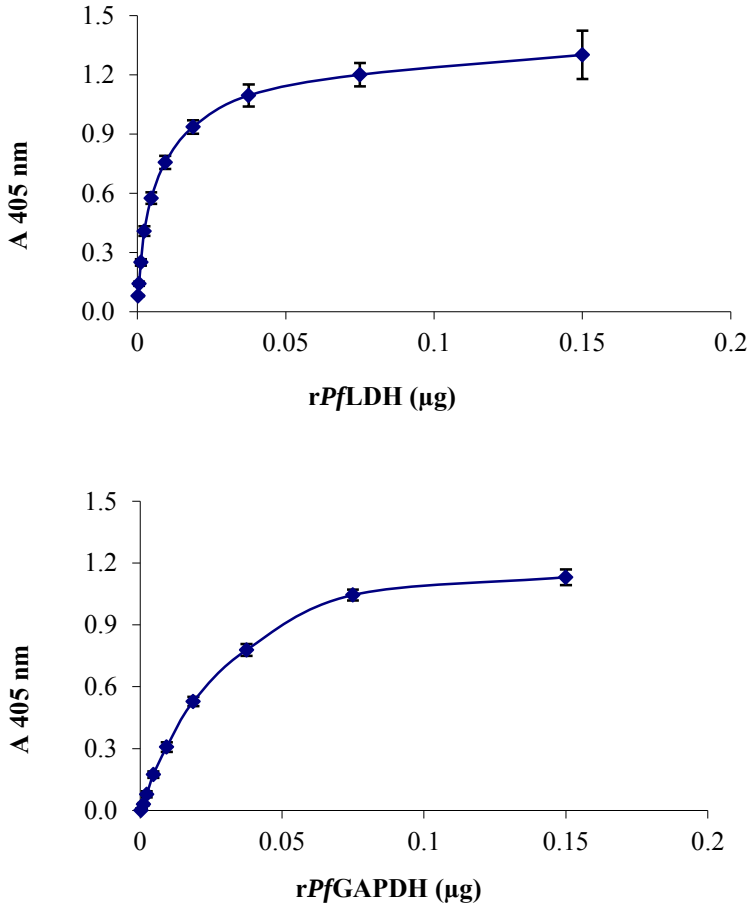


**Figure 5.10 Standard curves showing limits of detection of r*Pf*LDH and r*Pf*GAPDH using anti-recombinant IgY.**
ELISA plates were coated with a range of concentrations of recombinant protein from 0.15 µg (1 µg/ml) to 0.0003 µg. Anti-recombinant IgY antibodies were used as the primary antibodies at 6.25 µg/ml and a 1/15000 dilution of a rabbit anti-chicken HRPO secondary antibody. An average of triplicate readings with standard deviations was shown.

Both anti-recombinant protein antibodies detected their target antigens. The anti-r*Pf*LDH curve seemed to have a steeper initial increase compared to the anti-r*Pf*GAPDH curve. The slope of the curve suggests that the anti-r*Pf*LDH antibodies have higher avidity for the target antigen than the anti-r*Pf*GAPDH antibodies.

Using the standard curves, the approximate concentrations of native *Pf*LDH and *Pf*GAPDH in *Pf*(D10) lysate material were estimated. These results were shown in Figure 5.11.

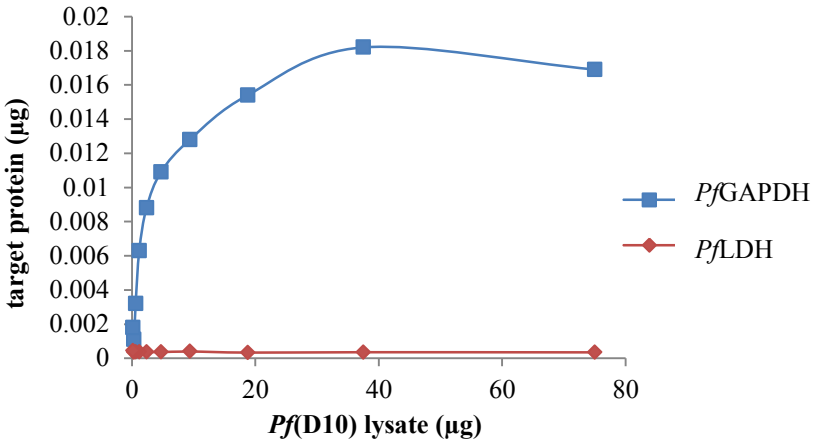


**Figure 5.11 Detection of native *Pf*LDH and *Pf*GAPDH in *Pf*(D10) lysate using anti-recombinant IgY.** ELISA plates were coated with a range of *Pf*(D10) lysate protein from 75 µg (0.5 mg/ml) to 0.15 µg. The antigens were detected with anti-r*Pf*LDH or anti-r*Pf*GAPDH IgY antibodies at 6.25 µg/ml and a rabbit anti-chicken HR PO labelled secondary antibody at 1/15000 dilution. The $A_{405}$ values were converted to concentrations of native antigen using the antigen specific standard curves. All data points were average values of triplicate readings.

The anti-r*Pf*GAPDH antibodies detected an increasing concentration of native *Pf*GAPDH as the lysate concentration increased (Figure 5.11). The anti-r*Pf*LDH antibodies, however, did not detect native *Pf*LDH within the ELISA. The above experiment was repeated using double the lysate concentration, starting at 150 µg of total lysate protein (1 mg/ml), however, there was no change in the detection of native *Pf*LDH. The detection of *Pf*GAPDH increased as expected with approximately 0.059 µg of native *Pf*GAPDH detected at a parasite lysate concentration of 150 µg (data not shown), therefore just more than double that detected in Figure 5.11, as was expected.

Not all proteins bind equally well to ELISA plates. Since protein binding can be pH dependent, an experiment was performed using either PBS pH 7.4 or carbonate buffer pH 9.6 (data not shown), where PBS gave the best result.

There are a number of proteins within a lysate, which each have different affinities for binding to the ELISA wells. It was hypothesized that the proteins in the lysate samples were out-competing native *Pf*LDH and *Pf*GAPDH for binding to ELISA wells. This would explain the poor absorbance readings for *Pf*LDH in Figure 5.11. To assess this hypothesis an experiment was designed in which parasite lysate and uninfected red blood cell lysates were

"spiked" with r*Pf*LDH or r*Pf*GAPDH protein and detected in a direct ELISA (Figures 5.12 and 5.13).

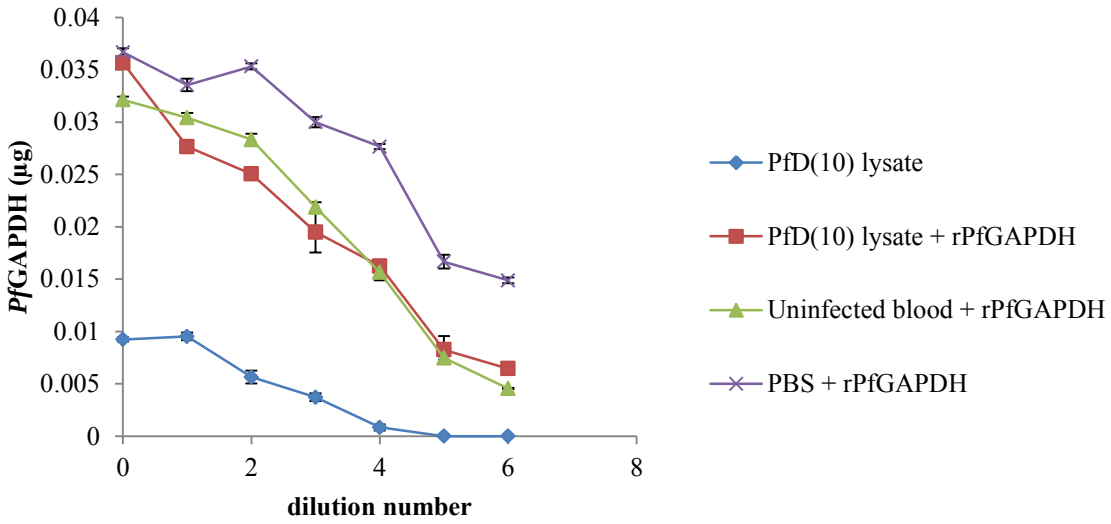


**Figure 5.12 Lysates "spiked" with r*Pf*GAPDH to assess competitive binding between lysate proteins and *Pf*GAPDH.**
Malaria *Pf*(D10) lysate samples and uninfected type "O" blood samples at 15 µg were spiked with r*Pf*GAPDH. The samples were diluted for a total of 6 doubling dilutions and detected with anti-r*Pf*GAPDH IgY and a rabbit anti-chicken-HRPO secondary antibody at 1/15000 dilution. All data sets were done in triplicate and standard deviations are displayed.

Approximately 0.01 µg of native *Pf*GAPDH was detected in the *Pf*(D10) lysate sample without the addition of r*Pf*GAPDH, as seen in Figure 5.12, which correlated to levels detected in Figure 5.11 at a similar lysate concentration. As a general trend the concentration of *Pf*GAPDH detected declined with increasing dilution of the samples as was expected. Detection of r*Pf*GAPDH in the PBS control sample showed highest levels of antigen. In comparison lower readings with the "spiked" infected red blood cell lysate and "spiked" uninfected red blood cell lysate samples suggested there were other proteins present in lysates that were competing for binding to the ELISA wells, thus reducing the detected level of *Pf*GAPDH.

A similar result was obtained for *Pf*LDH (Figure 5.13). Samples "spiked" with r*Pf*LDH in this case also showed increased detection of recombinant antigen, but a similar lack of detection of the native antigen as seen previously in Figure 5.11. There seemed to be a sharper decline in the detection of the recombinant antigen in the lysate samples in comparison to the PBS control. This suggested a higher competition for binding ELISA wells

between *Pf*LDH and other proteins within the lysate samples than was the case for *Pf*GAPDH.

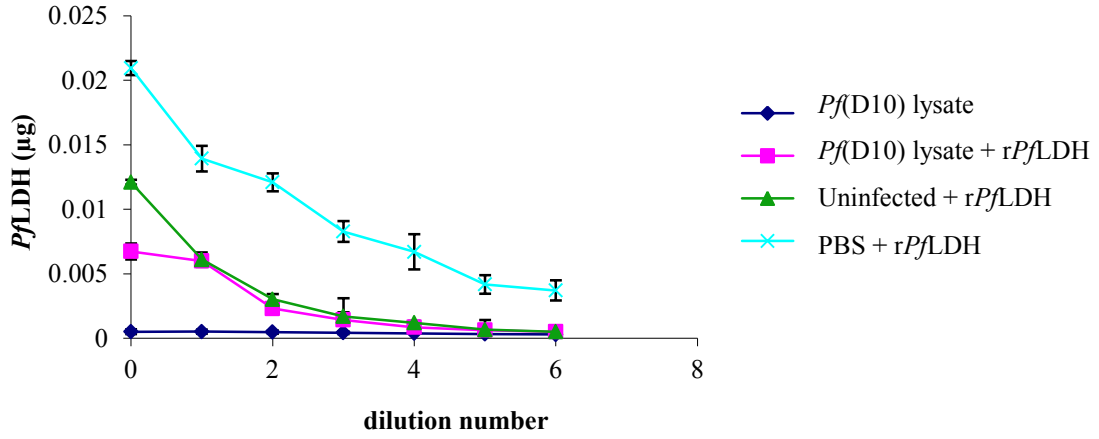


**Figure 5.13 Lysates "spiked" with r*Pf*LDH to assess competitive binding between lysate proteins and *Pf*LDH.**
Malaria lysate samples and uninfected type "O" blood samples at 15 µg were "spiked" with r*Pf*LDH. The samples were diluted for a total of 6 doubling dilutions and detected with anti-r*Pf*LDH IgY and a rabbit anti-chicken-HRPO secondary antibody at 1/15000 dilution. All data sets were done in triplicate and standard deviations are displayed.

Detection of native protein using a direct ELISA approach would thus be an underestimation of the real concentration present within the lysate samples due to an apparent competition in binding of proteins within a lysate sample for the ELISA plate. An immune-capture method in the form of a double antibody sandwich ELISA (DAS-ELISA) was then evaluated.

### 5.2.4 Development of a double antibody sandwich (DAS) ELISA for detection of native *Pf*GAPDH and *Pf*LDH

The anti-recombinant IgY antibodies raised against both protein targets were used as detection antibodies, with anti-peptide antibodies used as the capture antibodies in the DAS ELISA. The detection antibodies were thus labelled with HRPO and the concentration to be used in the DAS-ELISA was optimised as shown in Figure 5.14.

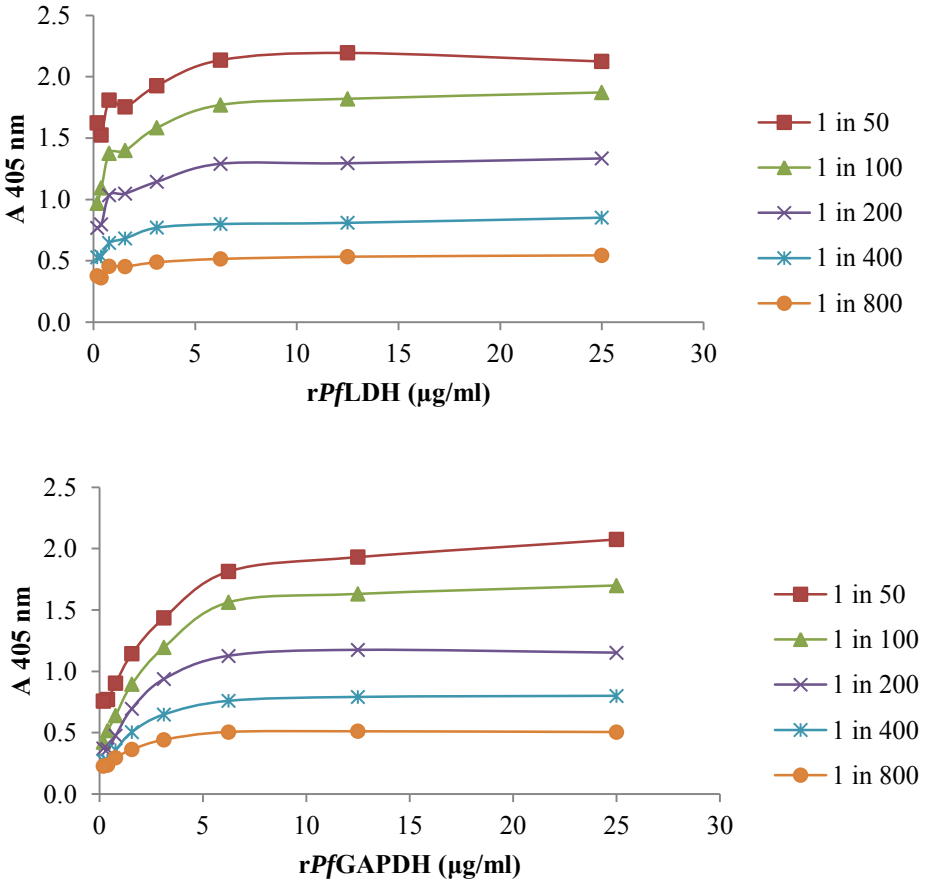


**Figure 5.14 ELISA to optimise the concentration of HRPO-labelled anti-recombinant IgY to use in the DAS-ELISA.**
96-well ELSIA plates were coated with r*Pf*LDH or r*Pf*GAPDH at an initial concentration of 25 µg/ml and diluted for 7 doubling dilutions across the plate. Doubling dilutions of the anti-r*Pf*LDH-HRPO or anti-r*Pf*GAPDH-HRPO were prepared separately starting at a 1 in 50 dilution to a 1 in 800 dilution. These were then tested across the range of antigen concentrations coated on the plates.

The chosen antibody dilution was a compromise between conserving the amount of antibody used to get a good signal. A 1 in 200 dilution (5 µg/ml) of HRPO coupled antibody was chosen for both anti-r*Pf*LDH and anti-r*Pf*GAPDH as these gave good $A_{405}$ readings across the antigen range tested in Figure 5.14.

Standard curves were set up to relate protein concentration to $A_{405}$ values (Figure 5.15).

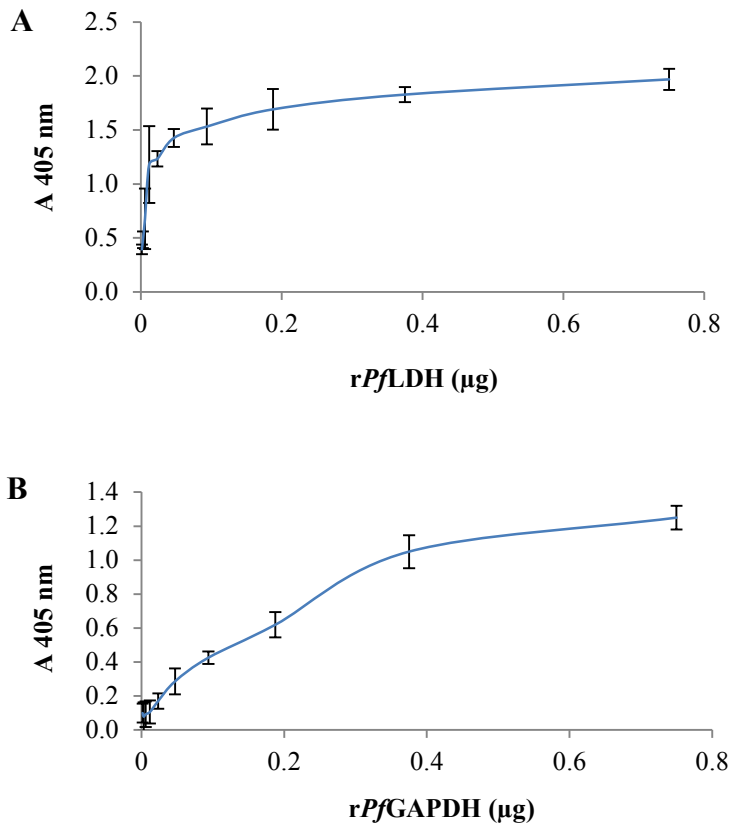


**Figure 5.15 Standard curves indicating limit of detection of the DAS-ELISA assay, used for estimating levels of native proteins.**
96-well ELISA plates were coated with the pan-malarial anti-peptide antibodies at 1 µg/ml as the capture antibodies. The anti-APG (pan LDH) antibody was used for the capture of *Pf*LDH (A) and the anti-VMG (pan GAPDH) antibody for *Pf*GAPDH (B). Standard curves were prepared using r*Pf*LDH or r*Pf*GAPDH at starting concentrations of 0.75 µg and double diluted a total of 9 times. The prepared HRPO-labeled anti-r*Pf*LDH or anti-r*Pf*GAPDH was then added as the detection antibody at a 1/200 dilution. The resulting standard curves are average values of triplicate samples with standard deviations shown.

The anti-r*Pf*LDH-HRPO standard curve showed a far more pronounced increase in $A_{405}$ at low r*Pf*LDH concentration, reaching saturation at approximately 0.2 µg. In comparison the anti-r*Pf*GAPDH-HRPO standard curve still showed increasing detection at 0.8 µg of r*Pf*GAPDH (Figure 5.15). No cross reactivity was detected in a control experiment where r*Pf*GAPDH was added to *Pf*LDH and the same for r*Pf*LDH added to *Pf*GAPDH (data not shown). Standard curves and detection of native *Pf*LDH and *Pf*GAPDH within *Pf*(D10) lysates were run on the same plate to avoid inter-plate inconsistencies. The resulting detection of the native proteins was shown in Figure 5.16, where the corresponding standard curves used were shown in Figure 5.15.

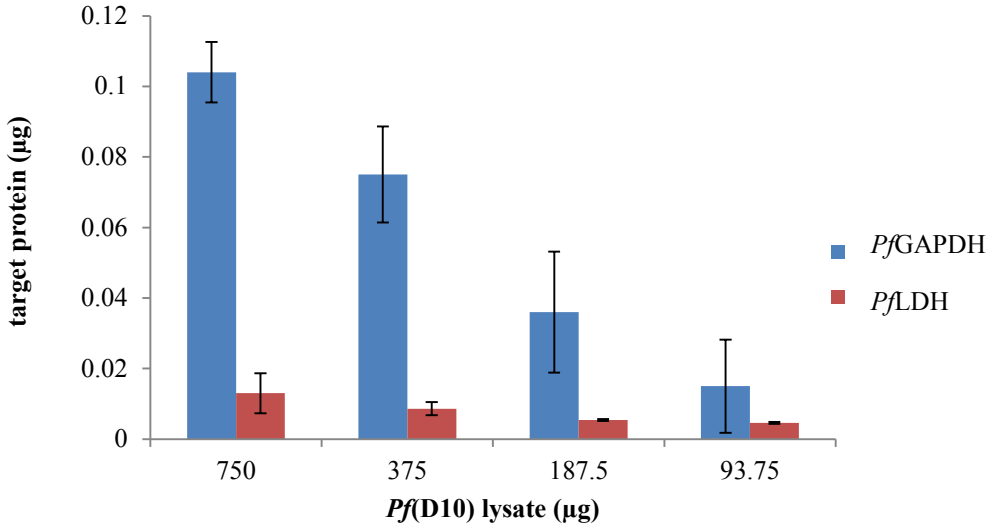


**Figure 5.16 Detection of native *Pf*LDH and *Pf*GAPDH in *Pf*(D10) lysate material.**
Separate ELISA plates were coated with the pan-malarial anti-peptide antibodies at 1 µg/ml as the capture antibodies. The anti-APG antibody was used for the capture of *Pf*LDH and the anti-VMG antibody for *Pf*GAPDH. Total parasite lysate was then added at an initial concentration of 750 µg and double diluted 3 times. The resulting $A_{405}$ values were converted to protein concentration values using prepared standard curves and the average values of triplicate readings were plotted with standard deviations shown.

*Pf*GAPDH was consistently detected at higher levels than *Pf*LDH, being present at 4 to 8 times the amount of *Pf*LDH (Figure 5.16). The concentrations determined by DAS-ELISA correlated with those using the direct ELISA method for *Pf*GAPDH. At approximately 150 µg and 75 µg *Pf*(D10) lysate the respective concentrations were around 59 and 17 ng of *Pf*GAPDH for the direct ELISA approach. For the DAS-ELISA results, the approximate concentrations were 36 and 15 ng of *Pf*GAPDH at lysate concentrations of approximately 187.5 and 93.75 µg respectively. As for the detection of *Pf*LDH, this was not the case. With the DAS-ELISA the concentrations of *Pf*LDH were higher than those in the direct ELISA. The levels were around 1 ng in the direct ELISA regardless of the lysate concentration, whereas they increased from 4 to 13 ng in the DAS-ELISA assay for *Pf*(D10) lysate concentrations of 93.75 to 750 µg. These results translate to an estimated 259.5 ng /ml of *Pf*LDH within the original 15 % lysate and 2.1 µg/ml of *Pf*GAPDH. For comparison to a paper by Martin *et al.,* (2009) the levels in a 1 % lysate would be approximately 17.3 ng/ml and 138.5 ng/ml respectively.

## 5.3 Discussion

Antibody specificity is important for the detection of antigens. Both the anti-peptide and anti-recombinant chicken antibodies raised in chapter 4 were used and characterised here. The aim was to compare the concentrations of the two target antigens *Pf*LDH and *Pf*GAPDH within *P. falciparum* lysate samples. Since both target antigens shared similar molecular masses of around 35 kD, differentiation based on size was not possible. It was important to show that the antibodies detected two separate antigens in solution and not the same 35 kD protein before further analysis was done. Western blotting, immunoprecipitation and ELISA assays were used to assess antibody specificity.

The anti-recombinant as well as anti-peptide antibodies detected only their respective recombinant antigens on a Western blot. In Western blots of *Pf*(D10) lysate samples bands of around 35 kD were detected using the anti-recombinant antibodies, with no proteins detected in uninfected blood samples. Using enhanced chemiluminescence both anti-recombinant antibodies also showed specificity by detecting only a single band. The *Pf*LDH band (around 34 kD) was slightly lower than that of *Pf*GAPDH (around 36 kD). This would correlate with PlasmoDB values predicted to be 34.4 kD for *Pf*LDH and 36.6 kD for *Pf*GAPDH based on the amino acid composition. With respect to the ECL results, the samples were prepared differently to the immunoprecipitation and ELISA samples. This was due to signal development between haemoglobin and the ECL substrate, as luminol is known to react with metal ions (Hartkopf and Delumyea, 1974), hence haemoglobin had to be removed by several wash steps.

With Western blotting proteins are detected in their fully denatured states, thus antibodies recognise linear epitopes of their target antigens (Towbin *et al*., 1979). Both *Pf*LDH and *Pf*GAPDH share similar tertiary structures forming tetramers in solution (chapter 3). They also bind the same cofactor $NAD^{+}(H)$; both have Rossmann fold motifs (Daubenberger *et al.*, 2000; Gomez *et al.*, 1997; Granchi *et al*., 2010) and share 47 % identity. The antibodies may therefore still cross react by detecting conformational epitopes on *Pf*LDH and *Pf*GAPDH. Through immunoprecipitation antibodies have the opportunity of binding antigens in their native conformation and could potentially recognise and bind conformational epitopes. The proteins precipitated using the anti-recombinant antibodies were recognised by their respective anti-peptide antibodies on Western blots with no cross reaction. To add to this sequential precipitations were also performed and showed that two separate antigens of around 35 kD were being precipitated from the same initial *Pf*(D10) lysate sample using the

anti-recombinant antibodies. These results support the specificity of the antibodies for their antigens, showing no cross-reaction with linear or conformational epitopes.

Detection of higher molecular weight bands around 65 to 68 kD in immunoprecipitation Western blots were not dimers of the native proteins, as the bands were also present in the uninfected red blood cell control lanes. These bands match the estimated size of the IgY heavy chain (Schade *et al.*, 1993), which would have been detected by the secondary rabbit anti-IgY-HRPO antibody used in the Western blots. These were not seen before in Figure 5.6 possibly because a new secondary antibody was used in these Western blots and may have been more reactive in this case. The smaller band around 50 kD may be a dimerization of IgY light chains.

In a direct ELISA format, ELISA plates were coated with the target antigen which was then detected with a specific antibody. Coating plates with a target protein causes slight denaturation of the protein due to protein-plastic interactions (van Regenmortel, 1988). PBS pH 7.4 was optimal for coating, however for some reason native *Pf*LDH appeared not to bind well to ELISA plate wells under these conditions and from spiked ELISAs it seemed that other proteins in solution were competing with native *Pf*LDH. This also showed that quantitation by direct ELISA is not ideal due to such competition and would likely result in an under estimation of the actual protein concentration. For this reason a double antibody sandwich ELISA was used (DAS-ELISA) for quantitation of native *Pf*LDH and *Pf*GAPDH.

The standard curves for the direct ELISA did suggest a higher avidity between the anti-r*Pf*LDH antibody and r*Pf*LDH than the avidity between anti-r*Pf*GAPDH and r*Pf*GAPDH. This result was similar for the DAS-ELISA standard curves. The higher avidity suggests that the detection of higher levels of native *Pf*GAPDH to *Pf*LDH in immunoprecipitation experiments may be more significant than observed in Figure 5.8, since the antibody concentrations used were the same. According to transcription data from Le Roch *et al.,* (2003) the relative levels of *Pf*GAPDH should be approximately 4 times greater than the corresponding level of *Pf*LDH (see appendix). This is clearly greater than that observed for the immunoprecipitation results. Nirmalan *et al.,* (2004) showed the relative protein levels of both *Pf*LDH and *Pf*GAPDH to exceed those of the mRNA levels at the trophozoite and schizont stages of the parasite red blood cell cycle. A similar finding was made by Smit *et al.,* (2009), which both support the transcription data and suggest there to be posttranscriptional regulation of these genes. The DAS-ELISA data thus far suggest there to be between 4-8

times more *Pf*GAPDH than *Pf*LDH, which corresponds with the mRNA levels from Le Roch *et al.,* (2003). It was concerning that the levels detected were still very low, and further optimisation of this assay will be done to allow more accurate quantitation. It would be interesting to quantify the levels of these protein targets at each stage of the parasite red blood cell cycle for comparison to the transcription data.

A study by Martin *et al.,* (2009) quantified the levels of LDH and histidine rich protein within the *P. falciparum* Dd2 strain. This strain does not express HRP-2, but they measured the levels of HRP-1 and HRP-3. The concentration of *Pf*LDH was estimated at 28.9 ng/ml for a 1 % parasite culture. The DAS-ELISA data shown here suggest there to be 17.3 ng/ml of *Pf*LDH in a 1 % parasitemia lysate. The DAS-ELISA data in this study suggest there to be approximately 138.5 ng/ml *Pf*GAPDH within a 1 % parasitemia lysate.

These results showed the anti-recombinant as well as the anti-peptide antibodies to be specific to their respective target antigens. They did not cross-react with any human blood proteins or any other parasite proteins. These antibodies consistently detected greater levels of *Pf*GAPDH to *Pf*LDH except in ECL results, where sample preparation may have played a role. In a DAS-ELISA assay approximately 4 times greater levels of *Pf*GAPDH in comparison to *Pf*LDH were detected. These results support *Pf*GAPDH as a possible alternative diagnostic target for RDTs.

# Chapter 6
# General discussion

## 6.1 Brief review

Malaria causes severe disease and is often fatal, especially in children under the age of 5 (WHO The Global Burden of Disease, 2008; WHO malaria fact sheet no. 94, January 2009). With no vaccine currently available, disease control and prevention relies on vector control methods, diagnosis and anti-malarial treatment (Betson *et al.*, 2009; Kappe *et al*., 2010; Moody, 2002). Developing countries in the tropics, which often lack the required infrastructure and funding to effectively control malaria are the worst affected (Hay *et al*., 2009). Field hospitals in rural areas therefore require diagnostic tests that are rapid, easy to perform and interpret, yet sensitive and specific at the same time (Makler *et al*., 1998; Moody, 2002; Perkins and Bell, 2008). Microscopy using Giemsa staining has served as and still is the gold standard for malaria diagnosis, detecting around 50 parasites per microliter. Preparation of samples for microscopy is cheap and infections can be quantified, however expertise is required to specifically identify the infecting species of *Plasmodium* (Moody, 2002; Suh *et al*., 2004). Various alternate methods have been developed in attempts to improve diagnosis, such as PCR, which can detect infections below 5 parasites per microliter (Demas *et al*., 2011). Most of these methods including microscopy require either expensive equipment or laboratory conditions to perform optimally (Makler *et al*., 1998; Moody, 2002; Perkins and Bell, 2008). Malaria immunochromatographic or rapid diagnostic tests (RDTs) have been developed to simplify malaria diagnosis and to be implemented in the field. The current tests target histidine rich protein 2 (HRP-2), lactate dehydrogenase (LDH) and aldolase and take between 15 to 20 minutes to perform with a detection limit of around 100 parasites per microliter (Ashley *et al*., 2009; Khairnar, 2009; Makler *et al*., 1998; Murray *et al*., 2008, Perkins and Bell, 2008). In order for RDTs to detect asymptomatic infections which would act as reservoirs of infection, the limits of detection will have to be improved to below 100 parasites per microliter (Suh *et al*., 2011).

## 6.2 The aims and objectives of this study

The main aims of this study were first to find a new *Plasmodium falciparum* protein target glyceraldehyde-3-phosphate dehydrogenase (*Pf*GAPDH) and to compare it to a current diagnostic target lactate dehydrogenase (*Pf*LDH). A second aim was to detect *Pf*GAPDH and *Pf*LDH within parasite lysate material using polyclonal chicken antibodies (IgY). To do this both proteins were recombinantly expressed, affinity purified and used to raise IgY. Additional IgY against specific peptide epitopes identified on the surface of *Pf*LDH and *Pf*GAPDH were also raised.

## 6.3 Main findings, conclusions and future work

The gene inserts used for expression of *Pf*LDH and *Pf*GAPDH were confirmed by size and PCR, where the PCR amplicons were sequenced, and had between 96 to 98 % homology with their respective DNA coding sequences. Both recombinant proteins were expressed at sizes slightly larger than the predicted native protein sizes due to additional $His_6$-tags similar to results from other groups (Berwal *et al*., 2008; Daubenberger *et al*., 2003; Satchell *et al*., 2005; Turgut-Balik *et al*., 2004). This did not seem to affect their quaternary structure as assessed by molecular exclusion chromatography (gel filtration chromatography) and was also demonstrated by Berwal *et al*., (2008) and Satchell *et al*., (2005), however enzyme activity assays for *Pf*GAPDH (Daubenberger *et al*., 2000; Ferdinand *et al*., 1964) and *Pf*LDH (Berwal *et al*., 2008; Gomez *et al*., 1997) would be useful to confirm the correct folding of the respective enzymes.

Peptide epitopes were identified on both *Pf*LDH and *Pf*GAPDH by sequence alignment and using an epitope prediction program Predict7$^{TM}$. The locations of the individual peptides identified were shown to be on the surface of their respective 3D protein crystal structure models (Dunn *et al*., 1996; Satchell *et al*., 2005). This approach allowed for *in silico* assessment of the target epitopes ensuring their specificity prior to the immunisation of experimental animals. This avoids the selection process involved in raising monoclonal antibodies (Pluschke *et al*., 1998) saving time, money and experimental animals. It would be interesting to compare the sensitivity of the polyclonal anti-LDH-peptide antibodies raised here to the monoclonal antibodies against *Plasmodial* LDH currently used in RDTs.

Isolation of IgY yields approximately 7 times more specific antibodies than comparative yields of IgG from rabbits and avoids bleeding of experimental animals (Schade *et al*., 1991).

In addition IgY lacks an Fc portion and does not cross react with mammalian complement proteins, Rheumatoid factors and anti-nuclear antibodies (Schade *et al*., 1991), which has been a cause of false positives in malaria RDTs using mammalian antibodies (Iqbal *et al*., 2000). Chicken antibodies (IgY) were raised against both the selected peptide epitopes for both *Pf*LDH and *Pf*GAPDH as well as both recombinant proteins. The antibodies were specific and did not cross react with other human blood proteins. Further work needs to be done to compare the sensitivities of the respective antibodies, as well as assessing their specificity using LDH and GAPDH from other malaria species. The anti-peptide antibody sensitivities will be assessed using a direct ELISA approach as was done with the anti-recombinant antibodies, as well as in a DAS-ELISA format, where the recombinant antigens will be captured by the anti-peptide antibodies and detected using an anti-$His_6$ tag antibody.

Native *Pf*LDH and *Pf*GAPDH were successfully "pulled down" using the anti-recombinant whole protein antibodies and also detected in DAS-ELISA experiments in *Pf*(D10) lysates. *Pf*GAPDH was consistently detected at higher levels than *Pf*LDH. The rapid saturation of the *Pf*LDH standard curve for the DAS-ELISA assay was concerning and this could be tested by using the other anti-peptide antibody as the capture antibody. By comparing the level of *Pf*GAPDH with the level of *Pf*LDH detected in this study as well as by Martin *et al*., (2009), *Pf*GAPDH in these assays appears to be present at a higher level than *Pf*LDH. This correlated with transcription data from Le Roch *et al*., (2003), however, it would be interesting to quantify protein levels at each stage within the red blood cell cycle, as Kuss *et al*., (2012) and Lasonder *et al*., (2002) have shown that protein levels may not necessarily correlate with mRNA levels due to posttranscriptional or posttranslational regulation. Semi-quantitative analyses of protein levels by Nirmalan *et al*., (2004) and Smit *et al*., (2009) have shown increasing trends in *Pf*LDH and *Pf*GAPDH levels from ring to schizont stages, however, therefore supporting the Le Roch *et al*., (2003) data.

The antibodies raised here remain to be tested in an RDT format. This would not only allow for comparison with other RDTs, but at the same time the heat stability of the IgY in an RDT format could be assessed. IgY antibodies have been shown to be stable at 4 °C for prolonged periods (Goldring and Coetzer, 2003). Chiodini *et al*., (2007) highlighted the need for a cold chain to ensure RDTs remain of a high functional quality in the field. The recombinant proteins and the peptides used in this study could also be used for quality assurance of RDTs as described by Lon *et al*., (2005).

In order to eliminate malaria, RDTs would have to detect asymptomatic infections at parasite loads below 100 / µl (Faechem *et al*., 2009). By identifying and targeting proteins expressed at higher levels than the current RDT targets, the limits of detection of RDTs may be lowered. Alternatively targeting a pool of malarial antigens may also improve RDTs and this could also be tested using the antibodies and recombinant proteins available in this study.

Another school of thought is that RDTs should not only be focused on detecting low parasitemia levels. In malaria endemic regions the adult population often develop natural, non-sterilizing immunity against malaria, therefore they remain susceptible to infection but are asymptomatic (Hafalla *et al*., 2011; Miller *et al*., 1994). As a result detecting and treating an asymptomatic malaria infection in such patients does not necessarily treat the cause of the disease which may be due to a different pathogen and thus require alternate drug treatment to treat the disease.

The ultimate aim with RDTs would be to quantify the extent of infection, as this will allow clinicians to monitor patients during drug treatment and will allow them to determine whether alternate drug treatments are necessary to clear infections. By targeting glycolytic proteins for malaria diagnosis in this study we hope to allow RDTs to do this. It was shown that LDH based RDTs return to negative between 2 to 7 days after drug clearance of infections (Iqbal *et al*., 2004; Murray *et al*., 2008). This will have to be assessed in an RDT format using GAPDH as the target antigen.

Future studies concerning the application of this research for the improvement of rapid diagnostic malaria kits can be broken down into three criteria:

1) Comparative studies of the newly identified diagnostic target *Pf*GAPDH to the known target *Pf*LDH can be conducted.

   This would include the further optimisation of the double antibody sandwich assay described in this study, as well as the use of enhanced chemiluminescence for comparison of the relative levels of the protein targets to each other. Comparison of *Pf*LDH and *Pf*GAPDH gene transcription and expression levels at the different stages of the malaria parasite red blood cell cycle would also be interesting.

2) Comparative studies of the antibodies raised in this study to each other as well as to the commercial antibodies used in current RDTs would be interesting.

The antibodies raised in this study could be evaluated for their affinity for their target antigens by measuring their affinity constants ($K_D$). This can be done to compare the affinities of the anti-peptide antibodies to each other, and to assess which target peptide has greatest antigenicity which would also assess the Predict7$^{TM}$ data used here. This could also be done for monoclonal antibodies used in current RDTs.

The antibodies raised here could also be tested for their specificity for their target antigens, especially in the case of the species specific anti-peptide antibodies. To add to this it would be interesting to assess the possibility of targeting *P. knowlesi* specific peptides.

3) The antibodies raised here will have to be assessed in an RDT format, as the antibodies may perform differently under RDT conditions than they do in optimised laboratory settings.

   RDT specificity and sensitivities could be assessed. The heat stability of these RDTs would also be of interest in comparison to commercial RDTs using monoclonal antibodies. This is a concern raised in the literature for current RDTs used in the field.

   The use of RDTs targeting *Pf*GAPDH for monitoring infections also has to be assessed, possibly with the use of a mouse model in which infections are cleared with drug treatment.

   Further studies which are of interest are to address the possibility of using RDTs to detect the severity of infections in terms of % parasitemia. This may involve a larger number of test lines on RDTs detecting antigen, and in this way relating amount of antigen detected to the level of parasitemia for example.

## References

**Aebersold R. and Mann M.** (2003). Mass spectrometry-based proteomics. *Nature,* **422** (6928)**,** 198-207.

**Akinyi S., Gaona J., Meyer E.V.S., Barnwell J.W., Galinski M.R., Corredor V.** (2008). Phylogenetic and structural information on glyceraldehyde-3-phosphate dehydrogenase (G3PDH) in *Plasmodium* provides functional insights. *Infection, Genetics and Evolution*. **8**, 205-212.

**Akler A.P., Lim P., Sem R., Shah N.K., Yi P., Bouth D.M., Tsuyuoka R., Maguire J.D., Fandeur T., Ariey F., Wongsrichanalai C., Meshnick S.R.** (2007). *Pfmdr1* and *in vivo* resistance to Artesunate-Mefloquine in *Falciparum* malaria on the Cambodian-Thai border. *American Journal of Tropical Medicine and Hygeine*. **76**, (4), 641-647.

**Anderios F., NoorRain A. and Vythilingam L.** (2009). In vivo study of human Plasmodium knowlesi in Macaca fascicularis. *Experimental parasitology,* **124,** 181-189.

**Anders R.F.** (2011). The case for a subunit vaccine against malaria. *Trends in Parasitology*. **27**, (8), 330-334.

**Andrews L., Andersen R.F., Webster D., Dunachie S., Walther R.M., Bejon P., Hunt-Cooke A., Bergson G., Sanderson F., Hill A.V.S. and Gilbert A.C.** (2005). Quantitative Real-time Polymerase Chain Reaction for Malaria Diagnosis and its use in Vaccine Clinical Trials. *Amercan Journal of Tropical Medicine and Hygiene,* **73** (1)**,** 191-198.

**Anthony L.C., Suzuki H. and Filutowicz M.** (2004). Tightly regulated vectors for the cloning and expression of toxic genes. *Journal of Microbiological Methods,* **58,** 243-250.

**Antia R., Yates A. and de Roode J.C.** (2008). The dynamics of acute malaria infections. I. Effect of the parasite's red blood cell preference. *Proceedings of the Royal Society,* **275,** 1449-1458.

**Ashley E. A., Touabi M., Ahrer M., Hutagalung R., Htun K., Luchavez J., Dureza C., Proux S., Leimanis M., Min Lwin M., Koscalova A., Comte E., Hamade P., Page A-L., Nosten F. and Guerin P. J.** (2009). Evaluation of three parasite lactate dehydrogenase-based rapid diagnostic tests for the diagnosis of falciparum and vivax malaria. *Malaria Journal,* **8,** 241.

**Aurrecoechea C., Brestelli J., Brunk B., Dommer J., Fischer S., Gajria B., Gao X., Gingle A., Grant G., Harb O.S., Heiges M., Innamorato F., Iodice J., Kissinger J.C., Kraemer E., Li W., Miller J.A., Nayak V., Pennington C., Pinney D.F., Roos D.S., Ross C., Stoeckert C.J.Jr., Treatman C. and Wang H.** (2009). PlasmoDB: a functional genomic database for malaria parasites. *Nucleic Acids Research,* **37** (suppl 1), D539-D543, doi: 10.1093/nar/gkn814

**Bahl A., Brunk B., Coppel R., Crabtree J., Diskin S.J., Fraunholtz M.J., Grant G.R., Gupta D., Huestis R.L., Kissinger J.C., Labo P., Li L., McWeeney S.K., Milgram A.J., Roos D.S., Schug J. and Stoekert C.J.Jr.** (2002). PlasmoDB: the *Plasmodium* genome resource. An integrated database providing tools for accessing, analyzing and mapping expression and sequence data (both finished and unfinished). *Nucleic Acids Research,* **30** (1)**,** 87-90.

**Baird J.K.** (2009). Resistance to therapies for infection by Plasmodium vivax. *Clinical microbiology reviews,* **22** (3)**,** 508.

**Baker J., Ho M-F., Pelecanos A., Gatton M., Chen N., Abdullah S., Albertini A., Ariey F., Barnwell J., Bell D., Cunningham J., Djalle D., Echeverry D.F., Gamboa D., Hii J., Kyaw M.P., Luchavez J., Membi C., Menard D., Murillo C., Nhem S., Ogutu B., Onyor P., Oyibo W., Wang S.Q., McCarthy J. and Cheng Q.** (2010). Global sequence variation in the histidine-rich proteins 2 and 3 of Plasmodium falciparum: implications for the performance of malaria rapid diagnostic tests. *Malaria Journal,* **9** (129), doi:10.1186/1475-2875-9-129

**Baldacci P. and Ménard R.** (2004). The elusive malaria sporozoite in the mammalian host. *Molecular Microbiology,* **54** (2)**,** 298-306.

**Bannister L.H., Hopkins J.M., Fowler R.E., Krishna S. and Mitchell G.H.** (2000). A Brief Illustrated Guide to the Ultrastructure of *Plasmodium falciparum* Asexual Blood Stages. *Molecular Approaches to Malaria,* **16** (10)**,** 427-433.

**Berwal R., Gopalan N., Chandel K., Prasad G. and Prakash S.** (2008). Plasmodium falciparum: Enhanced soluble expression, purification and biochemical characterization of lactate dehydrogenase. *Experimental parasitology,* **120** (2)**,** 135-141.

**Betson M., Jawara M. and Awolola T.S.** (2009). Status of insecticide susceptibility in Anopheles gambiae s.I. from malaria surveillance sites in The Gambia. *Malaria Journal,* **8,** 187.

**Bhattarai A., Ali A.A., Kachur P., Martensson A., Abbas A.K., Khatib R., Al-mafazy A., Ramsan M., Rotllant G., Gerstenmaier J.F., Molteni F., Abdulla S., Montgomery S.M., Kaneko A. and Björkman A.** (2007). Impact of Artemisinin-Based Combination Therapy and Insecticide-Treated Nets on Malaria Burden in Zanzibar. *PLoS Med,* **4** (11), doi:10.1371/journal.pmed.0040309

**Bisoffi Z., Gobbi F., Angheben A. and Van den Ende J.** (2009). The Role of Rapid Diagnostic Tests in Managing Malaria. *PLoS Med,* **6** (4), doi:10.1371/journal.pmed.1000063

**Bissati K.E., Zufferey R., Witola W.H., Carter N.S., Ullman B. and Mamoun C.B.** (2006). The plasma membrane permease PfNT1 is essential for purine salvage in the human malaria parasite Plasmodium falciparum. *PNAS,* **103** (24)**,** 9286-9291.

**Black R.E., Morris S.S. and Bryce J.** (2003). Where and why are 10 million children dying every year? *The Lancet,* **361,** 2226-2234.

**Blanford S., Wangpeng S., Christian R., Marden J.H., Koekemoer L.L., Brooke B.D., Coetzee M., Read A.F. and Thomas M.B.** (2011). Lethal and Pre-Lethal Effects of a Fungal Biopesticide Contribute to Substantial and Rapid Control of Malaria Vectors. *PLoS ONE,* doi:10.1371/journal.pone.0023591

**Bozdech Z., Llinas M., Pulliam B.L., Wong E.D., Zhu J. and DeRisi J.L.** (2003). The transcriptome of the intraeryhtrocytic developmental cycle of Plasmodium falciparum. *Plos Biology,* **1,** 1-16.

**Bradford M.M.** (1976). A Rapid and Sensitive Method for the Quantitation of Microgram Quantities of Protein Utilizing the Principle of Protein-Dye Binding. *Analytical Biochemistry,* **72,** 248-254.

**Broedel S.E., Papciak S.M. and LJones W.R.** (2001). The Selection of Optimum Media Formulations for Improved Expression of Recombinant Proteins in *E. coli*. *Technical Bulletin,* **2**, 1-8.

**Buppan P., Putaporntip C., Pattanawong U., Seethamchai S. and Jongwutiwes S.** (2010). Comparative detection of Plasmodium vivax and Plasmodium falciparum DNA in saliva and urine samples from symptomatic malaria patients in a low endemic area. *Malaria Journal,* **9** (72), doi:10.1186/1475-2875-9-72.

**Campanale N., Nickel C., Daubenberger C.A., Wehlan D.A., Gorman J.J., Klonis N., Becker K., Tilley L.** (2003). Identification and Characterisation of Heme-interacting Proteins in the Malaria Parasite, *Plasmodium falciparum*. *The Journal of Biological Chemistry*. **278**, (30), 27354-27361.

**Cármenes R.S., Freije J.P., Molina M.M. and Martín J.M.** (1989). Predict7, a program for protein structure prediction. *Biochemical and Biophysical Research Communications,* **159** (2)**,** 687-693.

**Carugo O. and Argos P.** (1997). NADP Dependent enzymes. I: Conserved stereochemistry of cofactor binding. *Proteins: Structure, Function, and Bioinformatics,* **28** (1)**,** 10-28.

**Chae H.Z., Uhm T.B. and Rhee S.G.** (1994). Dimerization of thiol-specific antioxidant and the essential role of cysteine 47. *Proceedings of the national academy of science USA: Biochemistry,* **91,** 7022-7026.

**Chapel H.M. and August P.J.** (1976). Report of nine cases of accidental injury to man with Freund's complete adjuvant. *Clinical Experimental Immunology,* **24**, 538-541.

**Chin W., Contacos P.G., Coatney G.R., Kimball H.R.** (1965). A Naturally Acquired Quotidian-type Malaria in Man Transferable to Monkeys. *Science*, **149**, (3686), 865.

**Chiodini P.L., Bowers K., Jorgensen P., Barnwell J.W., Grady K.K., Luchavez J., Moody A.H., Cenizal A. and Bell D.** (2007). The heat stability of Plasmodium lactate dehydrogenase-based and histidine-rich protein 2-based malaria rapid diagnostic tests. *Transactions of the Royal Society of Tropical Medicine and Hygiene,* **101,** 331-337.

**Chou P.Y. and Fasman G.D.** (1978). Prediction of beta-turns. *Biophysical Journal*, **26**, (3), 367-383.

**Chuangchaiya S., Jangpatarapongsa K., Chootong P., Sirichaisinthop J., Sattabongkot J., Pattanapanyasat K., Chotivanich K., Troye-Blomberg M., Cui L. and Udomsangpetch R.** (2009). Immune response to Plasmodium vivax has a potential to reduce malaria severity. *Clinical and Experimental Immunology*, **160** (2), 233-239.

**Clark A.G. and Whittam T.S.** (1992). Sequencing Errors and Molecular Evolutionary Analysis. *Molecular Biology and Evolution,* **9** (4), 744-752.

**Coetzer T.H.T.** (1985). Preparation and characterisation of antibodies against mouse Ig (all classes). *Internal Reports, Bioclones, (Pty.) Ltd. Immunology Group, Stellenbosch.*

**Collins W.E. and Jeffery G.M.** (2005). Plasmodium ovale: parasite and disease. *Clinical microbiology reviews,* **18** (3)**,** 570.

**Collins W.E. and Jeffery G.M.** (2007). Plasmodium malariae: parasite and disease. *Clinical microbiology reviews,* **20** (4)**,** 579.

**Cox-Singh J., Davis T.M.E., Lee K.S., Shamsul S.S.G., Matusop A., Ratnam S., Rahman H.A., Conway D.J., Singh B.** (2008). Plasmodium knowlesi malaria in humans is widely distributed and potentially life threatening. *Clinical Infectious Diseases,* **46**, (2), 165.

**Craig M.H., Bredenkamp B.L., Vaughan Williams C.H., Rossouw E.J., Kelly V.J., Kleinschmidt I., Martineau A. and Henry F.J.** (2002). Field and laboratory comparative evaluation of ten rapid malaria diagnostic tests. *Transactions of the Royal Society of Tropical Medicine and Hygiene,* **96,** 258-265.

**D'Acremont V., Lengeler C. and Genton B.** (2010). Reduction in the proportion of fevers associated with *Plasmodium falciparum* parasitemia in Africa: a systematic review. *Malaria Journal,* **9,** 240.

**Daneshvar C., Davis T.M.E., Cox-Singh J., Rafa'ee M.Z., Zakarai K., Divis P.C.S. and Singh B.** (2009). Clinical and Laboratory Features of Human *Plasmodium knowlesi* Infection. *Clinical Infectious Diseases,* **49** (6)**,** 852-860.

**Daneshvar C., Davis T.M.E., Cox-Singh J., Rafa'ee M.Z., Zakaria S.K., Divis P.C.S. and Singh B.** (2010). Clinical and parasitological response to oral chloroquine and primaquine in uncomplicated human *Plasmodium knowlesi* infections. *Malaria Journal,* **9** (1)**,** 238.

**Daubenberger C.A., Pölt-Frank F., Jiang G., Lipp J., Certa U., Pluschke G.** (2000). Identification and recombinant expression of glyceraldehyde-3-phosphate dehydrogenase of *Plasmodium falciparum*. *Gene*. **246**, 255-264.

**Daubenberger C.A., Tisdale E.J., Curcic M., Diaz D., Silvie O., Mazier D., Eling W., Bohrmann B., Matile H., Pluschke G.** (2003). The N'-Terminal Domain of Glyceraldehyde-3-phosphate Dehydrogenase of the Apicomplexan *Plasmodium falciparum* Mediates GTPase Rab2-Dependent Recruitment to Membranes. *Biological Chemistry*. **384**, 1227-1237.

**David P.H., Hommel M., Miller L.H., Udeinya I.J. and Oligino L.D.** (1983). Parasite sequestration in Plasmodium falciparum malaria: Spleen and antibody modulation of cytoadherence of infected erythrocytes. *Proc. Natl. Acad. Sci. USA,* **80,** 5075-5079.

**de Boer H.A., Comstock L.J. and Vasser M.** (1983). The *tac* promoter: A functional hybrid derived from the *trp* and *lac* promoters. *Proceedings of the national academy of science USA: Biochemistry,* **80,** 21-25.

**De Gregorio, E., D'ORO U., WACK A.** (2009). Immunology of TLR-independent vaccine adjuvants. *Current Opinion in Immunology***, 21** (3), 339-345.

**Delves P.J., Martin S.J., Burton D.R. and Roitt I.M.** (2006). *Roitt's Essential immunology*. Blackwell Publishing Ltd., London, 37-38; 57; 112; 221-223.

**Demana P.H., Fehske C., White K., Rades T. and Hook S.** (2004). Effect of incorporation of the adjuvant Quil A on structure and immune stimulatory capacity of liposomes. *Immunology and Cell Biology,* **82,** 547-554.

**Demas A., Oberstaller J., DeBarry J., Lucchi N.W., Srinivasamoorthy G., Sumari D., Kabanywanyi A.M., Vigellas L., Escalante A.A., Kachur S.P., Barnwell J.W., Peterson D.S., Udhayakumar V. and Kissinger J.C.** (2011). Applied Genomics: Data Mining Reveals Species-Specific Malaria Diagnositc Targets More Sensitive than 18S rRNA. *Journal of Clinical Microbiology,* **49** (7)**,** 2411-2418.

**Dostert C., Guarda G., Romero J.F., Menu P., Gross O., Tardivel A., Suva M., Stehle J., Kopf M., Stamenkovic I., Corradin G. and Tschopp J.** (2009). Malaria Hemozoin Is a Nalp3 Inflammasome Activating Danger Signal. *PLoS One*, **4** (8), doi:10.1371/journal.pone.0006510.

**Duffy P.E. and Mutabingwa T.K.** (2005). Rolling back a malaria epidemic in South Africa. *PLoS Med,* **2** (11), doi:10.1371/journal.pmed.0020368.

**Dunn C.R., Banfield M.J., Barker J.J., Higham C.W., Moreton K.M., Turgut-Balik D., Brady R.L. and Holbrook J.J.** (1996). The structure of lactate dehydrogenase from Plasmodium falciparum reveals a new target for anti-malarial design. *Nature Structural Biology*, **3** (11)**,** 912-915.

**Egan T.J., Ncokazi K.K.** (2005). Quinoline antimalarials decrease the rate of β-hematin formation. *Journal of Inorganic Biochemistry.* **99**, 1532-1539.

**Emini E.A., Hughes J.V., Perlow D.S., Boger J.** (1985). Induction of hepatitis A virus-neutralizing antibody by a virus-specific synthetic peptide. *Journal of Virology*, **55**, (3), 836-839.

**Faechem R.G.A., Phillips A.A. and Targett G.A., (editors).** (2009). *Shrinking the Malaria Map: A Prospectus on Malaria Elimination*. The Global Health Group: Global Health Sciences, San Francisco, 23, 89, 133.

**Feliu J.X., Cubarsi R. and Villaverde A.** (1997). Optimized Release of Recombinant Proteins by Ultrasonication of E. coli Cells. *Biotechnology and Bioengineering,* **58** (5)**,** 536-540.

**Ferdinand W.** (1964). The Isolation and Specific Activity of Rabbit-Muscle Glyceraldehyde Phosphate Dehydrogenase. *Biochemistry Journal,* **92**, 578.

**Fernandes de Oliviera M.R., de Catro Gomez A. and Toscano C.M.** (2010). Cost effectiveness of OptiMal® rapid diagnostic test for malaria in remote areas of the Amazon Region, Brazil. *Malaria Journal,* **9** (1)**,** 277.

**Fernando G.J. P., Stenzel D.J., Tindle R.W., Merza M.S., Morein B. and Frazer I.H.** (1995). Peptide polymerisation facilitates incorporation into ISCOMs and increases antigen-specific IgG2a production. *Vaccine,* **13** (15)**,** 1460-1467.

**Ferreira M.U. and Katzin A.M.** (1995). The assessment of antibody affinity distribution by thiocyanate elution: a simple dose-response approach. *Journal of Immunological Methods,* **187,** 297-305.

**Forney J.R., Magill A.J., Wongsrichanalai C., Sirichaisinthop J., Bautista C.T., Heppner D.G., Miller R.S., Ockenhouse C.F., Gubanov A., Shafer R., DeWitt C.C., Quino-Ascurra H.A., Kester K.E., Kain K.C., Walsh D.S., Ballou W.R. and Gasser R.A.Jr.** (2001). Malaria Rapid Diagnostic Devices: Performance Characteristics of the *Para*Sight F Device Determined in a Multisite Field Study. *Journal of Clinical Microbiology,* **39** (8)**,** 2884-2890.

**Foth B.J., Zhang N., Chaal B.K., Sze S.K., Preiser P.R. and Bozdech Z.** (2011). Quantitative time-course profiling of parasite and host cell proteins in the human malaria parasite Plasmodium falciparum. *Molecular and Cellular Proteomics,* **10** (8), doi:10.1074/mcp.M110.006411

**Foth B.J., Zhang N., Mok S., Preiser P.R. and Bozdech Z.** (2008). Quantitative protein expression profiling reveals extensive post-transcriptional regulation and post-translational modifications in schizont-stage malaria parasites. *Genome biology,* **9** (12)**,** R177.

**Francis Crick.** (1970). Central Dogma of Molecular Biology. *Nature,* **227**, 561-563.

**Friesen J., Silvie O., Putrianti E.D., Hafalla J.C.R., Matuschewski K. and Borrmann S.** (2010). Natural Immunization Against Malarai: Causal Prophylaxis with Antibiotics. *Malaria,* **2** (40), 40ra49, doi: 10.1126/scitranslmed.3001058.

**Fujioka H. and Aikawa M.** (2002). Malaria Parasites and Disease, Structure and Lifecycle. *Malaria Immunology,* 80, 1-26.

**Gamboa D., Ho M-F., Bendezu J., Torres K., Chiodini P.L., Barnwell J.W., Incardona S., Perkins M., Bell D., McCarthy J. and Cheng Q.** (2010). A Large Proportion of P. falciparum Isolates in the Amazon Region of Peru Lack pfhrp2 and pfhrp3: Implications for Malaria Rapid Diagnostic Tests. *Plos one,* **5** (1)**,** e8091.

**Gbotosho G.O., Happi C.T., Folarin O., Keyamo O., Sowunmi A. and Oduola A.M.J.** (2010). Rapid Detection of Lactate Dehydrogenase and Genotyping of *Plasmodium falciparum* in Saliva of Children with Acute Uncomplicated Malaria. *Amercan Journal of Tropical Medicine and Hygiene,* **83** (3)**,** 496-501.

**Gillet P., Mori M., Van den Ende J. and Jacobs J.** (2010). Buffer substitution in malaria rapid diagnostic tests causes false-positive results. *Malaria Journal,* **9** (215), doi:10.1186/1475-2875-9-215.

**Gillet P., Mori M., Van Esbroeck M., Van den Ende J. and Jacobs J.** (2009). Assessment of the prozone effect in malaria rapid diagnostic tests. *Malaria Journal,* **8** (271), doi:10.1186/1475-2875-8-271.

**Gkrania-Klotsas E. and Lever A.M.L.** (2007). An update on malaria prevention, diagnosis and treatment for the returning traveller. *Blood Reviews,* **21,** 73-87.

**Glenny A.T., Pope C.G., Waddington H., Wallace U.** (1926). Immunological notes XVII to XXIV. *Journal of Pathology,* **29**, 31-40.

**Goldman M. and Lambert P.H.** (2004). *Immunological safety of vaccines: Facts, hypotheses and allegations. Novel vaccination strategies,* Weinhem, Wiley-VCH, 595-611.

**Goldring J.P.D. and Coetzer T.H.T.** (2003). Isolation of Chicken Immunoglobulins (IgY) from Egg Yolk. *Biochemistry and Molecular Biology Education*, **31**, 185-187.

**Golenser J., Waknine J.H., Krugliak M., Hunt N.H. and Grau G.E.** (2006). Current perspectives on the mechanism of action of artemisinins. *International Journal for Parasitology,* **36,** 1427-1441.

**Golgi C.** (1886). Sull'infezione malarica. *Arch. Sci. Medicine*, **10**, 109-135.

**Gomez M.S., Piper R.C., Hunsaker L.A., Royer R.E., Deck L.M., Makler M.T. and Vander Jagt D.L.** (1997). Substrate and cofactor specificity and selective inhibition of lactate dehydrogenase from the malarial parasite P. falciparum. *Molecular and Biochemical Parasitology,* **90,** 235-246.

**Good M.F.** (2011). A whole parasite vaccine to control the blood stages of *Plasmodium* – the case for lateral thinking. *Trends in Parasitology*. **27**, (8), 335-340.

**Gove, S.** (1997) WHO Working Group on guidelines for IMCI. Integrated Management of Childhood Illness by outpatient health workers: technical basis and overview. *Bull WHO,* **75** (Suppl 1)**,** 7-24.

**Granchi C., Bertini S., Macchia M., Minutolo F.** (2010). Inhibitors of Lactate Dehydrogenase Isoforms and their Therapeutic Potentials. *Current Medicinal Chemistry*. **17**, 672-697.

**Grassi B.** (1900). *Studi di uno Zoologo Sulla Malaria*. Academia dei Lincei, Rome, 296.

**Grassi B. and Feletti R.** (1890). Parasites malariques chez les oiseaux. Arch. Ital. de Biologie **13**, 297-300.

**Graz B., Willcox M., Szeless T. and Rougemont A.** (2011). "Test and treat" or presumptive treatment for malaria in high transmission situations? A reflection on the latest WHO guidelines. *Malaria Journal,* **10** (136), doi:10.1186/1475-2875-10-136.

**Gregoriadis G., Allison A.C., Poste G.** (1989). *Immunological adjuvants and vaccines.*, Plenum Publishing Corporation, New York, 244.

**Guermonprez P., Saveanu L., Kleijmeer M., Davoust J., van Endert P. and Amigorena S.** (2003). ER-phagosome fusion defines an MHC class I cross-presentation compartment in dendritic cells. *Nature,* **425,** 397-402.

**Gupta R.K., Siber G.R.** (1995). Adjuvants for human vaccines-current status, problems and future prospects. *Vaccine,* **13**, 1263-1276.

**Gwer S., Newton C.R.J.C. and Berkley J.A.** (2007). Over-diagnosis and Co-Morbidity of Severe Malaria in African Children: A Guide for Clinicians. *American Journal of Tropical Medicine and Hygeine,* **77,** 6-13.

**Hafalla J.C., Silvie O. and Matuschewski K.** (2011). Cell biology andimmunology of malaria. *Immunological Reviews,* **240,** 297-316.

**Hall N., Karras M., Raine J.D., Carlton J.M., Kooij T.W.A., Berriman M., Florens L., Janssen C.S., Pain A., Christophides G.K., James K., Rutherford K., Harris B., Harris D., Churcher C., Quail M.A., Ormond D., Doggett J., Trueman H.E., Mendoza J., Bidwell S.L., Rajandream M-A., Carucci D.J., Yates III J.R., Kafatos F.C., Janse C.J., Barrell B., Turner C.M.R., Waters A.P. and Sinden R.E.** (2005). A Comprehensive Survey of the Plasmodium Life Cycle by Genomic, Transcriptomic, and Proteomic Analyses. *Science,* **307** (82)**,** 82-86.

**Hänscheid T., Frita R., Längin M., Kremsner P.K. and Grobush M.P.** (2009). Is flow cytometry better in counting malaria pigment-containing leukocytes compared to microscopy? *Malaria Journal,* **8** (255), doi:10.1186/1475-2875-8-255.

**Hänscheid T., Melo-Cristino J. and Pinto B.G.** (2001). Automated detection of malaria pigment in white blood cells for the diagnosis of malaria in Portugal. *American Journal of Tropical Medicine and Hygeine,* **64** (5, 6)**,** 290-292.

**Harris I., Sharrock W.W., Bain L.M., Gray K., Bobogare A., Boaz L., Lilley K., Krause D., Valley A., Johnson M., Gatton M.L., Shanks G.D. and Cheng Q.** (2010). A large proportion of asymptomatic *Plasmodium* infections with low and sub-microscopic parasite densities in the low transmission setting of Temotu Province, Solomon Islands: challenges for malaria diagnostics in an elimination setting. *Malaria Journal,* **9** (1)**,** 254.

**Hartkopf A. and Delumyea R.** (1974). Use of The Luminol Reaction for Metal Ion Detection in Liquid Chromatography. *Analytical Letters,* **7** (1)**,** 79-88.

**Hay S.I., Guerra C.A., Gething P.W., Patil A.P., Tatem A.J., Noor A.M., Kabaria C.W., Manh B.H., Elyazar I.R.F., Brooker S., Smith D.L., Moyeed R.A. and Snow R.W.** (2009). A World Malaria Map: Plasmodium falciparum Endemicity in 2007. *PLoS MED,* **6** (3), e1000048. doi:10.1371/journal.pmed.1000048.

**Herbert W.J.** (1968). The Mode of Action of Mineral-Oil Emulsion Adjuvants on Antibody Production in Mice. *Immunology,* **14** (3), 301-318.

**Hill F., Gemünd C., Benes V., Ansorge W., Gibson J.** (2000). An estimate of large-scale sequencing accuracy", *EMBO Reports,* **1**, 29–31.

**Hopp T.P. and Woods K.R.** (1981). Prediction of protein antigenic determinants from amino acid sequences. *Proceedings of the National Academy of Science USA,* **78**, 3824.

**Houde M., Bertholet S., Gagnon E., Brunet S., Goyette G., Laplante A., Princiotta M.F., Thibault P., Sacks D. and Desjardins M.** (2003). Phagosomes are competent organelles for antigen cross-presentation. *Nature,* **425,** 402-406.

**Houze S., Hubert V., Le Pessec G., Le Bras J. and Clain J.** (2011). Combined Deletions of pfhrp2 and pfhrp3 Genes Result in Plasmodium falciparum Malaria False-Negative Rapid Diagnostic Test *Journal of Clinical Microbiology,* **49** (7)**,** 2694-2696.

**Howard R.J., Uni S., Aikawa M., Aley S.B., Leech J.H., Lew A.M., Wellems T.E., Rener J. and Taylor D.W.** (1986). Secretion of a Malarial Histidine-rich Protein (Pf HRP II) from Plasmodium falciparum-infected Erythrocytes. *The Journal of Cell Biology,* **103,** 1269-1277.

**Hurdayal R., Achilonu I., Choveaux D., Coetzer T.H.T. and Goldring J.P.D.** (2010). Anti-peptide antibodies differentiate between plasmodial lactate dehydrogenases. *Peptides,* **31,** 525-532.

**Iqbal J., Sher A., Rab A.** (2000). *Plasmodium falciparum* Histidine-Rich Protein 2-Based Immunocapture Diagnostic Assay for Malaria: Cross-Reactivity with Rheumatoid Factors. *Journal of Clinical Microbiology*. **38**, (3), 1184-1186.

**Iqbal J., Siddique A., Jameel M. and Hira P.R.** (2004). Persistent histidine-rich protein 2, parasite lactate dehydrogenase, and panmalarial antigen reactivity after clearance of Plasmodium falciparum monoinfection. *Journal of Clinical Microbiology,* **42** (9)**,** 4237.

**Ishengoma D.S., Lwitho S., Madebe R.A., Nyagonde N., Persson O., Vestergaard L.S., Bygbjerg I.C., Lemnge M.M. and Alifrangis M.** (2011). Using rapid diagnostic tests as source of malaria parasite DNA for molecular analyses in the era of declining malaria prevalence. *Malaria Journal,* **10** (6), doi:10.1186/1475-2875-10-6.

**Ishihama Y., Oda Y., Tabata T., Sato T., Nagasu T., Rappsilber J. and Mann M.** (2005). Exponentially modified protein abundance index (emPAI) for estimation of absolute protein amount in proteomics by the number of sequenced peptides per protein. *Molecular and Cellular Proteomics,* **4** (9)**,** 1265-1272.

**Jackson K.E., Habib S., Frugier M., Hoen R., Khan S., Pham J.S., de Pouplana L.R., Royo M., Santos M.A.S., Sharma A. and Ralph S.A.** (2011). Protein translation in Plasmodium parasites. *Trends in Parasitology,* **27** (10)**,** 467-476.

**Jackson K.E., Spielmann T., Hanssen E., Adisa A., Separovic F., Dixon M.W.A., Trenholme K.R., Hawthorne P.L., Gardiner D.L., Gilberger T. and Tilley L.** (2007). Selective permeabilization of the host cell membrane of *Plasmodium falciparum*-infected red blood cells with streptolysin O and equinatoxin II. *Biochemical Journal,* **403,** 167-175.

**Jameson B.A., Wolf H.** (1988). The antigenic index: a novel algorithm for predicting antigenic determinants. *Computer Applications in the Biosciences,* **4**, (1), 181-186.

**Jiang H.L., Kang M.L., Quan J.S., Kang S.G., Akaike T., Yoo H.S., Cho C.S.** (2008). The potential of mannosylated chitosan microspheres to target macrophage mannose receptors in an adjuvant-delivery system for intranasal immunization. *Biomaterials*. **29**, 1931-1939.

**Johansson J., Ledina A., Vernerssona M., Lövgren-Bengtsson K., Hellman L.** (2004). Identification of adjuvants that enhance the therapeutic antibody response to host IgE *Vaccine,* **22**, 2873-2880.

**Jorgensen P., Chanthap L., Rebueno A., Tsuyuoka R. and Bell D.** (2006). Malaria Rapid Diagnostic Tests In Tropical Climates: The Need For A Cool Chain. *American Journal of Tropical Medicine and Hygeine,* **74** (5)**,** 750-754.

**Källander K., Nsungwa-Sabiiti J. and Peterson S.** (2004). Symptom overlap for malaria and pneumonia – policy implications for home management strategies. *Acta Tropica,* **90,** 211-214.

**Kanzok S.M. and Jacobs-Lorena M.** (2006). Entomopathogenic fungi as biological insecticides to control malaria. *Trends in Parasitology,* **22** (2)**,** 49-51.

**Kappe S.H.I., Vaughan A.M., Boddey J.A., Cowman A.F.** (2010). That was then but this is now: Malaria Research in the time of an eradication agenda. *Science*. **328**, 862-866.

**Kawai S., Hirai M., Haruki K., Tanabe K. and Chigusa Y.** (2009). Cross-reactivity in rapid diagnostic tests between human malaria and zoonotic simian malaria parasite Plasmodium knowlesi infections. *Parasitology International,* **58** (3)**,** 300-302.

**Kebaier C., Voza T. and Vanderberg J.** (2009). Kinetics of Mosquito-Injected *Plasmodium* Sporozoites in Mice: Fewer Sporozoites Are Injected into Sporozoite-Immunized Mice. *PLoS PATHOGENS,* **5** (4), e1000399. doi:10.1371/journal.ppat.1000399.

**Khairnar K., Martin D., Lau R., Ralevski F. and Pillai D.** (2009). Multiplex real-time quantitative PCR, microscopy and rapid diagnostic immuno-chromatographic tests for the detection of Plasmodium spp: performance, limit of detection analysis and quality assurance. *Malaria Journal,* **8** (284), doi:10.1186/1475-2875-8-284.

**Khetan, S. K.** (2001). *Microbial pest control*. CRC Press, 300.

**Kidane G. and Morrow R.H.** (2000). Teaching mothers to provide home treatment of malaria in Tigray, Ethiopia: a randomized trial. *Lancet*, **356**, 550-555.

**Kiefer F., Arnold K., Künzli M., Bordoli L. and Schwede T.** (2009). The SWISS-MODEL Repository and associated resources. *Nucleic Acids Research,* **37**, D387–D392, doi:10.1093/nar/gkn750.

**Kifude C.M., Rajasekariah H.G., Sullivan Jr. D.J., Stewart V., Angov E., Martin S.K., Diggs C.L. and Waitumbi J.N.** (2008). Enzyme-linked immunosorbent assay for detection of Plasmodium falciparum histidine-rich protein 2 in blood, plasma, and serum. *Clinical and vaccine immunology,* **15** (6)**,** 1012.

**Kiszewski A., Mellinger A., Spielman A., Malaney P., Sachs S.E. and Sachs J.** (2004). A Global Index Representing the Stability of Malaria Transmission. *Amercan Journal of Tropical Medicine and Hygiene,* **70** (5)**,** 486-498.

**Kodisinghe H.M., Perera K.L.R.L., Premawansa S., de S. Naotunne T., Wickramasinghe A.R. and Mendis K.N.** (1997). The ParaSight™-F dipstick test as a routine diagnostic tool for malaria in Sri Lanka. *Transactions of the Royal Society of Tropical Medicine and Hygiene,* **91** (4)**,** 398-402.

**Koenderink J.B., Kavishe R.A., Rijpma S.R. and Russel F.G.M.** (2010). The ABCs of multidrug resistance in malaria. *Trends in Parasitology,* **26,** 440-446.

**Kopp J. and Schwede T.** (2003). The SWISS-MODEL Repository of annotated three-dimensional protein structure homology models. *Nucleic Acids Research,* **32**, D230–D234, doi: 10.1093/nar/gkh008.

**Kristensen T., Lopez R., Prydz H.** (1992). An estimate of the sequencing error frequency in the DNA sequence databases, *DNA Sequence*, **2**, 343–346.

**Kublin J.G., Dzinjalamala F.K., Kamwendo D.D., Malkin E.M., Cortese J.F., Martino L.M., Mukadam R.A.G., Rogerson S.J., Lescano A.G., Molyneux M.E., Winstanley P.A., Chimpeni P., Taylor T.E., Plowe C.V.** (2002). Molecular Markers for Failure of Sulfadoxine-Pyrimethamine and Chlorproguanil-Dapsone Treatment of *Plasmodium falciparum* Malaria. *The Journal of Infectious Diseases*, **185**, 380-388.

**Kuss C., Gan C.S., Gunalan K., Bozdech Z., Sze S.K., Preiser P.R.** (2012). Quantitative Proteomics Reveals New Insights into Erythrocyte Invasion by *Plasmodium falciparum*. *Molecular and Cellular Proteomics*, **11**, (2), doi: 10.1074/mcp.M111.010645.

**Kyte J., Doolittle R.F.** (1982). A simple method for displaying the hydropathic character of a protein. *Journal of Molecular Biology*, **157**, (1), 105-132.

**Laemmli U.K.** (1970). Cleavage of structural proteins during the assembly of the head of bacteriophage T. *Nature*. **277**, 680-685.

**Lalloo D.G., Shingadia D., Pasvol G., Chiodini P.L., Whitty C.J., Beeching N.J., Hill D.R., Warrell D.A., Bannister B.A.** (2007). UK malaria treatment guidelines. *Journal of Infection,* **54** (2), 111-121.

**Lamperti E.D., Kittelberger J.M., Smith T.F., Villakomaroff L.** (1992). Corruption of genomic databases with anomalous sequence. *Nucleic Acids Research*, **20**, 2741–2747.

**Lasonder E., Ishihama Y., Andersen J.S., Vermunt A.M.W., Pain A., Sauerwein R.W., Eling W.M.C., Hall N., Waters A.P., Stunnenberg H.G. and Mann M.** (2002). Analysis of the *Plasmodium flaciparum* proteome by high-accuracy mass spectrometry. *Nature,* **419**, 537-542.

**Laveran A.** (1880). Note sur un nouveau parasite trouve dans le sang de plusiers maladies attients de fievre palustre. *Bulletins of Academy of Medicine*, **9**, 1235-1236.

**Lau Y., Fong M., Mahmud R., Chang P., Palaeya V., Cheong F., Chin L., Anthony C.N., Al-Mekhlafi M. and Chen Y.** (2011). Specific, sensitive and rapid detection of human *Plasmodium knowlesi* infection by loop-mediated isothermal amplification (LAMP) in blood samples. *Malaria Journal,* **10** (197), doi:10.1186/1475-2875-10-197.

**Le Roch K.G., Zhou Y., Blair P.L., Grainger M., Moch J.K., Haynes J.K., De la Vega P., Holder A.A., Batalov S., Carucci D.J. and Winzeler E.A.** (2003). Discovery of Gene Function by Expression Profiling of the Malaria Parasite Life Cycle. *Science,* **301,** 1503-1508.

**Lee, K. S., Cox-Singh J. and Singh B.** (2009). Morphological features and differential counts of Plasmodium knowlesi parasites in naturally acquired human infections. *Malaria Journal,* **8,** 73-73.

**Lee N., Baker J., Andrews K.T., Gatton M.L., Bell D., Cheng Q. and McCarthy J.** (2006). Effect of Sequence Variation in Plasmodium falciparum Histidine-Rich Protein 2 on Binding of Specific Monoclonal Antibodies: Implications for Rapid Diagnostic Tests for Malaria. *Journal of Clinical Microbiology,* **44** (8)**,** 2773-2778.

**Lee N., Baker J., Bell D., McCarthy J. and Cheng Q.** (2006). Assessing the Genetic Diversity of the Aldolase Genes of Plasmodium falciparum and Plasmodium vivax and Its Potential Effect on Performance of Aldolase-Detecting Rapid Diagnostic Tests. *Journal of Clinical Microbiology,* **44** (12)**,** 4547-4549.

**Leitgeb A.M., Blomqvist K., Cho-Ngwa F., Samje M., Nde P., Titanji V. and Wahlgren M.** (2011). Low Anticoagulant Heparin Disrupts *Plasmodium falciparum* Rosettes in Fresh Clinical Isolates. *Amercan Journal of Tropical Medicine and Hygiene,* **84** (3)**,** 390-396.

**Levine R.S., Peterson A.T., Benedict M.Q.** (2004). Geographic and ecologic distributions of the *Anopheles gambiae* complex predicted using a genetic algorithm. *American Journal of Tropical Medicine and Hygeine.* **70**, 105-109.

**Li X., Nakano T., Sunwoo H.H., Paek B.H., Chae H.S. and Sim J.S.** (1998). Effects of Egg and Yolk Weights on Yolk Antibody (IgY) Production in Laying Chickens. *Poultry Science,* **77,** 266-270.

**Lindblad E.B.** (2004). Aluminium adjuvants—in retrospect and prospect. *Vaccine,* **22**, 3658-3668.

**Lon C.T., Alcantara S., Luchavez J., Tsuyuoka R. and Bell D.** (2005). Positive control wells: a potential answer to remote-area quality assurance of malaria rapid diagnostic tests. *Transactions of the Royal Society of Tropical Medicine and Hygiene,* **99,** 493-498.

**Luchavez J., J., B., S., A., Belizario V.Jr., Cheng Q., McCarthy J.S. and Bell D.** (2011). Laboratory demonstration of a prozone-like effect in HRP2-detecting malaria rapid diagnostic tests: implications for clinical management. *Malaria Journal,* **10** (286), doi:10.1186/1475-2875-10-286.

**Mackinnon M.J., Li J., Mok S., Kortok M.M., Marsh K., Prieser P.R. and Bozdech Z.** (2009). Comparative Transcriptional and Genomic Analysis of *Plasmodium falciparum* Field Isolates. *PLoS PATHOGENS,* **5** (10), e1000644. doi:10.1371/journal.ppat.1000644.

**Makler M.T., Palmer C.J. and Ager A.L.** (1998). A review of practical techniques for the diagnosis of malaria. *Annals of tropical medicine and parasitology,* **92** (4)**,** 419-433.

**Maltha J., Gillet P., Cnops L., van den Ende J., van Esbroeck M. and Jacobs J.** (2010). Malaria rapid diagnostic tests: Plasmodium falciparum infections with high parasite densities may generate false positive Plasmodium vivax pLDH lines. *Malaria Journal,* **9** (198), doi:10.1186/1475-2875-9-198.

**Marshall J.C., Powell J.R. and Caccone A.** (2005). Short Report: Phylogenetic Relationship of the Anthrophilic *Plasmodium falciparum* Malaria Vectors in Africa. *Amercan Journal of Tropical Medicine and Hygiene,* **73** (4)**,** 749-752.

**Martin S.K., Rajasekariah H.G., Awinda G., Waitumbi J.N. and Kifude C.** (2009). Unified Parasite Lactate Dehydrogenase and Histidine-Rich Protein ELISA for Quantification of *Plasmodium falciparum*. *Amercan Journal of Tropical Medicine and Hygiene,* **80** (4), 516-522.

**Martinez-Torres D., Chandre F., Williamson M.S., Darriet F., Berge J.B., Devonshire A.L., Guillet P., Pasteur N., Pauron D.** (1998). Molecular characterisation of pyrethroid knockdown resistance (*kdr*) in the major malaria vector *Anopheles gambiae s.s. Insect Molecular Biology*. **7**, (2), 179-184.

**Matteeli A., Castelli F., Caligaris S.,** (1997). *Handbook of Malaria Infection in the Tropics.* University of Brescia (Italy), 17-23.

**McCutchan T.F., Piper R.C., Makler M.T.** (2008). Use of malaria rapid diagnostic test to identify *Plasmodium knowlesi* infection. *Emerging Infectious Diseases*, **14**, (11), 1750-1752.

**McNeela E.A. and Mills K.H.G.** (2001). Manipulating the Immune system: humoral versus cell-mediated immunity. *Advanced Drug Delivery Reviews*, **51**, (1), 43-54.

**McMorrow M.L., Masanja M.I., Abdulla S.M.K., Kahigwa E. and Kachur S.P.** (2008). Challenges in Routine Implementation and Quality Control of Rapid Diagnostic Tests for Malaria-Rufiji District, Tanzania. *American Journal of Tropical Medicine and Hygeine,* **79** (3)**,** 385-390.

**Mens P.F., Matelon R.J., Nour B.Y.M., Newman D.M. and Schallig H.D.F.H** (2010). Laboratory evaluation on the sensitivity and specificity of a novel and rapid detection method for malaria diagnosis based on magneto-optical technology (MOT). *Malaria Journal,* **9** (207), doi:10.1186/1475-2875-9-207.

**Miller L.H., Good M.F. and Milon G.** (1994). Malaria Pathogenesis. *Science,* **264,** 1878-1883.

**Moody, A.** (2002). Rapid Diagnostic Tests for Malaria Parasites. *Clinical microbiology reviews,* **15** (1), 66-78.

**Morein B., Hub K.F., Abusugrab I.** (2004). Current status and potential application of ISCOMs in veterinary medicine *Advanced Drug Delivery Reviews,* **56**, 1367-1382.

**Murray C.K. and Bennett J.W.** (2009). Rapid Diagnosis of Malaria. *Interdisciplinary Perspectives on Infectious Diseases***, 1**, 1-7.

**Murray C.K., Gasser R.A.Jr., Magill A.J. and Miller R.S.** (2008). Update on Rapid Diagnostic Testing for Malaria. *Clinical microbiology reviews,* **21** (1)**,** 97-110.

**Nakane P.K. and Kawaoi A.** (1974). Peroxidase-Labeled Antibody A New Method Of Conjugtion. *The Journal of Histochemistry and Cytochemistry*, **22** (12)**,** 1084-1091.

**Ng O.T., Ooi E.E., Lee C.C., Lee P.J., Ng L.C., Wong P.S., Tu T.M., Loh J.P. and Leo Y.S.** (2008). Naturally Acquired Human Plasmodium knowlesi Infection, Singapore. *Emerging Infectious Diseases,* **14** (5)**,** 814-816.

**Nirmalan N., Sims P.F.G. and Hyde J.E.** (2004). Quantitative proteomics of the human malaria parasite Plasmodium falciparum and its application to studies of development and inhibition. *Molecular Microbiology,* **52** (4)**,** 1187-1199.

**Notomi T., Okayama H., Masubuchi H., Yonekawa T., Watanabe K., Amino N. and Hase T.** (2000). Loop-mediated isothermal amplification of DNA. *Nucleic Acids Research,* **28** (12)**,** e63.

**Nussenzweig R.S., Vanderberg J., Most H., Orton C.** (1967). Protective Immunity produced by the Injection of X-irradiated Sporozoites of *Plasmodium berghei*. *Nature*. **216**, 160-162.

**Nyalwidhe J. and Lingelbach K.** (2006). Proteases and chaperones are the most abundant proteins in the parasitophorous vacuole of Plasmodium falciparum-infected erythrocytes. *Proteomics,* **6,** 1563-1573.

**Oakley M.S., Gerald N., McCutchan T.F., Aravind L. and Kumar S.** (2011). Clinical and molecular aspects of malaria fever. *Trends in Parasitology,* **27** (10)**,** 442-449.

**Okiro E.A. and Snow R.W.** (2010). The relationship between reported fever and Plasmodium falciparum infection in African children. *Malaria Journal,* **9** (99), doi:10.1186/1475-2875-9-99.

**Olszewski K.L. and Llinas M.** (2011). Central carbon metabolism of *Plasmodium* parasites. *Molecular and Biochemical Parasitology,* **175,** 95-103.

**Palm N. W., Medzhitov R.** (2009). Immunostimulatory activity of haptenated proteins. *PNAS,* **106**, 4782-4787.

**Palmer C.J., Lindo J.F., Klaskala W.I., Quesada J.A., Kaminsky R., Baum M.K. and Ager A.L.** (1998). Evaluation of the OptiMAL Test for Rapid Diagnosis of Plasmodium vivax and Plasmodium falciparum Malaria. *Journal of Clinical Microbiology*, **36** (1)**,** 203-206.

**Penna-Coutinho J., Cortopassi W.A., Oliviera A.A., Franca T.C.C., Krettli A.U.** (2011). Antimalarial Activity of Potential Inhibitors of *Plasmodium falciparum* Lactate Dehydrogenase Enzyme Selected by Docking Studies. *PLoS ONE*, **6**, (7), e21237. doi:10.1371/journal.pone.0021237.

**Pereira Arias-Bouda L.M., Kuijper S., Van Der Werf A., Nguyen L.N., Jansen H.M. and Kolk A.H.J.** (2003). Changes in avidity and level of immunoglobulin G antibodies to Mycobacterium tuberculosis in sera of patients undergoing treatment for pulmonary tuberculosis. *Clinical and Diagnostic Laboratory Immunology,* **10** (4)**,** 702-709.

**Perkins M.D. and Bell D.R.** (2008). Working without a blindfold: the critical role of diagnostics in malaria control. *Malaria Journal,* **7**(Suppl 1):S5 doi:10.1186/1475-2875-7-S1-S5.

**Peterson D.S., Walliker D., Wellems T.E.** (1998). Evidence that a point mutation in dihydrofolate reductase-thymidylate synthase confers resistance to pyrimethamine in falciparum malaria. *Proceedings of the National Academy of Science USA*, **85**, 9114-9118.

**Petrovsky N. and Aguilar J.C.** (2004). Vaccine adjuvants: Current state and future trends. *Immunology and Cell Biology,* **82,** 488-496.

**Piper R., Lebras J., Wentworth L., Hunt-Cooke A., Houze S., Chiodini P. and Makler M.** (1999). Immunocapture diagnostic assays for malaria using Plasmodium Lactate Dehydrogenase (pLDH. *American Journal of Tropical Medicine and Hygeine,* **60** (1)**,** 109-118.

**Pluschke G., Joss A., Marfurt J., Daubenberger C., Kashala O., Zwickl M., Steif A., Sansig G., Schlapfer B., Linkert S., van der Putten H., Hardman N. and Schröder M.** (1998). Generation of chimeric monoclonal antibodies from mice that carry human immunoglobulin Cγ1 heavy of Cκ light chain gene segments. *Journal of Immunological Methods,* **215,** 27-37.

**Polson A., Coetzer T.H.T., Kruger J., von Maltzahn E., van der Merwe K.J.** (1985). Improvements in the isolation of IgY from the yolks of eggs laid by immunized hens. *Immunological Investigations*. **14**, 323-327.

**Reed S.G., Bertholet S., Coler R.N. and Friede M.** (2008). New horizons in adjuvants for vaccine development. *Trends in Immunology*, **30**, (1), 23-32.

**Rimaniol A.C., Gras G., Verdier F., Capel F., Grigoriev V.B., Porcheray F., Sauzeat E., Fournier J.G., Clayette P., Siegrist C.A., Dormont D.** (2004). Aluminium hydroxide adjuvant induces macrophage differentiation towards a specialized antigen presenting cell type. *Vaccine,* **22**, 3127-3135.

**Rodriguez-del Valle M., Quakyi I.A., Amuesi J., Quaye J.T., Nkrumah F.K. and Taylor D.W.** (1991). Detection of Antigens and Antibodies in the Urine of Humans with Plasmodium falciparum Malaria. *Journal of Clinical Microbiology,* **29** (6)**,** 1236-1242.

**Rogers D.J. and Randolph S.E.** (2000). The Global Spread of Malaria in a Future, Warmer World. *Science,* **289,** 1763-1765.

**Ross R.** (1897). On some peculiar pigmented cells found in two mosquitoes fed malaria blood. *British Medical Journal*, **2**, 1786-1788.

**Rozendaal J.A.** (1997). *Vector control: methods for use by individuals and communities*. World Health Organization, 1-3.

**Sabbatani S., Fiorino S. and Manfredi R.** (2010). The emerging of the fifth malaria parasite (Plasmodium knowlesi). A public health concern? *The Brazilian Journal of Infectious Diseases,* **14** (3)**,** 299-309.

**Saravanan P. and Kumar S.** (2009). Diagnostic and immunoprophylactic applications of synthetic peptides in veterinary microbiology. *Microbiology research,* **1**, (1), doi: 10.4081/mr.2010.e1.

**Satchell J.F., Malby R.L., Luo C.S., Adisa A., Alpyurek A.E., Klonis N., Smith B.J., Tilley L., Colman P.M.** (2005). Structure of glyceraldehyde-3-phosphate dehydrogenase from *Plasmodium falciparum*. *Biological Crystallography*. **61**, 1213-1221.

**Say R.F. and Fuchs G.** (2010). Fructose 1,6-bisphosphate aldolase/phophatase may be an ancestral gluconeogenic enzyme. *Nature,* **464,** 1077-1081.

**Schade R., Staak C., Hendriksen C., Erhard M., Hugl H., Koch G., Larsson A., Pollmann W., van Regenmortel M., Rijke E., Spielmann H., Steinbusch H., Straughan D.** (1993). The Production of Avian (Egg Yolk) Antibodies: IgY – The Report and Recommendations of ECVAM Workshop 21. *ATLA* **24**, 925-934.

**Schade, R., Pfister, C., Halatsch, R. and Henklein, P.** (1991). Polyclonal IgY antibodies from chicken egg yolk - an alternative to the production of mammalian IgG type antibodies in rabbits. *ATLA* **19**, 403-419.

**Schein C.H. and Noteborn M.H.M.** (1988). Formation of soluble recombinant proteins in *Escherichia coli* is favored by lowering growth temperature. *Biotechnology*, **6**, 291-294.

**Schumann W. and Ferreira C.S.** (2004). Production of recombinant proteins in Escherichia coli. *Genetics and Molecular Biology,* **27** (3)**,** 442-453.

**She R.C., Rawlins M.L., Mohl R., Perkins S.L., Hill H.R., Litwin C.M.** (2007). Comparison of Immunofluorescence Antibody Testing and Two Enzyme Immunoassays in the Serologic Diagnosis of Malaria. *Journal of Travel Medicine*. **14**, (2), 105-111.

**Shortt H.E., Garnham P.C.C., Covell G., Shute P.** (1948). Pre-Erythrocytic Stage of Human Malaria, Plasmodium Vivax. *British Medical Journal,* **1**, (4550), 547.

**Singh B., Lee K.S., Matusop A., Radhakrishnan A., Shamsul S.S.G., Cox-Singh J., Thomas A., Conway D.J.** (2004). A large focus of naturally acquired *Plasmodium knowlesi* infections in human beings. *Lancet*, **363**, 1017-24.

**Sirima S.B., Konate A., Tiono A.B., Convelbo N., Cousens S., Pagnoni F.** (2003). Early treatment of childhood fevers with pre-packaged antimalarial drugs in the home reduces severe malaria morbidity in Burkina Faso. *Tropical Medicine and Interantional Health*, **8**, (2), 133-139.

**Smit S., Stoychev S., Louw A.I. and Birkholtz L.M.** (2009). Proteomic Profiling of Plasmodium falciparum through Improved, Semiquantitative Two-Dimesional Gel Electrophoresis. *Journal of Proteome research,* **9,** 2170-2181.

**Smith J.D. and Craig A.D.** (2005). The surface of the Plasmodium falciparum-infected erythrocyte. *Current Issues in Molecular Biology,* **7,** 81-94.

**Smith L.A., Bruce J., Gueye L., Helou A., Diallo R., Gueye B., Jones C. and Webster J.** (2010). From fever to anti-malarial: the treatment-seeking process in rural Senegal. *Malaria Journal,* **9** (1)**,** 333.

**Snow R.W., Craig M.H., Newton C.R.J.C., Steketee R.W.** (2003). *The Public Health Burden of Plasmodium falciparum Malaria in Africa: Deriving the Numbers.* Working Paper No. 11, Disease Control Priorities Project, Bethesda, Maryland: Fogarty International Center, National Institutes of Health.

**Sorensen H.P. and Mortensen K.K.** (2005). Advanced genetic strategies for recombinant protein expression in *Escherichia coli*. *Journal of Biotechnology,* **115,** 113-128.

**Sousa-Figueiredo J.C., Oguttu D., Adriko M., Besigye F., Nankasi A., Arinaitwe M., Namukuta A., Betson M., Kabatereine N.B. and Stothard J.R.** (2010). Investigating portable fluorescent microsocpy (CyScope®) as an alternative rapid diagnostic test for malaria in children and women of child-bearing age. *Malaria Journal,* **9,** 245.

**Sridaran S., McClintock S.K., Syphard L.M., Herman K.M., Barnwell J.W. and Udhayakumar V.** (2010). Anti-folate drug resistance in Africa: meta-analysis of reported dihydrofolate reductase (*dhfr*) mutant genotype frequencies in African *Plasmodium falciparum* parasite populations. *Malaria Journal,* **9** (1)**,** 247.

**Suh K.N., Kain K.C. and Keystone J.S.** (2004). Malaria. *Canadian Medical Association Journal,* **170** (11), 1693-1702.

**Sun J., Jiang Z., Hu S.** (2008). Effect of four adjuvants on immune response to F4 fimbriae in chickens. *Veterinary Immunology and Immunopathology*. **121**, 107-112.

**Tadei W.P., Thatcher B.D., Santos J.M.M., Scarpassa V.M., Rodrigues I.B. and Rafael M.S.** (1998). Ecologic Observations on Anopheline Vectors of Malaria in the Brazilian Amazon. *Amercan Journal of Tropical Medicine and Hygiene,* **59** (2)**,** 325-335.

**Tademir D., Sanabria D., Lauinger I.L., Tarun A., Herman R., Perozzo R., Zloh M., Kappe S.H., Brun R. and Carballeira N.M.** (2010). 2-Hexadecynoic acid inhibits plasmodial FAS-II enzymes and arrests eryhtrocytic and liver stage *Plasmodium* infections. *Bioorganic and Medicinal Chemistry,* **18,** 7475-7485.

**Takahashi M., Lee L., Shi Q., Gawad Y. and Jackowski G.** (1996). Use of Enzyme Immunoassay for Measurement of Skeletal Troponin-I Utilizing Isoform-Specific Monoclonal Antibodies. *Clinical Biochemistry,* **29** (4)**,** 301-308.

**Talman A.M., Duval L., Legrand E., Hubert V., Yen S., Bell D., Le Bras J., Ariey F. and Houze S.** (2007). Evaluation of the intra- and inter-specific genetic variability of Plasmodium lactate dehydrogenase. *Malaria Journal,* **6** (140), doi:10.1186/1475-2875-6-140.

**Taylor S.M., Molyneux M.E., Simel D.L., Meshnick S.R. and Juliano J.J.** (2010). Does This Patient Have Malaria? *JAMA: The Journal of the American Medical Association,* **304** (18)**,** 2048.

**te Witt R., van Wolfswinkel M.E., Petit P.L., van Hellemond J.J., Koelewijn R., van Belkum A. and van Genderen P.J.J.** (2010). Neopterin and procalcitonin are suitable biomarkers for exclusion of severe *Plasmodium falciparum* disease at the initial clinical assessment of travellers with imported malaria. *Malaria Journal,* **9,** (255), doi:10.1186/1475-2875-9-255.

**Teklehaimanot A., McCord G.C. and Sachs J.D.** (2007). Scaling up Malaria Control in Africa: An Economic and Epidemiological Assessment. *Amercan Journal of Tropical Medicine and Hygiene,* **77,** 138-144.

**Tjitra E., Suprianto S., McBroom J., Currie B.J. and Anstey N.M.** (2001). Persistent ICT Malaria P.f/P.v Panmalarial and HRP2 Antigen Reactivity after Treatment of Plasmodium falciparum Malaria Is Associated with Gametocytemia and Results in False-Positive Diagnoses of Plasmodium vivax in Convalescence. *Journal of Clinical Microbiology,* **39** (3)**,** 1025-1031.

**Tomar D., Biswas S., Tripathi V. and Rao D.N.** (2006). Development of diagnostic reagents: Raising antibodies against synthetic peptides of PfHRP-2 and LDH using microsphere delivery. *Immunobiology,* **211,** 797-805.

**Tonnang H.E.Z., Kangalawe R.Y.M. and Yanda P.Z.** (2010). Predicting and mapping malaria under climate change scenarios: the potential redistribution of malaria vectors in Africa. *Malaria Journal,* **9** (111), doi:10.1186/1475-2875-9-111.

**Towbin H., Staehelin T., Gordon J.** (1979). Electrophoretic transfer of proteins from polyacrylamide gels to nitrocellulose sheets: procedure and applications. *Proceedings of the National Academy of Science USA*. **76**, 4350-4354.

**Tristan C., Shahani N., Sedlak T.W., Sawa A.** (2010). The diverse functions of GAPDH: Views from different subcellular compartments. *Cellular Signalling*, **23**, (2), 317-323.

**Turgut-Balik D., Akbulut E., Shoemark D.K., Celik V., Moreton K.M., Sessions R.B., Holbrook J.J. and Brady R.L.** (2004). Cloning, sequence and expression of the lactate dehydrogenase gene from the human malaria parasite, Plasmodium vivax. *Biotechnology Letters,* **26,** 1051-1055.

**Turgut-Balik D., Shoemark D.K., Moreton K.M., Sessions R.B. and Holbrook J.J.** (2001). Over-production of lactate dehydrogenase from Plasmodium falciparum opens a route to new antimalarials. *Biotechnology Letters,* **23**, (11), 917-921.

**Uzochukwu B.S.C., Obikeze E.N., Onwujekwe O.E., Onoka C.A. and Griffiths U.K.** (2009). Cost-effectiveness analysis of rapid diagnostic test, microscopy and syndromic approach in the diagnosis of malaria in Nigeria: implications for scaling-up deployment of ACT. *Malaria Journal,* **8** (265), doi:10.1186/1475-2875-8-265.

**Van den Eede P., Vythilingam I., Ngo Duc T., Van T N., Hung L H., D'Alessandro U. and Erhart A.** (2010). Plasmodium knowlesi malaria in Vietnam: some clarifications. *Malaria Journal,* **9** (20), doi:10.1186/1475-2875-9-20.

**van Hellemond J.J., Rutten M., Koelewijn R., Zeeman A-M., Verweij J., Wismans P., Kocken C.H. and van Genderen J.J.** (2009). Human Plasmodium knowlesi Infection Detected by Rapid Diagnostic Tests for Malaria. *Emerging Infectious Diseases,* **15** (9)**,** 1478-1480.

**van Regenmortel, M.H.V.** (1993). Eggs as protein and antibody factories. *Proceedings of the European Symposium on the Quality of Poultry Meat*, 257-263.

**van Weemen B.K. and Schuurs A.H.W.M.** (1971). Immunoassay using antigen-enzyme conjugates. *FEBS Letters,* **15** (3)**,** 232-236.

**Veron V. and Carme B.** (2006). Short Report: Recovery and use of *Plasmodium* DNA from Malaria Rapid Diagnositc Tests. *Amercan Journal of Tropical Medicine and Hygiene,* **74** (6)**,** 941-943.

**Versteeg I., Mens P.F.** (2009). Development of a stable positive control to be used for quality assurance of rapid diagnostic tests for malaria. *Diagnostic Microbiology and Infectious Disease*. **64**, 256-260.

**Vincent M., Xu Y. and Kong H.** (2004). Helicase-dependent isothermal DNA amplification. *EMBO reports,* **5** (8)**,** 795-800.

**Voet D. and Voet J.G.** (2004). *Biochemistry*. John Wiley and sons, inc., 70; 131; 503; 604-607.

**Welch W.H.** (1897). *Malaria: definition, synonyms, history, and parasitology. System of Practical Medicine.* Columbia University Libraries, Americana, **1**, 17-76.

**Wellems T.E., Hayton K. and Fairhurst R.M.** (2009). The impact of malaria parasitism: from corpuscles to communities. *Journal of Clinical Investigation,* **119** (9)**,** 2496-2505.

**Wesche P.L., Gaffney D.J. and Keightley P.D.** (2004). DNA Sequence Error Rates in Genbank Records Estimated using the Mouse Genome as a Reference. *DNA Sequence,* **15** (5/6)**,** 362-364.

**Wever P.C., Henskens Y.M.C., Kager P.A., Dankert J. and van Gool T.** (2002). Detection of Imported Malaria with the Cell-Dyn 4000 Hematology Analyzer. *Journal of Clinical Microbiology,* **40** (12)**,** 4729-4731.

**WHO.** (2006). Evaluation of rapid diagnostic tests: malaria. *Nature Reviews Microbiology*, **4**, doi:10.1038/nrmicro1524.

**WHO.** (2008). Update on WHO Procedures for Procurement and Quality Assurance of Malaria Rapid Diagnostic Tests. Available at http://www.wpro.who.int/NR/rdonlyres/3659F207-C0B3-4D59-83BD-446CD9847ED1/0/WHOmalariaQAupdate_052008.pdf

**WHO.** (2008). The Global Burden of Disease: 2004 update. *World health organization: geneva.*

**Reyburn, H.** (2010) New WHO guidelines for the treatment of malaria. *BMJ,* **340**, c2637.

**WHO.** (2009) Malaria fact sheet number 94, 2006, *World Health Organization, Geneva,* Available at http://www. who. int/inf-fs/en/fact094. html.

**Wilson N.O., Adjei A.A., Anderson W., Baidoo S. and Stiles J.K.** (2008). Short Report: Detection of *Plasmodium falciparum* Histidine-rich Protein II in Saliva of Malaria Patients. *Amercan Journal of Tropical Medicine and Hygiene,* **78** (5)**,** 733-735.

**Wilson-Welder J.H., Torres M.P., Kipper M.J., Mallapragada S.K., Wannemuehler M.J. and Narasimhan B.** (2009). Vaccine Adjuvants: Current Challenges and Future Approaches. *Journal of Pharmaceutical Sciences*, **98**, (4), 1278-1316.

**Wongsrichanalai C., Barcus M.J., Muth S., Sutamihardja A., Wernsdorfer W.A.** (2007). A review of malaria diagnostic tools: microscopy and rapid diagnostic test (RDT). *The American Society of Tropical Medicine and Hygiene*, **77**, (6), 119–127.

**Yakob L., Bonsall M.B. and Yan G.** (2010). Modelling knowlesi malaria transmission in humans: vector preference and host competence. *Malaria Journal,* **9,** 329.

**Zocher K., Fritz-Wolf K., Kehr S., Fischer M., Rahlfs S., Becker K.** (2012). Biochemical and structural characterisation of *Plasmodium falciparum* glutamate dehydrogenase 2. *Molecular and Biochemical Parasitology*, **183**, 52-62.